Building and Environment

Mapping the spatial distribution of nocturnal urban heat island based on Local Climate Zone framework

--Manuscript Draft--

Manuscript Number:	BAE-D-22-04658R1
Article Type:	Original Research Paper
Keywords:	Urban heat island; local climate zone; urban morphology; Mobile Traverse Measurement; Spatial Mapping; Hong Kong
Corresponding Author:	Yong XU Guangzhou University Hong Kong, CHINA
First Author:	YINGSHENG ZHENG, Ph.D.
Order of Authors:	YINGSHENG ZHENG, Ph.D.
	Chao REN
	Yuan SHI
	Steve H.L. YIM
	Derrick Y.F. LAI
	Yong XU
	Can FANG
	Wenjie LI
Abstract:	A spatial understanding of street-scale urban heat island (UHI) is essential but challenging in Hong Kong, due to its highly heterogeneous urban environment and a limited weather station monitoring network. Night-time mobile measurements were conducted during the summertime of 2014 to monitor UHI variation at local level. Three measurement routes and a total of 80 sample sites were selected according to the Local Climate Zone (LCZ) framework. The measured climatic data and urban morphology data were synergized and analyzed at LCZ scale through Geographical Information System (GIS). Stepwise Multiple Linear Regression (MLR) and Partial Least Square Regression (PLSR) were applied to quantify the connections between urban form and local UHI conditions of LCZ. Mean sky view factor, total street length, and pervious surface fraction of LCZ sites have been found to be the most explanatory variables of local UHI intensity, and over 50% of UHI variations can be explained by both statistical models of stepwise MLR and PLSR. An UHI evaluation map of urban areas in Hong Kong has been developed based on the statistical models, through which UHI hotspots have been identified. LCZ-based UHI mitigation strategies were further developed for climatic planning of Outline Zoning Plan areas. The results indicate that urban forms have significant influences on UHI development at local scale, and an optimal design of urban morphology is necessary for UHI mitigation and climate adaptation.

COVER LETTER

Dear Editor,

Thank you for editor's and reviewers' comments and providing the opportunity for us to submit the revised manuscript **"BAE-D-22-04456"-"Mapping the spatial distribution of nocturnal urban heat island based on Local Climate Zone framework"** authored by **Yingsheng ZHENG, Chao REN, Yuan SHI, Steve H.L. YIM, Derrick Y.F. LAI, Yong XU*, Can FANG, and Wenjie LI** for the consideration of publication as a research article in your prestigious journal. Comments and ssuggestions from editors and reviewers are quite helpful for us and we incorporate them in the revised manuscript.

By submitting our study to your prestigious journal, we would like to take this precious opportunity to share our findings and experience in the subtropical high-density city of Hong Kong with urban climate researchers and urban planners around the world and facilitate interdisciplinary communication.

Best regards,
Yong XU

ETHICS IN PUBLISHING
• The research meets all applicable standards with regard to the ethics of experimentation and research integrity, and the following is being certified/declared true.
• Along with co-authors of concerned field, the paper has been submitted with full responsibility, following due ethical procedure, and there is no duplicate publication, fraud, plagiarism, or concerns about animal or human experimentation.

DECLARATION OF INTEREST
• None of the authors of this paper has a financial or personal relationship with other people or organizations that could inappropriately influence or bias the content of the paper.
• It is to specifically state that "No Competing interests are at stake and there is No Conflict of Interest" with other people or organizations that could inappropriately influence or bias the content of the paper.

CORRESPONDING AUTHOR:
Yong XU
School of Geography and Remote Sensing, Guangzhou University
E-mail: xu1129@gzhu.edu.cn

Declaration of Interest Statement

The authors declare that they have no known competing financial interests or personal relationships that could have appeared to influence the work reported in this paper.

Dear Editor and Reviewers,

We highly appreciate the valuable comments of reviewers on our manuscript of "BAE-D-22-04456 Mapping the spatial distribution of nocturnal urban heat island based on Local Climate Zone framework ". Suggestions are quite helpful for us and we incorporate them in the revised manuscript.

Response to Editor:

In revising your manuscript, please pay particular attention to addressing the concerns raised by reviewer #2 below; particularly points 1 (novelty w.r.t. state of the art / geographical context) and 2 (justification of temporal focus; presumably on the grounds of the timing of peak UHI?).

Response to Editor:

Thank you for your comment.

1. Point 1 (novelty w.r.t. state of the art / geographical context):The needs for refined spatial understanding of local UHI in the high-density city of Hong Kong, and the possible methods for the observations and spatial analysis of UHI were discussed in **Section 1.2 on from line 24 page 3 to line 15 page 4** in the revised manuscript.

"Weather station network operated by Hong Kong Observatory provides long-term meteorological data in high temporal resolution, based on which spatial interpolation techniques could be applied in the heat risk assessment at city level (Morakinyo et al., 2019). However, as automatic weather stations are sparsely distributed in relatively open spaces, it is still hard to reveal the intra-urban variations of UHI at fine scale (Shi, Katzschner, & Ng, 2018). Remote sensing technique is another commonly used method in the spatial assessment of UHI through retrieving land surface temperature based on satellite images (Nwakaire, Onn, Yap et al., 2020). It is known that diurnal profiles of surface UHI differ from that of canopy UHI. Large SUHI generally occurs during the daytime while large canopy UHI generally occurs at night, and therefore spatial assessment of canopy UHI through remote sensing techniques at fine scale may introduce estimation error (Shi, Katzschner, et al., 2018).

Compared to above methods, mobile traverse measurement method is more applicable to the refined spatial assessment of UHI for its advantages in low cost, time efficiency, and high spatial resolution (Liu, Lin, Liu et al., 2017; Yan, Guo, Li et al., 2020). The climatic data collected through mobile measurements at street level is close to the local climatic conditions that pedestrians are exposed to. It could be employed to quantify the influence of urban forms on the climatic variation at local level (Chàfer, Tan, Cureau et al., 2022; Z. Wang, Zhao, & Peng, 2021)."

2. Point 2 (**justification of temporal focus; presumably on the grounds of the timing of peak UHI?)** was discussed in **Section 2.2 (2) Weather control and measurement time selection from line 4 page 8 to line 6 page 9** in the revised manuscript**:**

" Weather control and time selection is critical for UHI observation and analysis, as the spatial distribution patterns of UHI varies in different background weather conditions and the diurnal circle. Clear sky condition is ideal for UHI development, but it has low occurrence frequency below 2.5% in the summer of Hong Kong. Summertime peak UHI intensities mainly occurred in partly cloudy conditions with daily mean cloud amount of 2-7 Oktas (Zheng, Li, Fang et al., 2023). Thus, typical hot summer days with partly cloudy and weak wind conditions were selected for UHI observations.

Although the stationary observation records in Hong Kong show that UHI intensity is generally maximized in deep night or early morning, and the peak air temperature generally occurs at noon or early afternoon (Zheng, 2016), early night period of 20:00-22:00 would be more critical for UHI measurement since that: (1). Early night time when people get off work or school, urban areas would have more intense outdoor human activities than that at noon or at late night, as noontime or early afternoon when air temperature reaches peak in the whole day in summer, people generally prefer to stay indoor to avoid high temperature and strong solar radiation. (2). Daytime UHI is not that obvious as nocturnal UHI. High-density urban areas is highly possible to have cooler air temperature than rural areas at noon and early afternoon, i.e. urban cool island effects, mainly due to the shading effects and heat absorption/storage by dense buildings (Ren, Wang, Shi et al., 2021). Significant UHI intensity at early night would lead to air temperature elevation in urban areas and cause thermal discomfort or heat-related health problems to pedestrians. Based on the above consideration, early night period of 20:00-22:00 was determined as the critical time period for mobile traverse measurement of UHI effects."

We highly appreciate the encouragement and valuable comments on our manuscript. Suggestions are quite helpful for us to improve this study.

Response to Reviewer 1:

1. First, just some particular comments: line 12 page 2 Five times of mobile traverse measurements have been conducted… awkward phrasing

Response to reviewer: Thank you for your comment. It was revised as "Night-time mobile measurements were conducted during the summertime of 2014 to monitor UHI variation at local level" **in the abstract section on line 7 page 2** highlighted in yellow.

2. Line 37 page 3 variate significantly in Hong Kong… do you mean vary.

Response to reviewer: Thank you for your comment. It was revised as "local thermal environments and the associated heat exposure risks vary significantly in Hong Kong" **in section 1.2 on line 16 page 3** highlighted in yellow.

3. Line 31 page 7 Five times of mobile traverse measurements have been conducted… shows up here again.

Response to reviewer: Thank you for your comment. It was revised as "A total of five mobile measurements were completed under the typical hot weather condition of Hong Kong, to monitor local atmospheric environments of selected LCZ sample sites (Table 1)." **in section 2.3 (1) on line 9 page 9** highlighted in yellow.

4. Line 55 page 10 Meteorological data was collected… should be data are collected.

Response to reviewer: Thank you for your comment. It was revised according to the comment **in section 2.3 (3) on line 3 page 12** highlighted in yellow.

5. Line 60 page 10 what is the rural LCZ in LCZ classification. It's role in determining UHI? Would results vary with other choices? Is site chosen typical rural? how much variance is there in rural LCZ?

Response to reviewer: Thank you for your comment. Considerations of determining rural reference station for calculating UHI magnitude were revised in **section 2.3 (3). Stationary observation data from line 3 page 12 to line 11 page 13** highlighted in yellow:

”Meteorological data are collected from the Hong Kong Observatory for calculating UHI magnitude of LCZ sample sites and conducting temporal adjustments for measured air temperature. Determination of rural reference for UHI study is difficult for Hong Kong because local climate vary across different rural areas owing to the mountainous and coastal geographical conditions. Stations located near the coast such as Cheung Chau station and Waglan Island stations have been excluded from consideration, as the recorded daily temperature profiles could be significantly influenced by the seawater temperature (Sakakibara & Owa, 2005). Ta Kwu Ling (TKL) and Lau Fu Shan (LFS) stations have been commonly recognized as rural stations of Hong Kong (Fung, 2010; Memon, Leung, & Liu, 2009; Siu & Hart, 2013). TKL station is in the northeastern rural area with a small population and lush vegetation (Figure 6). LFS station is controversial due to its surrounding low-rise neighborhoods and proximity to high-rise residential developments in Tin Shui Wai, and some studies have classified LFS as a rural station (Leung, 2004; Leung & Ng, 1997), while recent studies have recognized it as an urban or suburban station as LFS station shows similar diurnal temperature profiles with the urban stations located in new towns of Hong Kong (Memon et al., 2009; Wu, Leung, Lui et al., 2009). Based on the above consideration, TKL station is determined as the rural reference in this study.”

6. Line 1 page 16 why LCZ4 2nd hottest among all the comparisons?

Response to reviewer: Thank you for your comment. Although mean UHI intensity of LCZ4 is 2nd hottest among all comparisons, it has wide range of 1.08 K – 3.62 K, which may be due to the influence of surrounding high-density urban environments. The reasons was discussed in **Section 3.1 from line 5 page 18 to line 3 page 19** highlighted in yellow:

” UHI intensities of LCZ sample sites in the six LCZ classes were shown in Figure 9. LCZ1 experienced the highest mean UHI level above 2.5 K among the six classes, and it showed wide range of 1.58 K – 4.49 K. LCZ2 and LCZ4 also observed considerable UHI intensity, with the mean values above 2.0 K. The mean value of LCZ4 was slightly higher than that of LCZ2, but it had wider range spanning from 1.08 K to 3.62 K. The high UHI intensities observed in some LCZ sample sites are possibly due to the influence of surrounding high-density urban environments. The open mid-rise class of LCZ5 and low-rise classes (LCZ3 and LCZ6) have recorded averaged UHI intensity below 2.0 K. LCZ5 had the lowest mean UHI level of 1.15 K. LCZ6 documented a slightly elevated UHI intensity compared to LCZ3 and LCZ5, which may be influenced by the heat release from the freeway near the sites.”

7. Page 19 would bootstrapping sampling aid in confidence levels in results? Especially for results shown in Table 8.

Response to reviewer: Thank you for your comment. Bootstrapping sampling method was used to evaluate confidence intervals of parameter estimates of UHI estimation model i**n section 3.2 from line 16 page 23 to line 4 page 24** highlighted in yellow:

“Bootstrap method was employed to evaluate confidence intervals of parameter estimates of UHI estimation model through 5000 bootstrapping replications (Gu & You, 2022). The results show that the original PLSR model has higher predictive performance (R2 = 0.53) than bootstrap-based models (R2 = 0.28).”

8. Page 22 clear days vs cloudier days? Any way in the sample to know results due to this?

Response to reviewer: Thank you for your comment. As clear sky conditions occur at low frequency in summer of Hong Kong, typical hot summer days with partly cloudy and calm wind conditions were selected

to conduct mobile traverse measurements. The content was presented in the revised manuscript **Section 2.2 (2) Weather control and measurement time selection on line 6 – line 9, page 8** highlighted in yellow:

" Clear sky condition is ideal for UHI development, but it has low occurrence frequency below 2.5% in the summer of Hong Kong. Summertime peak UHI intensities generally occurred in partly cloudy conditions with daily mean cloud amount of 2-7 Oktas (Zheng, Li, Fang et al., 2023). Thus, typical hot summer days with partly cloudy and weak wind conditions were selected for UHI observations."

This is a very nice article well executed.

Response to reviewer: We highly appreciate the encouragement and valuable comments on our manuscript. Suggestions are quite helpful for us to improve this study.

Response to Reviewer 2:

While this paper addresses an important topic, it has several limitations that should be addressed. Despite its significance, there are several weaknesses in the study design and execution that need to be addressed in order for the findings to be fully convincing:

1. This research method, although useful, has been utilized in various countries in the past and may not necessarily be considered groundbreaking or innovative in the field. In fact, similar studies have been conducted in multiple countries, which may make this study appear to lack originality.

Response to reviewer: Thank you for your comment.

Needs for refined spatial understanding of local UHI in the high-density city of Hong Kong, and the possible methods for the observations and spatial analysis of UHI were discussed in **Section 1.2 from line 24 page 3 to line 15 page 4** highlighted in yellow**:**

"Weather station network operated by Hong Kong Observatory provides long-term meteorological data in high temporal resolution, based on which spatial interpolation techniques could be applied in the heat risk assessment at city level (Morakinyo et al., 2019). However, as automatic weather stations are sparsely distributed in relatively open spaces, it is still hard to reveal the intra-urban variations of UHI at fine scale (Shi, Katzschner, & Ng, 2018). Remote sensing technique is another commonly used method in the spatial assessment of UHI through retrieving land surface temperature based on satellite images (Nwakaire, Onn, Yap et al., 2020). It is known that diurnal profiles of surface UHI differ from that of canopy UHI. Large SUHI generally occurs during the daytime while large canopy UHI generally occurs at night, and therefore spatial assessment of canopy UHI through remote sensing techniques at fine scale may introduce estimation error (Shi, Katzschner, et al., 2018).

Compared to the above methods, mobile traverse measurement method is more applicable to the refined spatial assessment of UHI for its advantages in low cost, time efficiency, and high spatial resolution (Liu, Lin, Liu et al., 2017; Yan, Guo, Li et al., 2020). The climatic data collected through mobile measurements at street level is close to the local climatic conditions that pedestrians are exposed to. It could be employed to quantify the influence of urban forms on the climatic variation at local level (Chàfer, Tan, Cureau et al., 2022; Z. Wang, Zhao, & Peng, 2021)."

Research gaps of UHI studies in Hong Kong were discussed in **Section 1.3, line 8 – line 24 on page 5,** highlighted in yellow:

"Many previous UHI studies in Hong Kong have conducted in situ measurements to monitor local UHI conditions, but mainly focused on certain LCZ types, such as high-rise residential developments and compact commercial areas (Giridharan, Lau, Ganesan et al., 2007; Lin, Lau, Qin et al., 2017; Tan, Lau, & Ng, 2016). The quantitative relationships between local UHI intensity and urban forms have not been fully explored based on UHI observations in a comprehensive set of sample sites. Knowledge about the spatial distribution pattern of UHI intensity at LCZ level is still limited, especially in the critical time period under typical hot summer weather conditions. Thus, standardized UHI observations and refined understanding about how urban morphology influences the spatial distribution of UHI in Hong Kong are needed for climatic planning and adaptation."

2. The study was only conducted in Hong Kong, so the conclusions may not be applicable to other cities. In addition, the study was only conducted during the summer season, so it may not accurately reflect the results in other seasons. Another limitation of this study is that it only focused on the UHI conditions during early nighttime in summer under the prevailing weather conditions in Hong Kong. Therefore, further research on local climate conditions during the daytime (especially in the early afternoon when the air temperature is at its peak) is necessary.

Response to reviewer: Thank you for your comment.

This study shows how the LCZ classification system could be applied to land surface classification, site selection, experimental design as well as data documentation and analysis for UHI studies. An integrative method of statistical analysis and spatial mapping has been employed to establish the urban morphology-based UHI estimation model of Hong Kong, which not only supports quantitative knowledge of key urban morphology parameters influencing local UHI development, but also provides intuitive spatial information about critical urban areas with urgent need for UHI mitigation. The LCZ-based "UHI observation-UHI estimation-UHI mitigation planning" method proposed by this study is helpful for cross-disciplinary communication between climatic researchers and planners, and also applicable to UHI study and climatic planning application in other cities.

The reasons why UHI measurements were conducted in early nighttime under typical summer weather conditions in Hong Kong were discussed **Section 2.2 (2) Weather control and measurement time selection from line 4 page 8 to line 6 page 9** highlighted in yellow:

"Weather control and time selection is critical for UHI observation and analysis, as the spatial distribution patterns of UHI varies in different background weather conditions and the diurnal circle. Clear sky condition is ideal for UHI development, but it has low occurrence frequency below 2.5% in the summer of Hong Kong. Summertime peak UHI intensities mainly occurred in partly cloudy conditions with daily mean cloud amount of 2-7 Oktas (Zheng, Li, Fang et al., 2023). Thus, typical hot summer days with partly cloudy and weak wind conditions were selected for UHI observations.

Although the stationary observation records in Hong Kong show that UHI intensity is generally maximized in deep night or early morning, and the peak air temperature generally occurs at noon or early afternoon (Zheng, 2016), early night period of 20:00-22:00 would be more critical for UHI measurement since that: (1). Early night time when people get off work or school, urban areas would have more intense outdoor human activities than that at late night or noon. Significant UHI intensity at early night would lead to air temperature elevation in urban areas and cause thermal discomfort or heat-related health problems of pedestrians. (2). Noontime or early afternoon when air temperature reaches peak in the whole day in summer, people generally prefer to stay indoor to avoid high temperature and strong solar radiation, and thus there are less outdoor activities at noon than that in the early evening. In addition, daytime UHI is not that obvious as nocturnal UHI. High-density urban areas is highly possible to have cooler air temperature

than rural areas at noon and early afternoon, i.e. Urban Cool Island, mainly due to the shading effects and heat absorption/storage by dense buildings (Ren, Wang, Shi et al., 2021). Based on the above consideration, early night period of 20:00-22:00 was determined as the critical time period for mobile traverse measurement of UHI effects."

Limitations of this study was discussed **in the conclusion section on line 3 page 34** highlighted in yellow:

"A limitation of this study is that it only focused on UHI conditions in the early night-time period in summer, when outdoor human activities are intense with high exposure risks to significant UHI effects. Further heat risk analysis during the daytime and other seasons is necessary, especially in the early afternoon with the air temperature at its peak level. In addition, obvious UHI variations in the dominant high-rise LCZ classes of LCZ1 and LCZ4 have been observed through mobile traverse measurements, which indicates the needs for further subclassification and refinement of LCZ framework in the high-density and heterogenous urban environments in Hong Kong."

3. While the Local Climate Zone (LCZ) classification system has been utilized in this study, it may not be without flaws. The LCZ classification may not adequately reflect the complexity of the urban environment, may not be sufficiently precise, may not adequately reflect differences between city areas, and may not adequately reflect changes in city.

Response to reviewer: Thank you for your comment. **The needs of further refinement of LCZ framework under local urban scenario** was discussed in **the conclusion section on line 6 page 34** highlighted in yellow:

"In addition, obvious UHI variations in the dominant high-rise LCZ classes of LCZ1 and LCZ4 have been observed through mobile traverse measurements, which indicates the needs for further subclassification and refinement of LCZ framework in the high-density and heterogenous urban environments in Hong Kong."

We highly appreciate the encouragement and valuable comments on our manuscript. Suggestions are quite helpful for us to improve this study.

Highlights

- Mobile measurements were conducted to achieve a refined spatial understanding of UHI conditions at local scale.
- Local Climate Zone (LCZ) framework was applied to standardize the mobile measurements of UHI.
- Urban morphology-based UHI estimation model of LCZ was established though bivariate and multivariate analysis.
- Hotspots of UHI in high-density urban areas of Hong Kong were identified.
- LCZ-based planning strategies for UHI mitigation were developed.

Mapping the spatial distribution of nocturnal urban heat island based on Local Climate Zone framework

Yingsheng Zheng[a,b], Chao Ren[c], Yuan Shi[d], Steve H.L. Yim[e,f,g], Derrick Y.F. Lai[h], Yong Xu[i*], Can Fang[a], Wenjie Li[a]

a. College of Architecture and Urban Planning, Guangzhou University, Guangzhou, China

b. School of Architecture, The Chinese University of Hong Kong, Hong Kong SAR, China

c. Division of Landscape Architecture, Department of Architecture, Faculty of Architecture, The University of Hong Kong, Hong Kong, SAR, China

d. Department of Geography and Planning, University of Liverpool, Liverpool, UK

e. Asian School of the Environment, Nanyang Technological University, Singapore

f. Lee Kong Chian School of Medicine, Nanyang Technological University, Singapore

g. Earth Observatory of Singapore, Nanyang Technological University, Singapore

h. Department of Geography and Resource Management, The Chinese University of Hong Kong, Hong Kong SAR, China

i. School of Geography and Remote Sensing, Guangzhou University, Guangzhou, China

Corresponding Author:
Yong XU
School of Geography and Remote Sensing, Guangzhou University
E-mail: xu1129@gzhu.edu.cn

Mapping the spatial distribution of nocturnal urban heat island based on Local Climate Zone framework

Abstract

A spatial understanding of street-scale urban heat island (UHI) is essential but challenging in Hong Kong, due to its highly heterogeneous urban environment and a limited weather station monitoring network. Night-time mobile measurements were conducted during the summertime of 2014 to monitor UHI variation at local level. Three measurement routes and a total of 80 sample sites were selected according to the Local Climate Zone (LCZ) framework. The measured climatic data and urban morphology data were synergized and analyzed at LCZ scale through Geographical Information System (GIS). Stepwise Multiple Linear Regression (MLR) and Partial Least Square Regression (PLSR) were applied to quantify the connections between urban form and local UHI conditions of LCZ. Mean sky view factor, total street length, and pervious surface fraction of LCZ sites have been found to be the most explanatory variables of local UHI intensity, and over 50% of UHI variations can be explained by both statistical models of stepwise MLR and PLSR. An UHI evaluation map of urban areas in Hong Kong has been developed based on the statistical models, through which UHI hotspots have been identified. LCZ-based UHI mitigation strategies were further developed for climatic planning of Outline Zoning Plan areas. The results indicate that urban forms have significant influences on UHI development at local scale, and an optimal design of urban morphology is necessary for UHI mitigation and climate adaptation.

Key Words: Urban Heat Island; Local Climate Zone; Urban Morphology; Mobile Traverse Measurement; Spatial Mapping; Hong Kong

1.Introduction

1.1. Challenges in climatic planning for urban heat island mitigation

Under the influence of local urbanization and global climate change, many cities over the world have experienced significant temperature increase in past decades (Masson-Delmotte, Zhai, Pörtner et al., 2018). The occurrence frequency, magnitude, and duration of high-temperature episodes are expected to continue rising in the second half of the 21st century (Dosio, Mentaschi, Fischer et al., 2018; Perkins-Kirkpatrick & Lewis, 2020). Urban heat island (UHI) effect which caused by the process of urbanization with changes in land surface structure and human behaviours, tends to be reinforced by high temperature periods. It results in additional hot days at local scale, associated with elevated energy consumption for cooling and increased heat-related health risks (Goggins, Chan, Ng et al., 2012; Ho, Lau, Ren et al., 2017; Morakinyo, Ren, Shi et al., 2019). Therefore, it is essential to identify hotspot areas of UHI and take climatic planning interventions for UHI mitigation.

1.2. Needs for refined spatial understanding of local UHI in the high-density city of Hong Kong

Hong Kong is a high-density city with a highly heterogeneous urban environment and mountainous-coastal geography. Due to the spatial variability of urban forms and geographical conditions, local thermal environments and the associated heat exposure risks vary significantly in Hong Kong (Hua, Zhang, Ren et al., 2021). In high-density urban areas with crowded buildings and dense population, UHI effects exacerbate the strength of high temperatures, and the high temperature weather generally accompanied by high air pressure and weak air flow further exacerbates the magnitude of UHI effects (Zou, Yan, Yu et al., 2021). Residents living in high-density urban areas are exposed to the strengthened high temperature weather and urban heat islands. In such cases, a refined spatial understanding of urban morphology and local UHI conditions is needed to support the planning decision-making for UHI mitigation.

Weather station network operated by Hong Kong Observatory provides long-term meteorological data in high temporal resolution, based on which spatial interpolation techniques

could be applied in the heat risk assessment at city level (Morakinyo et al., 2019). However, as automatic weather stations are sparsely distributed in relatively open spaces, it is still hard to reveal the intra-urban variations of UHI at fine scale (Shi, Katzschner, & Ng, 2018). Remote sensing technique is another commonly used method in the spatial assessment of UHI through retrieving land surface temperature based on satellite images (Nwakaire, Onn, Yap et al., 2020). It is known that diurnal profiles of surface UHI differ from that of canopy UHI. Large SUHI generally occurs during the daytime while large canopy UHI generally occurs at night, and therefore spatial assessment of canopy UHI through remote sensing techniques at fine scale may introduce estimation error (Shi, Katzschner, et al., 2018).

Compared to the above methods, mobile traverse measurement method is more applicable to the refined spatial assessment of UHI for its advantages in low cost, time efficiency, and high spatial resolution (Liu, Lin, Liu et al., 2017; Yan, Guo, Li et al., 2020). The climatic data collected through mobile measurements at street level is close to the local climatic conditions that pedestrians are exposed to. It could be employed to quantify the influence of urban forms on the climatic variation at local level (Chàfer, Tan, Cureau et al., 2022; Z. Wang, Zhao, & Peng, 2021).

1.3. Application of Local Climate Zone framework into the spatial assessment of UHI

To systematically differentiate the varying land surface types, Stewart and Oke (2012) have developed the Local Climate Zone (LCZ) framework as a land surface classification system to standardize the observation and report of UHI studies. The LCZ framework consists of 17 basic classes, including ten building classes and seven land cover classes. Previous studies of LCZ classification have shown that the existing LCZ classes can well describe the land surface properties and thermal environment variations at local scale (Jiang, Zhan, Dong et al., 2022; Francois Leconte, Bouyer, Claverie et al., 2015). Moreover, LCZ framework has proposed a set of guidelines in the aspects of representative site selection, site metadata documentation, weather control and time control for UHI observations and report. Following the standardized framework of LCZ, local climatic studies in different climatic regions over the world with varied built environment could be compared.

In the high-density city of Hong Kong, the highly heterogeneous land cover conditions have been described and quantified in LCZ classification maps through GIS method and remote sensing method (R. Wang, Ren, Xu et al., 2018; Zheng, Ren, Xu et al., 2017). The LCZ classification maps have been evaluated and validated by Shi, Lau, Ren et al. (2018) based on mobile traverse measurements, and the study found that the LCZ framework can well differentiate local thermal variation. The LCZ framework has been further applied in standardizing the observation and analysis of thermal comfort and thermal sensation in different LCZ types (Lau, Chung, & Ren, 2019; Tan, Lau, & Ng, 2017).

Many previous UHI studies in Hong Kong have conducted in situ measurements to monitor local UHI conditions, but mainly focused on certain LCZ types, such as high-rise residential developments and compact commercial areas (Giridharan, Lau, Ganesan et al., 2007; Lin, Lau, Qin et al., 2017; Tan, Lau, & Ng, 2016). The quantitative relationships between local UHI intensity and urban forms have not been fully explored based on UHI observations in a comprehensive set of sample sites. Knowledge about the spatial distribution pattern of UHI intensity at LCZ level is still limited, especially in the critical time period under typical hot summer weather conditions. Thus, standardized UHI observations and refined understanding about how urban morphology influences the spatial distribution of UHI in Hong Kong are needed for climatic planning and adaptation.

This study aims to (1) apply the LCZ framework to standardize the procedures of UHI observations in Hong Kong, and conduct traverse measurements to monitor local climate conditions in selected high-density urban areas under the prevailing summer weather condition of Hong Kong, (2) investigate the relationships between urban morphology parameters and UHI intensity at LCZ scale, and develop a morphological-based UHI estimation model through statistical analysis, (3) formulate a UHI estimation map as an intuitive information support of critical urban areas with urgent needs for UHI mitigation, and (4) integrate the LCZ-based UHI mitigation strategies into the statutory plan of Outline Zoning Plan in Hong Kong.

2.Method

2.1. Study area

Hong Kong is a high-density city located on the southeast coast of China, one of the core cities in the Guangdong-Hong Kong-Macao Greater Bay Area. The total land area of Hong Kong is about 1,114 square kilometers, of which more than 75% is a mountain country park reserve, and less than 25% of the land is allowed for urban development. The total population is about 7.4 million, with the highest subregion population density exceeding 55,000 people per square kilometre (HKGovernment, 2021).

Hong Kong has a subtropical maritime monsoon climate. Summertime in Hong Kong is associated with high air temperature, high relative humidity and weak winds, which may cause thermal discomfort and other heat-related health problems. Large population, limited land resources, and high urbanization level shape the high-density urban environment in Hong Kong, and considerable UHI intensity has been observed in high-density urban areas of Hong Kong.

2.2. Experimental design of mobile traverse measurement for UHI observation

(1). Sample sites selection and measurement routes design

The GIS-based Local Climate Zone classification map of Hong Kong developed by Zheng et al. (2017) was applied to identify the critical regions and potentially appropriate sites for urban heat island monitoring. Main LCZ types of urban areas of Hong Kong are LCZ1- LCZ6 (**Figure 1**), and dominant LCZ types in city centers are LCZ1 (Compact High-rise) and LCZ4 (Open High-rise). High density urban areas of northern Hong Kong Island (HKI), Kowloon Peninsula (KL) as well as the new town of Tuen Mun (TM) in the New Territories have been selected as study areas (**Figure 2**). A total of 80 typical LCZ sites (in 300m grid size) have been selected, including 32 sites in HKI, 33 sites in KL, and 15 sites in TM. Sample sites cover six LCZ types of LCZ1 – LCZ6. HKI and TM areas mainly comprise high-rise LCZ types of LCZ1 and LCZ4, while KL area covers six LCZ types from LCZ1 to LCZ6. Traverse measurement routes have been designed to pass through the central

part of sample sites, and the total length of HKI, KL, and TM routes are 16km, 25km and 12km respectively (**Figure 3**). A couple of pilot measurements were performed to ensure the measurement time was controlled within two hours to limit the background air temperature change during the measurement (Stewart, 2011).

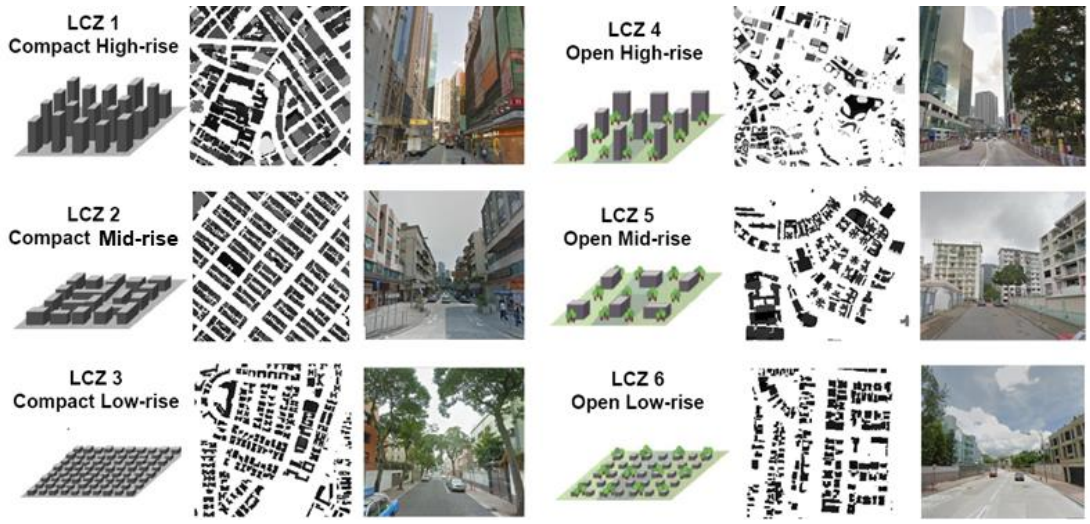

Figure 1. Examples of LCZ classes in Hong Kong (Zheng et al., 2017)

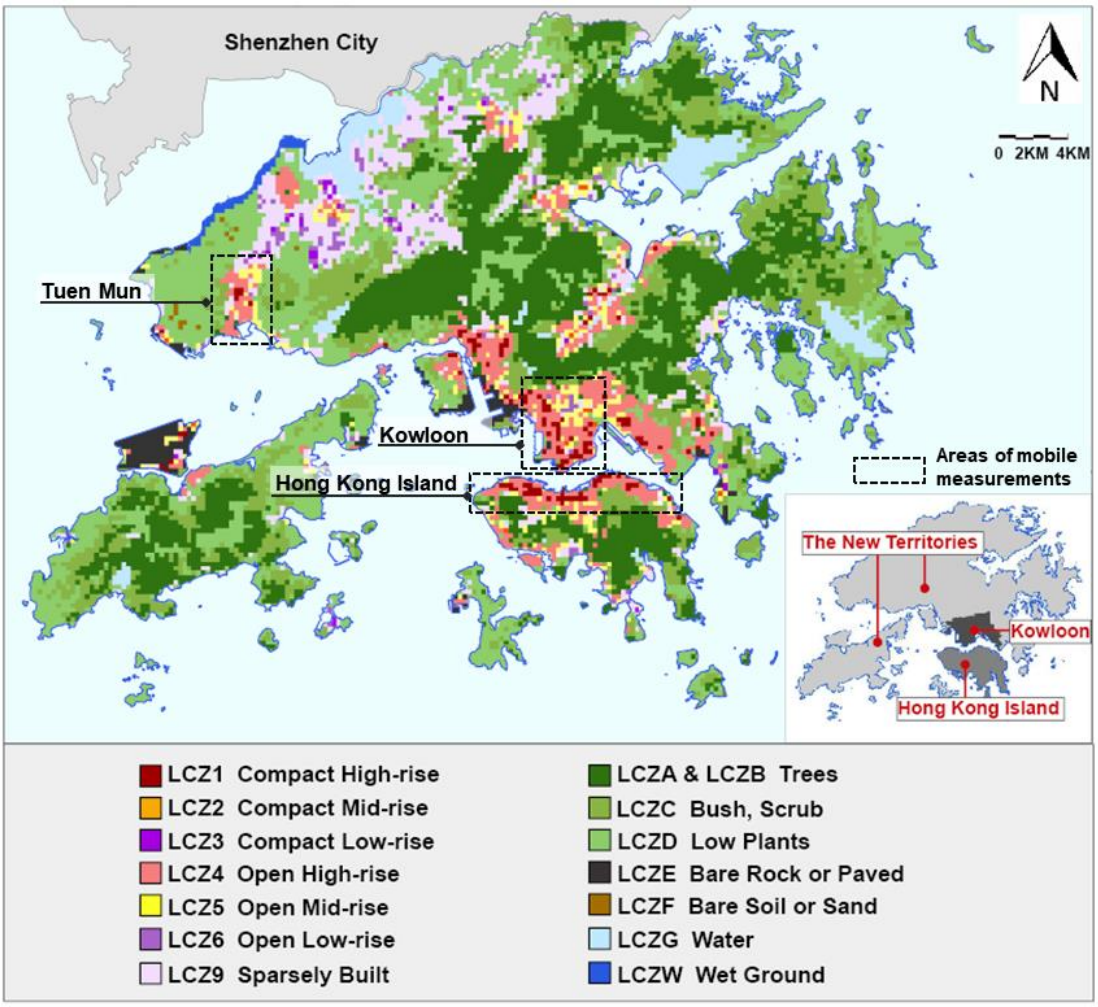

Figure 2. Study areas of traverse measurements based on the LCZ classification map in Hong Kong

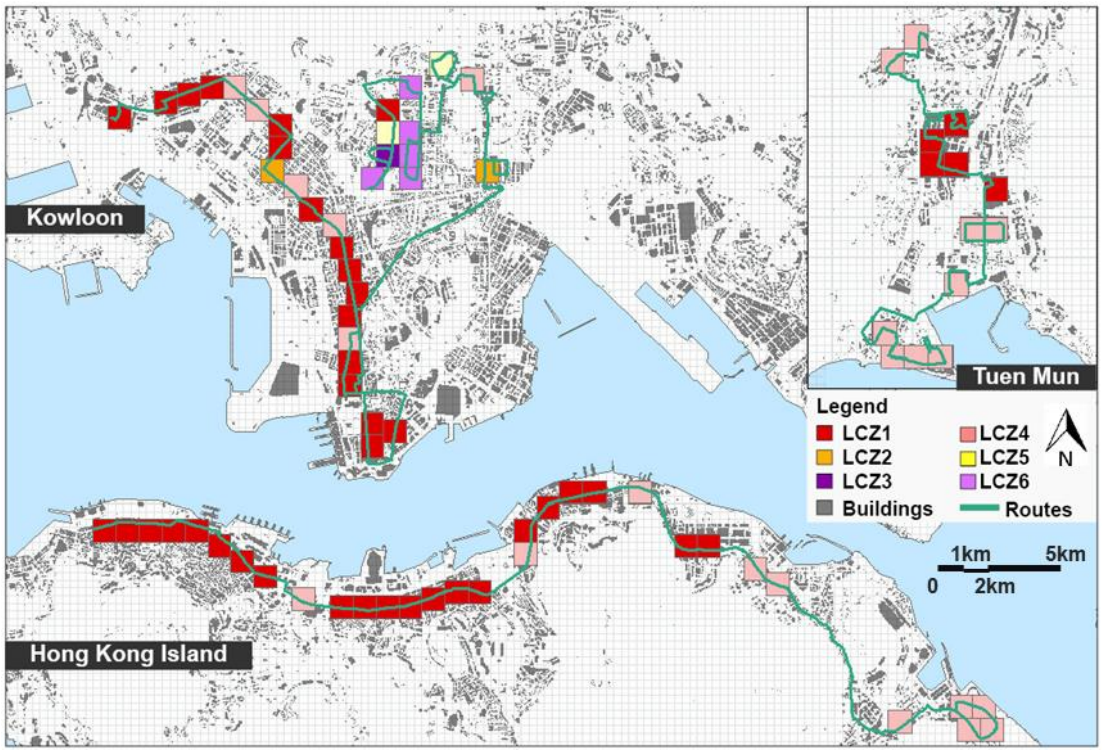

Figure 3. Sample sites selection and traverse measurement routes design

(2). Weather control and measurement time selection

Weather control and time selection is critical for UHI observation and analysis, as the spatial distribution patterns of UHI varies in different background weather conditions and the diurnal circle. Clear sky condition is ideal for UHI development, but it has low occurrence frequency below 2.5% in the summer of Hong Kong. Summertime peak UHI intensities mainly occurred in partly cloudy conditions with daily mean cloud amount of 2-7 Oktas (Zheng, Li, Fang et al., 2023). Thus, typical hot summer days with partly cloudy and weak wind conditions were selected for UHI observations.

Although the stationary observation records in Hong Kong show that UHI intensity is generally maximized in deep night or early morning, and the peak air temperature generally occurs at noon or early afternoon (Zheng, 2016), early night period of 20:00-22:00 would be more critical for UHI measurement since that: (1). Early night time when people get off work or school, urban areas would have more intense outdoor human activities than that at noon or at late night, as noontime or early afternoon when air temperature reaches peak in the whole day in summer, people generally prefer to stay indoor to avoid high temperature and strong solar radiation. (2). Daytime UHI is not that obvious as nocturnal UHI. High-density urban areas is highly possible to have cooler air temperature than

rural areas at noon and early afternoon, i.e. urban cool island effects, mainly due to the shading effects and heat absorption/storage by dense buildings (Ren, Wang, Shi et al., 2021). Significant UHI intensity at early night would lead to air temperature elevation in urban areas and cause thermal discomfort or heat-related health problems to pedestrians. Based on the above consideration, early night period of 20:00-22:00 was determined as the critical time period for mobile traverse measurement of UHI effects.

2.3. Data

(1). Traverse measurement data

A total of five mobile measurements were completed under the typical hot weather condition of Hong Kong, to monitor local atmospheric environments of selected LCZ sample sites (**Table 1**). There was no rainfall recorded in the past 24 hours before each measurement at the nearby weather stations of study areas.

Table 1. Background information of traverse measurements

Study Region	Measurement Date	Number of Typical LCZ Sample Sites						
		Sum	LCZ1	LCZ2	LCZ3	LCZ4	LCZ5	LCZ6
HKI	Jul 16, 2014 Aug 26, 2014	32	24	--	--	8	--	--
KL	Jul 30, 2014	33	17	2	1	6	2	5
TM	Aug 25, 2014 Sep 2, 2014	15	5	--	--	10	--	--

Air temperature and relative humidity were measured and recorded by TESTO 480 temperature and humidity probe and data logger (**Figure 4**). The air temperature and relative humidity probe of TESTO 480 was mounted on top of the van, 2.5m above ground. The estimated system accuracy of the air temperature is +/-0.5 K within the range from -20 K to +70 K, while the accuracy of the relative humidity is +/- 1% from 0 to 90%, and +/- 1.4 % from 90% to 100%. Data were recorded by the data logger of TESTO 480 at one-second interval while the Garmin 62s GPS system also recorded the location and driving velocity at one-second interval simultaneously. A driving

recorder was installed on the van to record the road conditions. During measurements, the van traveled at an average speed of around 20 km/h with its maximum speed controlled within 50 km/h.

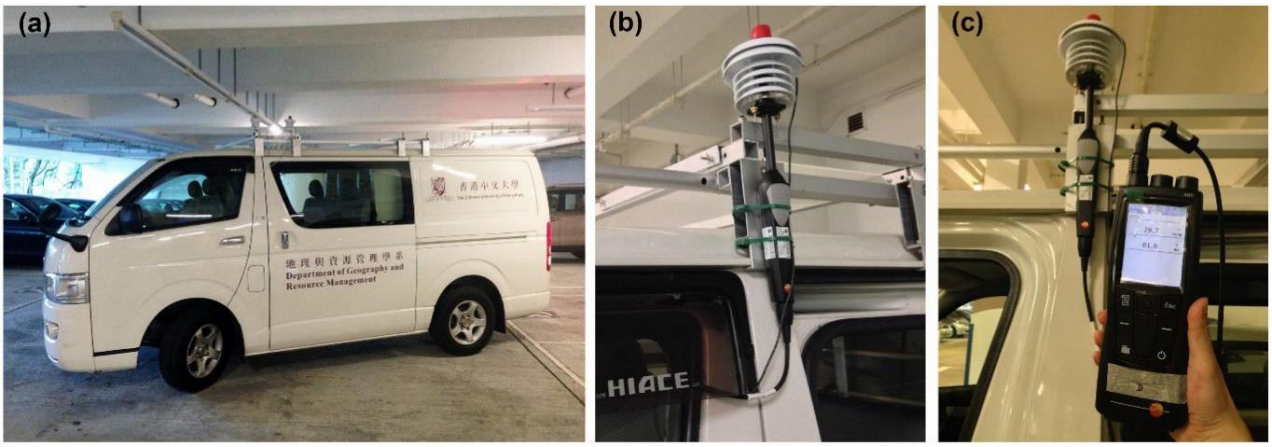

Figure 4. Measurement equipment
(a. Vehicle; b. Mounting of Testo 480 sensor; c. Testo 480 sensor and data logger)

The measured data was divided into two datasets for statistical modelling. Data in the HKI and KL areas was applied as the training dataset to quantify the correlation between UHI intensity and urban morphology parameters and develop the UHI estimation model. Data in TM was used as the validation dataset to evaluate the predictive accuracy of the UHI estimation model.

(2). Urban morphology data

Urban morphology data including buildings, streets, topography and land use in GIS format, as well as four remote sensing images of Landsat 8 (October 5, 2013, December 31, 2013, August 8, 2015, and October 18, 2015) were employed to quantify urban morphology parameters of LCZ sample sites following the GIS-based LCZ classification method (Zheng et al., 2017) (**Figure 5**). The urban morphology parameters of LCZ include building height (BH), building surface fraction (BSF, i.e. building coverage ratio), building volume density (BVD), sky view factor (SVF), aspect ratio (H/W), pervious surface fraction (PSF), impervious surface fraction (ISF), street coverage ratio (SCR), street width (SW), and elevation (DEM).

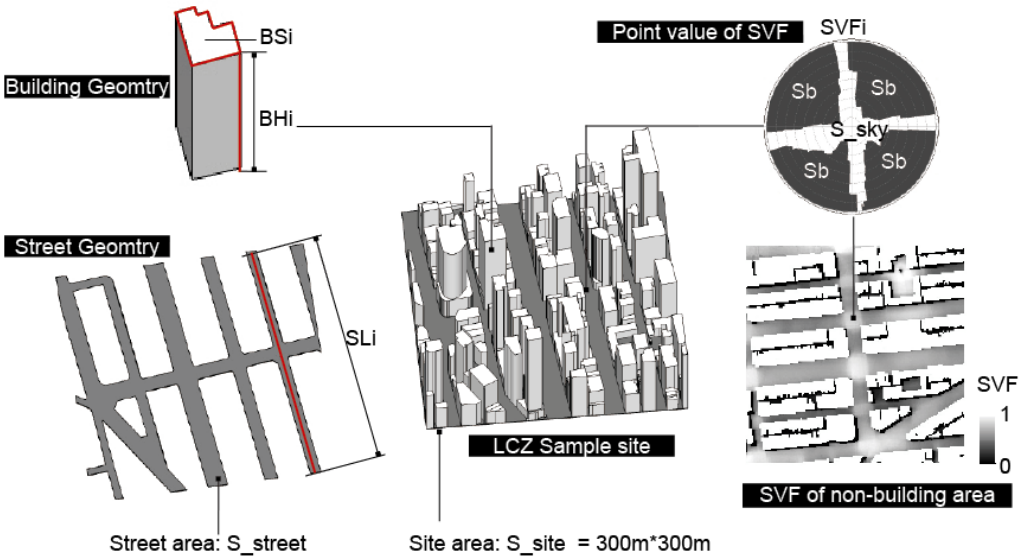

Figure 5. Urban morphology parameters calculation (Zheng et al., 2017)

Table 2. Definition and calculation methods of urban morphology parameters

Parameters	Definition	Basic Data	Calculation methods	Description
BH	Area weighted mean building height of sample sites	Building data	$BH = \frac{\sum_{i=1}^{n} BSi * BHi}{\sum_{i=1}^{n} BSi}$	n is the number of buildings of the LCZ sample site. BSi is the ground area of a building. BHi is the height of a building. $\sum_{i=1}^{n} BSi$ is the total building cover area of the site. $\sum_{i=1}^{n} BSi * BHi$ is the total building volume of the site.
BSF	Building surface fraction of sample sites	Building data	$BSF = \frac{\sum_{i=1}^{n} BSi}{S\_site}$	n is the number of buildings of the LCZ sample site. S_site is the total area of the site.
SVF	Areal mean SVF of non-building areas in sample sites (Chen, Ng, An et al., 2010)	Building and topography data	$SVF = \frac{\sum_{i=1}^{n} SVFi}{n}$ $SVFi = \frac{S\_Sky}{(S\_Sky + \sum Sb)}$	SVFi is the SVF value of a certain point in non-building area (point area 1m*1m) in the LCZ sample site. n is the number of SVF points (1m*1m) in non-building area of the site. S_Sky and $\sum Sb$ represent the area of sky and the area occupied by buildings in a certain point respectively. $S_{Sky} + \sum Sb$ represents the entire hemispheric environment in a certain point.
H/W	Areal mean aspect ratio of sample sites	Building and street data	$H/W = \frac{BH}{SW}$	The ratio of mean building height to mean

				street width in the LCZ sample site.
BVD	Building volume density of sample sites (Ng, Yau, Wong et al., 2012)	Building data	$\mathrm{BVD} = \frac{\sum_{i=1}^{n} BSi * BHi}{S\_site}$	n is the number of buildings of the LCZ sample site. BSi is the ground area of a building. BHi is the height of a building. $\sum_{i=1}^{n} BSi$ is the total building cover area of the site. $\sum_{i=1}^{n} BSi * BHi$ is the total building volume of the site.
PSF	Pervious surface fraction of sample sites	Remote sensing data	$\mathrm{PSF} = \frac{\sum S\_per}{S\_site}$ $\sum S\_per$ is the total area of pervious surface, with NDVI above 0.2 (Weier & Herring, 2000)	$\sum S\_per$ is the total area of pervious surface, with NDVI above 0.2
ISF	Impervious surface fraction of sample sites	Building and remote sensing data	$\mathrm{ISF} = 1 - \mathrm{BSF} - \mathrm{PSF}$	Impervious surface fraction is defined as the fraction of surface not covered by pervious surface or buildings.
SCR	Street coverage ratio of sample sites	Street data	$\mathrm{SCR} = \frac{\sum S\_street}{S\_site}$	$\sum S\_street$ is the total area of streets in the site. S_site is the area of sample sites.
SL	Total street length of sample sites	Street data	$\mathrm{SW} = \sum_{i=1}^{n} SLi$	n is the number of streets in the LCZ sample site. $\sum_{i=1}^{n} SLi$ is the total length of streets in the site.
SW	Mean street width of sample sites	Street data	$\mathrm{SW} = \frac{\sum S\_street}{\sum_{i=1}^{n} SLi}$	n is the number of streets in the LCZ sample site. $\sum_{i=1}^{n} SLi$ is the total length of streets in the site. $\sum S\_street$ is the total area of streets in the site.
Elevation	Mean elevation of sample sites	Topography data	--	--

(3). Stationary observation data

Meteorological data are collected from the Hong Kong Observatory for calculating UHI magnitude of LCZ sample sites and conducting temporal adjustments for measured air temperature. Determination of rural reference for UHI study is difficult for Hong Kong because local climate vary across different rural areas owing to the mountainous and coastal geographical conditions. Stations located near the coast such as Cheung Chau station and Waglan Island stations have been excluded

from consideration, as the recorded daily temperature profiles could be significantly influenced by the seawater temperature (Sakakibara & Owa, 2005). Ta Kwu Ling (TKL) and Lau Fu Shan (LFS) stations have been commonly recognized as rural stations of Hong Kong (Fung, 2010; Memon, Leung, & Liu, 2009; Siu & Hart, 2013). TKL station is in the northeastern rural area with a small population and lush vegetation (Figure 6). LFS station is controversial due to its surrounding low-rise neighborhoods and proximity to high-rise residential developments in Tin Shui Wai, and some studies have classified LFS as a rural station (Leung, 2004; Leung & Ng, 1997), while recent studies have recognized it as an urban or suburban station as LFS station shows similar diurnal temperature profiles with the urban stations located in new towns of Hong Kong (Memon et al., 2009; Wu, Leung, Lui et al., 2009). Based on the above consideration, TKL station is determined as the rural reference in this study. UHI intensity of LCZ sample sites (UHII) was calculated as the mean air temperature difference between LCZ sample sites and TKL station during traverse measurements according to the definition of UHI (Kotharkar & Bagade, 2018; Stewart & Oke, 2012):

$$\text{UHII} = \Delta T_{U-R} = T_{LCZ\ Sites} - T_{TKL} \quad (1)$$

Figure 6. Panoramic view of rural reference station: TKL station

2.4. Post-processing of traverse measurement data

(1). Exclusion of contaminated data

Air temperature data measured when the mobile traverse vehicle with low driving speed is possible to be affected by heat release from nearby vehicles and insufficient ventilation of sensor. Previous study by Buttstädt and Schneider (2014) has excluded data collected at a driving speed lower than 18 km/h in order to ensure sufficient sensor ventilation. François Leconte, Bouyer, Claverie et al. (2016) have pointed out that low-driving-speed (below 15 km/h) data may have thermal

perturbations from other vehicles stopped nearby. Therefore, this study has not considered the data with driving speed lower than 15 km/h.

(2). Temporal adjustment and altitude correction of measured air temperature

As local climate conditions change with time during traverse measurements, temporal adjustment of measured data is necessary for synchronous analysis. Due to the geographical diversity and spatial heterogeneity of urban morphology in Hong Kong, this study has selected reference stations operated by Hong Kong Observatory for three traverse measurement regions separately. Hong Kong Park (HKP) and Shaw Kai Wan (SKW) stations in Hong Kong Island have been determined as reference stations for HKI region. Hong Kong Observatory headquarter station (HKOH), Kings Park (KP), Kowloon Town (KLT), and Sham Shui Po (SSP) stations in Kowloon have been determined as the reference stations for KL region, and TU1 station has been determined as a reference station for TM region (Mok, Wu, & Cheng, 2011).

Mean cooling rates during measurement time (8 pm - 10 pm) have been calculated based on hourly air temperature data of reference stations in each day. 9 pm is the reference time for the linear temporal adjustment. Measured data has been adjusted proportionally to the time difference between 9 pm and the measurement time. **Table 3** shows the mean cooling rates of reference stations between 20:00 and 22:00 in five measurement days. The mean cooling rates of reference stations were all below 0.25 K/h, and the overall temperature changes during two-hour measurements ranged from 0.15 K to 0.5 K.

Due to the elevation difference between LCZ sample sites and the reference rural station, the measured air temperature was corrected to the same elevation of TKL station (15m above mean sea level) to calculate the UHI intensity. Air temperature of each measured point has been corrected to the same elevation of TKL station (15m), to calculate the UHI intensity. The temperature lapse rate for UHI calculation was 0.01 K/m, as suggested by previous study in Hong Kong (Giridharan, 2005).

Table 3. Cooling rates of reference stations during the traverse measurements (8 pm - 10 pm)

Date	Mean Cooling Rate of Reference Stations (K/h)			
	HKI	KL	TM	Mean

	HKP	SKW	HKOH	KP	KLT	SSP	TU1	
Jul 16	0.15	0	*n/a*	*n/a*	*n/a*	*n/a*	*n/a*	0.075
Jul 30	*n/a*	*n/a*	0.15	0.1	0.2	0.25	n/a	0.175
Aug 25	*n/a*	*n/a*	*n/a*	*n/a*	*n/a*	*n/a*	0.25	0.25
Aug 26	0.15	0.3	*n/a*	*n/a*	*n/a*	*n/a*	*n/a*	0.225
Sep 2	*n/a*	*n/a*	*n/a*	*n/a*	*n/a*	*n/a*	0.2	0.2

(3). Collation of measured data into GIS

GPS information, which records the corresponding geographical location of each measurement data, was firstly imported into the GIS system in vector points. Secondly, the measured data (after temporal adjustment and exclusion of low-speed data) was related to each GPS point according to the measurement time. The measured data points were converted into high-resolution raster layer (in 1m resolution) in GIS. Then, the raster layer was processed through zonal statistics in GIS to calculate the mean air temperature of each LCZ site. Thirdly, mean air temperature of each LCZ site was subtracted by the mean air temperature of TKL station during 8 pm - 10 pm to get the UHI intensity of sample sites.

2.5. Bivariate and multivariate analysis

Bivariate analysis methods of Pearson Correlation and Partial Correlation were used to access the discrete association between every urban morphology parameter and UHI intensity. Pearson Correlation measures the linear correlation between two variables, which is an important approach to address the collinearity issue between the independent variables. However, multicollinearity is a common feature of urban morphology dataset, which can lead to inflation of the variance of predictive variables and cause biased inference statistics in multivariate analysis(Yu, Chen, & Wong, 2020). Therefore, Partial Correlation was compared with Pearson Correlation to examine the relationship between every two variables, with the effects of other variables removed (Chu, Venevsky, Wu et al., 2019; Shipley, 2016). It is essential for enhancing the reliability of statistical model when multicollinearity exists among the independent variables.

Multivariate analysis methods of stepwise Multiple Linear Regression (stepwise MLR) and Partial Least Squares (PLS) were conducted to identify the predictive variables of UHI intensity and establish the UHI estimation model at local scale. Bootstrap resampling method was employed to evaluate confidence intervals of UHI intensity (Houet & Pigeon, 2011). To identify the best fitting model, different combinations of urban morphology parameters were compared based on the Akaike Information Criterion (AIC)(Guo, Yang, Xiao et al., 2020; Yin, Yuan, Lu et al., 2018). According to the model selection rule of AIC, the combination of independent variables with minimum AIC value is preferred to establish the urban morphology based UHI estimation model. Based on the model, a UHI estimation map was formulated in GIS.

The workflow of this study is summarized as follows (**Figure 7**).

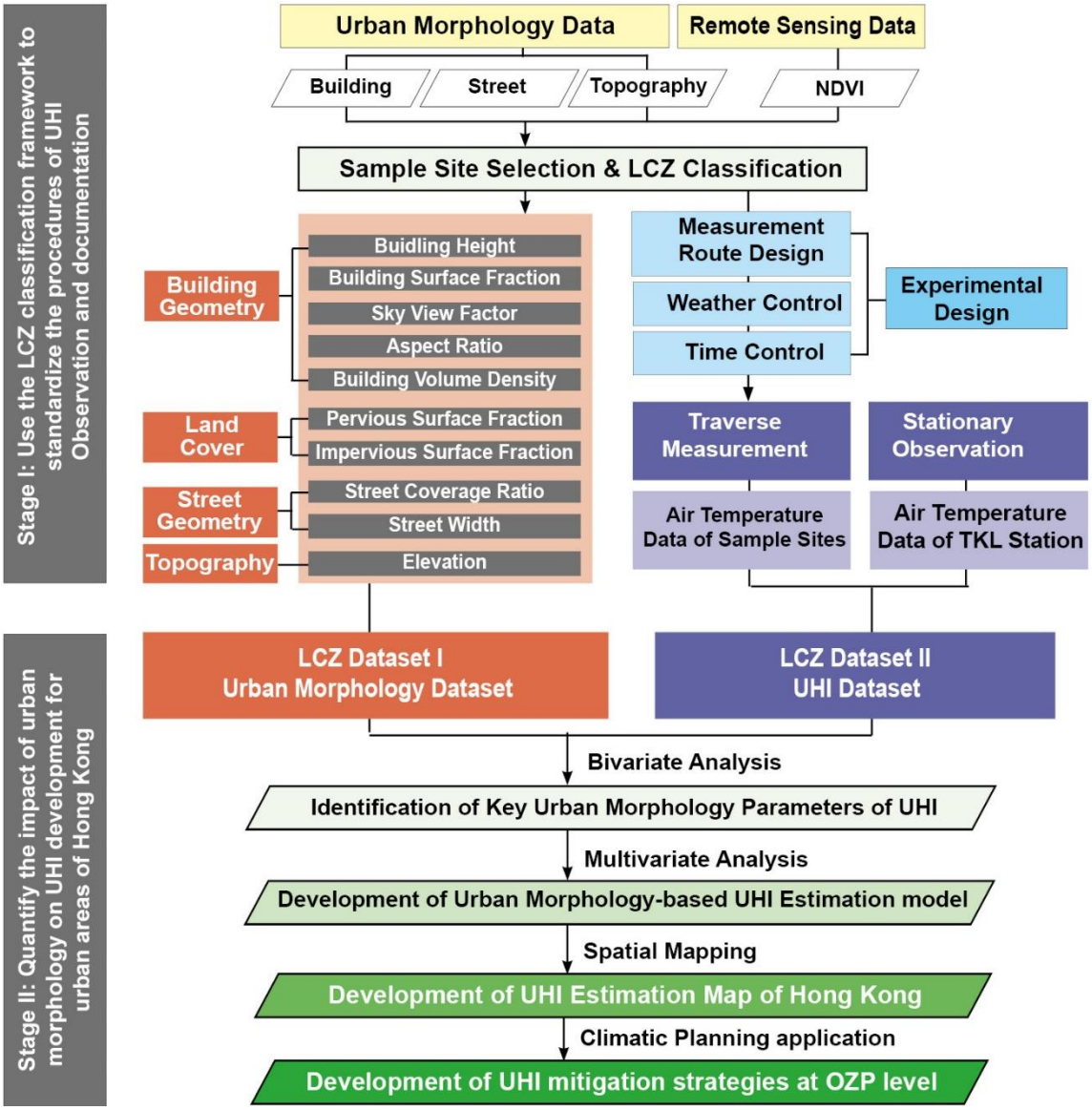

Figure 7. Workflow of this study

3. Results

3.1. UHI intensity and urban morphology statistics of LCZ sample sites

Figure 8 presents the mean UHI intensity of LCZ sample sites based on traverse measurement results. On average, a 3 K variation of UHI intensity has been observed, with maximum and minimum UHI intensity of around 4.2 K and 1.0 K, respectively. Wan Chai, Causeway Bay, North Point in HKI, as well as Jorden and Tin Hau Temple in KL were hot spot areas which have observed UHI intensity higher than 3.5 K. Sai Ying Pun, Sheung Wan, Admiralty and Fortress Hill in HKI, as well as Prince Edward and Yau Ma Tei in KL have observed UHI intensity of 3.0 - 3.5 K. All the above hot spot sites are LCZ1 (compact high-rise), except Tin Hau Temple is LCZ4 (open high-rise). The

sample sites in TM, mainly classified as LCZ4, experienced comparatively lower UHI intensity under 2.5 K.

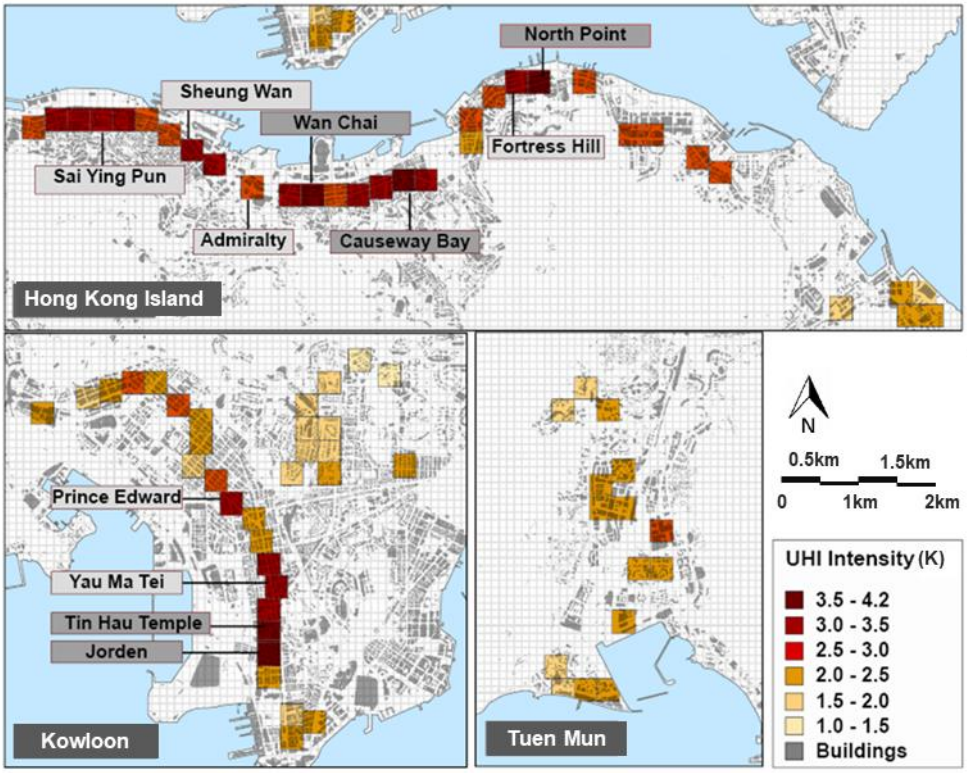

Figure 8. Mean UHI intensity of LCZ sample sites based on traverse measurements (Sample Size: 80)

UHI intensities and urban morphology parameters of LCZ sample sites in the six LCZ classes were shown in **Figure 9** and **Figure 10**. LCZ1 experienced the highest mean UHI level above 2.5 K among the six classes, and it showed wide range of 1.58 K – 4.49 K. LCZ2 and LCZ4 also observed considerable UHI intensity, with the mean values above 2.0 K. The mean value of LCZ4 was slightly higher than that of LCZ2, but it had wider range spanning from 1.08 K to 3.62 K. The high UHI intensities observed in some LCZ sample sites are possibly due to the influence of surrounding high-density urban environments. The open mid-rise class of LCZ5 and low-rise classes (LCZ3 and LCZ6) have recorded averaged UHI intensity below 2.0 K. LCZ5 had the lowest mean UHI level of 1.15 K. LCZ6 documented a slightly elevated UHI intensity compared to LCZ3 and LCZ5, which may be influenced by the heat release from the freeway near the sites.

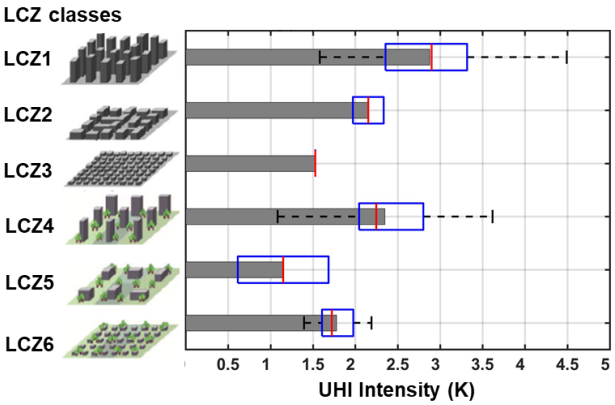

LCZ Type	UHI Intensity (K)					
	Mean	Median	Max	Min	Std Dev	Sample Size
LCZ1	2.88	2.90	4.49	1.58	0.62	46
LCZ2	2.15	2.15	2.33	1.97	0.26	2
LCZ3	1.53	1.53	1.53	1.53	-	1
LCZ4	2.36	2.25	3.62	1.08	0.53	24
LCZ5	1.15	1.15	1.68	0.61	0.75	2
LCZ6	1.78	1.72	2.19	1.39	0.29	5

Figure 9. UHI intensity of LCZ classes based on traverse measurement results (Sample Size: 80)

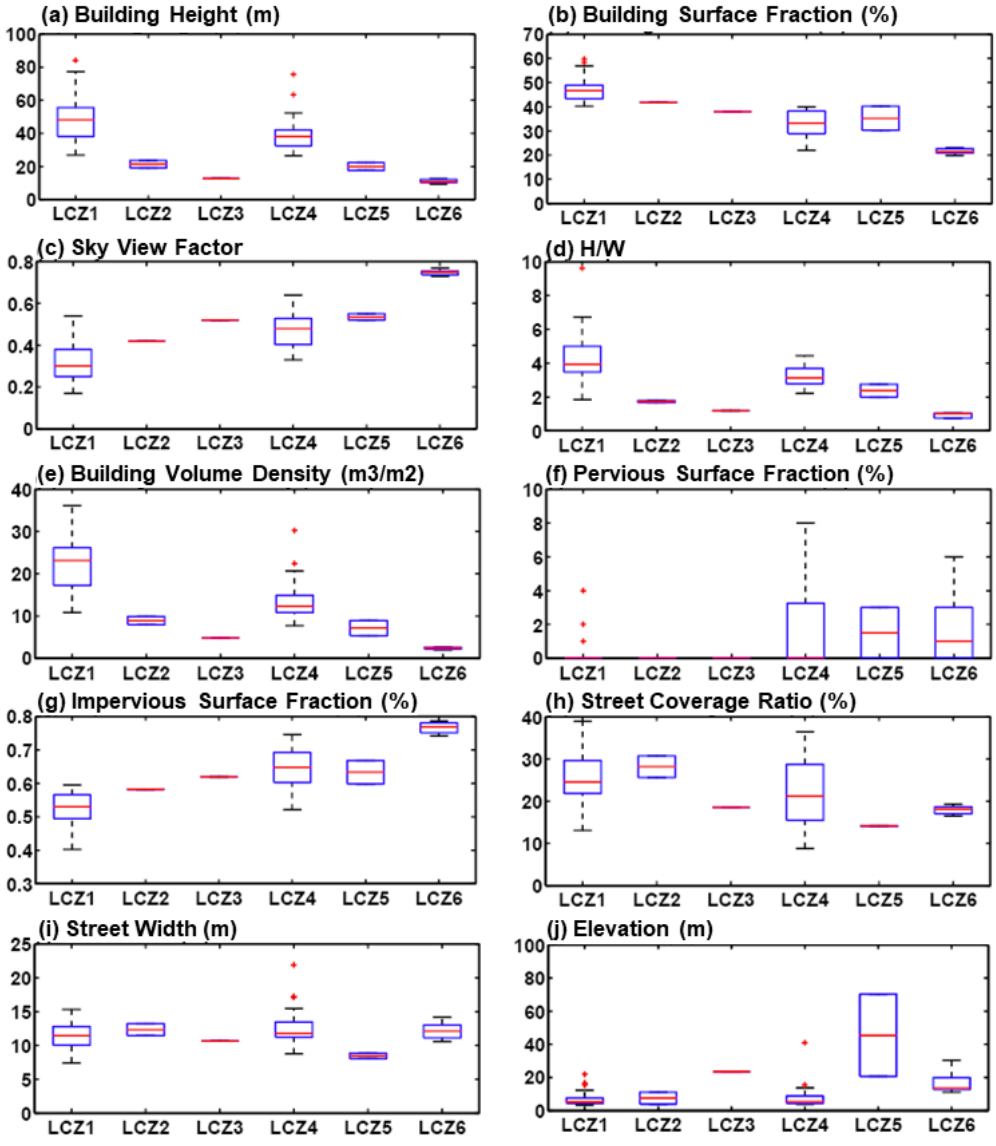

Figure 10. Boxplot of urban morphology parameters in LCZ sample sites (Sample Size: 80)

3.2. LCZ-based UHI estimation models by stepwise MLR and PLSR

(1). Bivariate analysis

The measurement data was divided into two datasets for statistical modelling. Data in the HKI and KL areas were used as the training dataset, as HKI and KL are early built high-density urban areas in Hong Kong. The training dataset was applied for quantifying the correlation between urban morphology parameters and UHI intensity, and develop the urban morphology-based UHI estimation model. TM measurement route is comparatively shorter with LCZ types consisting of LCZ4, so the data in TM was applied as the validation dataset for evaluating the predictive performance of the UHI estimation model.

First, bivariate correlation analysis methods (Pearson Correlation and Partial Correlation methods) were employed to analyze the discrete relationship between UHI intensity and each urban morphology parameter (**Table 4** and **Table 5**). Urban morphology parameters were classified into three categories: (1) building morphology parameters, including BH, BSF, SVF, H/W, and BVD; (2) land cover parameters: PSF and ISF; (3) traffic-related parameters: SCR, SL, and SW. The Pearson Correlation coefficients between UHI intensity and urban morphology parameters with the absolute value above 0.5 are as follows: (1) SVF (R = -0.67); (2) H/W (R = 0.51); (3) BVD (R = 0.52); (4) PSF (R = -0.62); (5) SCR (R = 0.59); and (9) SL (R = 0.66) (**Table 4**). Moreover, results show that collinearity exists between urban morphology parameters. For example, 3-d building geometry parameters of SVF, H/W, BVD are correlated to BH with R values of -0.56, 0.82 and 0.93, respectively, while SVF, H/W, BVD, and PSF are correlated to BSF with R values of -0.75, 0.55, 0.75, and -0.81, respectively.

In partial correlation analysis (**Table 5**), most of partial correlation coefficients between UHI intensity and multiple morphology parameters decrease to varying degrees compared to the results of Pearson Correlation analysis, with the influence of other urban morphology parameters removed. According to the analysis of Pearson correlation and partial correlation, SVF, PSF, and SL were identified as the most important indicators of UHI intensity in the building geometry, land cover, and street geometry categories respectively. SVF, PSF and SL were therefore applied as input variables for MLR and PLSR analysis.

Table 4. Pearson correlations between UHI intensity and multiple urban parameters based on training dataset (Training sample size: 65)

	Building Geometry					Land Cover		Street Geometry/ Traffic		
	BH (m)	**BSF (%)**	**SVF**	**H/W**	**BVD (m^3/m^2)**	**PSF (%)**	**ISF (%)**	**SCR (%)**	**SL (m)**	**SW (m)**
UHII (K)	0.49	0.43	-0.67	0.51	0.52	-0.62	0.47	0.59	0.66	-0.05
BH (m)	1.00	0.48	-0.56	0.82	0.93	-0.41	0.03	0.30	0.28	0.24
BSF (%)	0.48	1.00	-0.75	0.55	0.75	-0.81	-0.01	0.37	0.48	-0.17
SVF	-0.56	-0.75	1.00	-0.64	-0.71	0.79	-0.29	-0.59	-0.68	0.16
H/W	0.82	0.55	-0.64	1.00	0.84	-0.43	-0.04	0.12	0.37	-0.31
BVD (m^3/m^2)	0.93	0.75	-0.71	0.84	1.00	-0.62	0.01	0.37	0.41	0.09
PSF (%)	-0.41	-0.81	0.79	-0.43	-0.62	1.00	-0.57	-0.62	-0.64	0.04
ISF (%)	0.03	-0.01	-0.29	-0.04	0.01	-0.57	1.00	0.54	0.41	0.16
SCR (%)	0.30	0.37	-0.59	0.12	0.37	-0.62	0.54	1.00	0.80	0.31
SL (m)	0.28	0.48	-0.68	0.37	0.41	-0.64	0.41	0.80	1.00	-0.16
SW (m)	0.24	-0.17	0.16	-0.31	0.09	0.04	0.16	0.31	-0.16	1.00

Table 5. Partial correlations between UHI intensity and multiple urban parameters based on training dataset (Training sample size: 65)

	Building Geometry					Land Cover		Street Geometry/ Traffic		
	BH (m)	**BSF (%)**	**SVF**	**H/W**	**BVD (m^3/m^2)**	**PSF (%)**	**ISF (%)**	**SCR (%)**	**SL (m)**	**SW (m)**
UHII (K)	0.24	-0.16	-0.33	-0.16	-0.06	-0.14	0.04	-0.19	0.34	-0.20
BH (m)		-0.13	0.08	0.59	0.60	0.13	0.07	0.17	-0.24	0.55
BSF (%)	-0.13		-0.37	-0.29	0.46	-0.82	-0.75	-0.17	0.08	-0.31
SVF	0.08	-0.37		-0.24	0.01	-0.20	-0.22	-0.43	0.22	0.00
H/W	0.59	-0.29	-0.24		0.24	-0.16	-0.08	-0.31	0.25	-0.80
BVD (m^3/m^2)	0.60	0.46	0.01	0.24		-0.01	-0.04	0.00	0.10	0.18
PSF (%)	0.13	-0.82	-0.20	-0.16	-0.01		-0.89	-0.16	0.09	-0.22

ISF (%)	0.07	-0.75	-0.22	-0.08	-0.04	-0.89		-0.02	0.02	-0.13
SCR (%)	0.17	-0.17	-0.43	-0.31	0.00	-0.16	-0.02		0.82	0.16
SL (m)	-0.24	0.08	0.22	0.25	0.10	0.09	0.02	0.82		-0.14
SW (m)	0.55	-0.31	0.00	-0.80	0.18	-0.22	-0.13	0.16	-0.14	

Partialed with respect to all the other variables.

(2). Multivariate analysis

Forward stepwise MLR and PLSR were applied to establish urban morphology-based UHI estimation models. To prevent over-fitting caused by multicollinearity of explanatory variables, predictors were selected following the procedures suggested by Oukawa, Krecl, and Targino (2022) that variables with the highest correlation with UHI intensity in the three categories (building geometry, land cover, and street geometry/traffic) were identified and selected as the input variables in stepwise MLR and PLSR analysis. Based on the results of the bivariate analysis in the above section, SVF, PSF, and SL were selected as representative parameters of building geometry, land cover, and street geometry/traffic categories respectively, as input variables of multivariate analysis. In stepwise MLR analysis, forward selection started with no independent variable, and tested the influence of each newly added variables on the model. The testing process was based on stopping rule of Akaike Information Criterion (AIC). It kept variables that contributed most to the fitting performance of the model, and repeated testing until no newly-added variable further improved the model.

Table 6 shows the results of forward stepwise MLR analysis. In the forward step analysis, SVF was the first entered variable which was evaluated as the most decisive predictor of UHI intensity, as it can explain around 44% of the UHI variation independently, with the AIC value of 114.6. SL was the second entered variable, through which the predictive performance increased to 0.54 and the AIC value decreased to 104.4. When PSF was entered in the stepwise MLR model, the predictive performance remained the same, while the AIC value had slight increase to 106.7. Thus, a combination of SVF and SL were determined as the predictors of the finalized UHI estimation model

by stepwise MLR (R^2 = 0.54, RMSE = 0.52, AIC = 104.4). **Table 7** presents the best fitting model developed by stepwise MLR, which indicates that every 0.1 decreases in SVF, or 1km increase in the total street length (SL) of LCZ sites is associated with a rise of UHI intensity by 0.23 K, and 0.48 K, respectively.

Table 6. Model-fitting results of UHI intensity and urban geometric parameters based on training dataset (Training sample size: 65)

Forward Step-wise MLR					
Step	Parameter	Action	R^2	10-fold Cross Validation R^2	AIC
1	SVF	Entered	0.44	0.40	114.6
2	SL	Entered	0.54	0.51	104.4
3	PSF	Entered	0.54	0.49	106.7
4	*Best Model*	*Specific*	*0.54*	*0.51*	*104.4*

Table 7 Planning-based statistical model of UHI intensity using Stepwise MLR (Training sample size: 65)

Summary of Fit						
R^2	Adjusted R^2	RMSE	Mean of Response	P value	Observations	10-fold Cross Validation R^2
0.54	0.53	0.52	2.64	<0.0001 *	65	0.51

Parameter Estimates					
Independent Variable	Estimate	Std Error	Prob>|t|	VIF	Estimate (Z-value)
Intercept	2.53	0.46	<.0001*	n/a	n/a
SVF	-2.23	0.60	0.0006*	1.68	-0.43
SL	4.8×10^{-4}	1.3×10^{-4}	0.0004*	1.68	0.41
Stepwise MLR Model	UHII= 2.53 – 2.23×SVF + 4.8×10^{-4}×SL				

The PLSR with variables' importance of projection (VIP) approach (Li, Vilela, Tariq et al., 2022) was implemented to develop the UHI estimation model based on the NIPALS algorithm. SVF, PSF, and SL were applied as input variables for PLSR analysis. As **Table 8** shows, the minimum number of latent factors is one, and all the three input variables of SVF, PSF, and SL have the VIP value above 0.8. The latent factor developed by PLSR analysis can explain 80.39% variation of independent variables (SVF, SL and PSF) and 52.56% of dependent variable (UHI intensity). Bootstrap method was employed to evaluate confidence intervals of parameter estimates of UHI

estimation model through 5000 bootstrapping replications (Gu & You, 2022). The results show that the original PLSR model has higher predictive performance (R^2 = 0.53) than bootstrap-based models (R^2 = 0.28).

Method	Number of Factors	Percent Variation Explained for Cumulative X	Percent Variation Explained for Cumulative Y	Number of VIP > 0.8
NIPALS	1	80.39 %	52.56 %	3
Parameter Estimates				
		Bootstrap Method (5000 bootstrap samples)		
	Original	Mean	Median	95% Confidence Interval Upper	95% Confidence Interval Lower
Intercept	2.71	2.71	2.71	3.02	2.48
SVF	-1.50	-1.52	-1.50	-1.19	-1.93
SL	0.0003	0.0003	0.0003	0.0004	0.0003
PSF	-1.72	-1.75	-1.73	-1.30	-2.31
R2/Adjusted R2	0.53/0.52	0.28/0.27	0.28/0.26	-	-
PLSR Model	UHII = 2.71 - 1.50×SVF + 3.0×10-4×SL - 1.72×PSF				

Table 9 compared UHI estimation models developed by MLR and PLSR. It shows that the two methods have similar performance in predicting UHI intensity, and stepwise MLR has a slightly higher adjusted R^2 (0.53) than PLSR (adjusted R^2=0.52). The model by PLSR gives a more comprehensive consideration of the influence of building geometry (SVF), vegetated land cover (PSF) and street geometry/traffic conditions(SL) on UHI development, while stepwise MLR only takes SVF and SL into account through automatic variable selection procedures. Hence, the finalized model is determined as the PLSR model. It the PLSR model, for every 0.1 decrease in SVF, 10% decrease in PSF, or 1km increase in the total street length of LCZ sites, UHI intensity is associated with a rise of 0.15 K, 0.17 K, and 0.30 K, respectively.

Table 8. PLSR model summary in predicting UHI intensity at LCZ scale

Method	Number of Factors	Percent Variation Explained for Cumulative X	Percent Variation Explained for Cumulative Y	Number of VIP > 0.8
NIPALS	1	80.39 %	52.56 %	3
Parameter Estimates				
		Bootstrap Method (5000 bootstrap samples)		
	Original	Mean	Median	95% Confidence Interval Upper	95% Confidence Interval Lower
Intercept	2.71	2.71	2.71	3.02	2.48
SVF	-1.50	-1.52	-1.50	-1.19	-1.93

SL	0.0003	0.0003	0.0003	0.0004	0.0003
PSF	-1.72	-1.75	-1.73	-1.30	-2.31
R^2/Adjusted R^2	0.53/0.52	0.28/0.27	0.28/0.26	-	-
PLSR Model	UHII = 2.71 - 1.50×SVF + 3.0×10-4×SL - 1.72×PSF				

Table 9. Comparison of UHI estimation models by Stepwise MLR and PLSR

Summary of Fit						
	R^2	Adjusted R^2	RMSE	Mean of Response	P value	Observations
Stepwise MLR	0.54	0.53	0.52	2.64	<0.0001*	65
PLSR	0.53	0.52	0.52	2.64	<0.0001*	65
UHI Estimation Models by Stepwise MLR and PLSR						
	Intercept	SVF	SL	PSF	UHI Estimation Model	
Stepwise MLR	2.52	-2.23	4.8×10^{-4}	n/a	$UHII= 2.53 – 2.23\times SVF + 4.8\times10^{-4}\times SL$	
PLSR	2.71	-1.50	3.0×10^{-4}	-1.72	$UHII = 2.71 - 1.50\times SVF + 3.0\times10^{-4}\times SL - 1.72\times PSF$	
Finalized Model (PLSR)	UHII = 2.71 - 1.50×SVF + 3.0×10-4×SL - 1.72×PSF					

(3). Model validation

Traverse measurement data in TM was used to validate the UHI estimation model by PLSR. **Figure 11** illustrates the comparison of the observed data and the predicted data. Although there is variation between the measured and the predicted values, the overall pattern is predicted by the PLSR method. The statistical model explains 56% of UHI intensity diversity in TM, and the root mean square error is 0.19 K. The measured UHI intensity ranges from 1.6 K to slightly above 2.7 K, while the predicted value ranges from 1.4 K to 2.6 K.

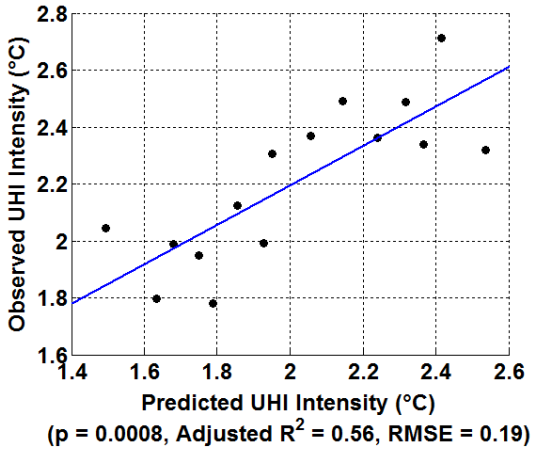

Figure 11. Validation of PLSR model based on traverse measurement data in Tuen Mun region (Validation sample size: 15)

3.3. UHI estimation map of urban areas in Hong Kong

According to the urban morphology-based UHI estimation model, an UHI estimation map for Outline Zoning Plan (OZP) (Ren, Ng, & Katzschner, 2011; Ren, Yang, Cheng et al., 2018) areas of Hong Kong has been developed (**Figure 12**). The raster grid of the map is 300m, which is consistent with the scale of LCZ unit. The UHI intensity of each raster grid was calculated using the urban morphology analysis maps of SVF, SL and PSF. As the UHI estimation map shows, hot spot areas with UHI intensity above 3 K are mainly distributed in KL and HKI areas. LCZ1 is the dominant LCZ type of hot spot areas according to the LCZ classification map (**Figure 2**). Large areas in Kowloon and northern HKI experience high-level UHI intensity ranging from 2.5 K to 3 K. Some areas in Tsuen Wan and Kwun Tong also have UHI intensity above 2.5 K. Open high-rise residential areas (LCZ4), which are mainly distributed in northern HKI, Kwun Tong, Sha Tin, Yuen Long, and TM, generally experience UHI intensity from 1.5 K to 2.5 K. The low-rise LCZ classes of LCZ5 and LCZ6, highly concentrated in the Sai Kung district and the northern part of Hong Kong, have UHI intensity of 0.5 K – 1.5 K.

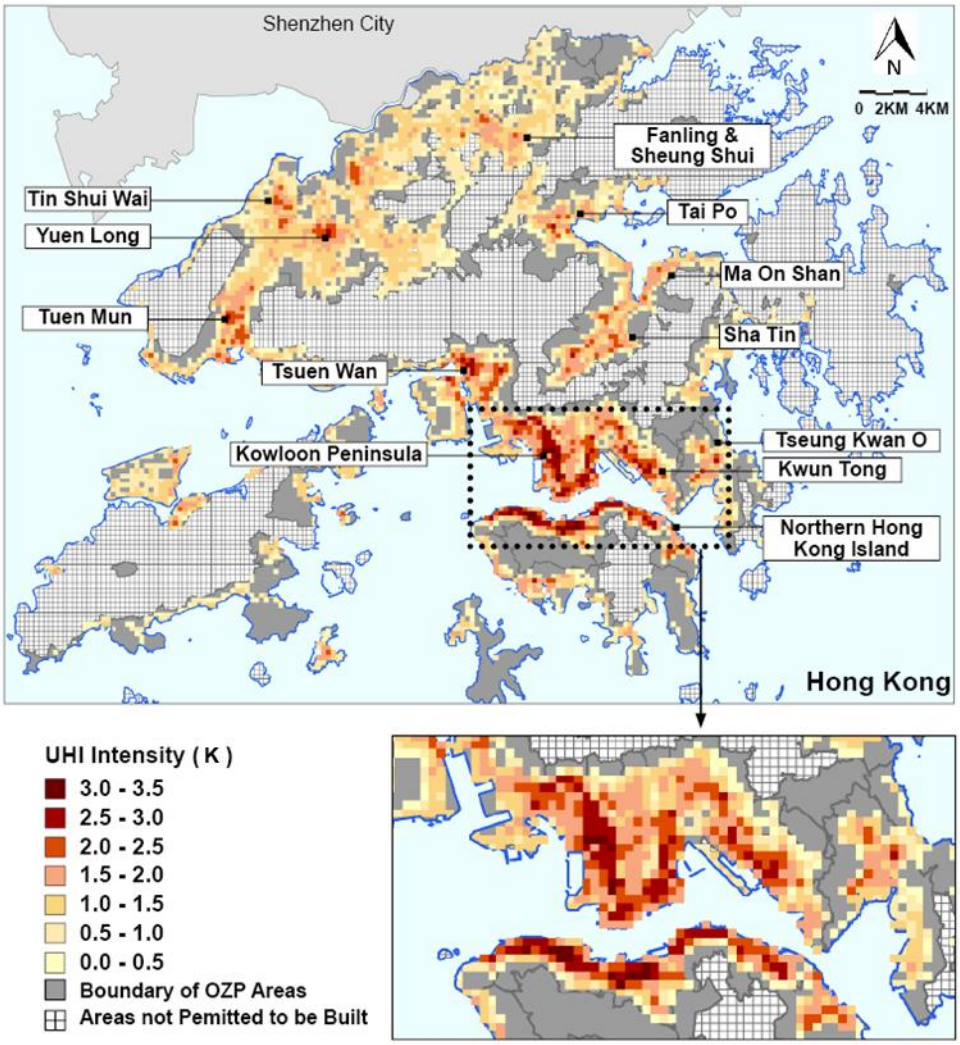

Figure 12. UHI Intensity Estimation Map for urban areas (covered by LCZ1-LCZ6) of Hong Kong

3.4. Identification of critical Outline Zoning Plan areas for UHI mitigation

Outline Zoning Plan (OZP) is the key statutory plan of Hong Kong at district level, which integrates various planning considerations in the provision of development, covering urban development purposes, environmental planning, natural landscape/habitat conservation, and cultural heritage/townscape conservation. Thus, the maximum UHI intensity (MUHII) of OZP was evaluated based on the UHI estimation map to identify critical planning zones for UHI mitigation (**Figure 13, Table 10**). 8% of OZP areas suffer MUHII above 3°C, which are distributed in KL Peninsula and the northern part of Hong Kong Island. LCZ sites with UHI intensity of 2.5°C - 3°C have been found in OZP areas along the northern coastline of Hong Kong Island, the western and eastern part of Kowloon, as well as New Towns such as Yuen Long, Tun Mun, Tsuen Wan, Sha Tin, Kwun Tong, and Tseung Kwan O. The OZP areas with MUHII above 2.5°C are generally covered by high-rise

LCZs. 34% OZP areas have MUHII from 1.5°C to 2.5°C, mainly located in marginal areas. OZP areas with MUHII under 1°C are dominated by mid-rise LCZs or low-rise LCZs.

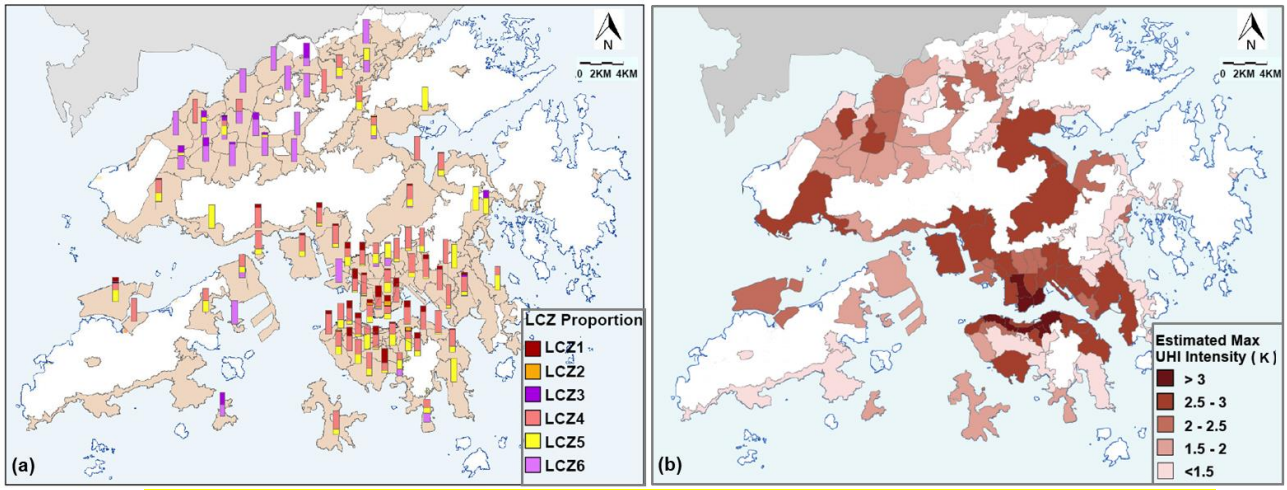

Figure 13. LCZ proportion and estimated maximum UHI intensity of OZP areas in Hong Kong ((a). LCZ proportion map (b). Estimated Maximum UHI intensity map)

Table 10. Frequency distribution of maximum UHI intensity in OZP areas

Maximum UHI Intensity (K)	>3	2.5 - 3	2 - 2.5	1.5 - 2	<1.5
Percentage of OZP areas	8%	24%	17%	17%	34%

4. Discussion

4.1. Applying LCZ framework in UHI observations and interdisciplinary communication

Spatial understanding of local climatic conditions is essential to the mitigation and adaptation of heat risks (Yuan, Zhou, Hu et al., 2022). This study applied LCZ framework in the experimental design, site selection, as well as data documentation and analysis of mobile traverse measurements. Sample sites and measurement routes were determined based on the LCZ classification map. LCZ sample sites consisted of built-up LCZ types of LCZ1-LCZ6. Measurement routes were designed to cover typical high-density urban areas of Hong Kong. Obvious intra-urban variations of local climatic conditions were monitored by the mobile measurements, and the results were analysed at LCZ scale.

Besides the application in standardizing the procedures of UHI observations , LCZ framework was employed to synergize climatic and urban morphology data to establish standardized LCZ datasets. LCZ datasets not only allow parametric analysis to investigate the links between urban morphology parameters and UHI intensity, but also provide spatial information for developing the

UHI estimation map based on the statistical models. The LCZ classification map and the UHI estimation map demonstrate the spatial distribution of urban morphology and UHI intensity using an easy-to-understand way, which may assist cross-field communication and cooperation between researchers, planners and policy makers (Perera & Emmanuel, 2018; Yang, Jin, Xiao et al., 2019).

4.2. Quantifying connections between urban morphology parameters and UHI development at local scale

Obvious intra-urban variation of UHI has been observed in the high-density and heterogenous urban environment of Hong Kong through mobile measurement. The results indicate that urban morphology has significant influence on UHI development. LCZ parameters in building density, street density, and impervious land cover has positive connections with UHI intensity, while elevation shows the opposite effect on UHI intensity. Quantitative connections between LCZ parameters of SVF, SL, PSF, and UHI intensity have been established through multivariate analysis of stepwise MLR and PLSR. Intra-urban variations of UHI intensity were characterized through the UHI estimation map, based on which urban areas with critical UHI conditions were identified.

Mobile measurement, numerical modelling and remote-sensing image analysis methods have been widely applied in quantifying the links between urban morphology and thermal environment at LCZ scale across different cities (Cilek & Cilek, 2021; Mughal, Li, & Norford, 2020; Yang, Zhan, Xiao et al., 2020). Kotharkar and Bagade (2018) have conducted mobile traverse surveys in winter of Nagpur, India. The study has found significant thermal variations across traditional LCZ types and LCZ subclasses, which helps identifying hot spots for prioritized UHI mitigation measures. Cao, Huang, Hong et al. (2022) employed numerical simulation methods to model the climatic conditions and thermal comfort at LCZ scale in Wuhan. Compact LCZ types have been found to be hotter and drier than open LCZ types both in daytime and nighttime, which may be due to the lack of open space and vegetation in urban core areas. Mushore, Dube, Manjowe et al. (2019) examined land surface temperature of LCZs based on remote sensing data of Landsat 8 in Harare, and found that LCZ types with high building surface cover had higher land surface temperature, while LCZ types with high

natural cover such as vegetation and water were cooler. Previous studies using different climatic observation and simulation methods have widely identified that compact LCZ types with the low natural surface cover of vegetation and water need planning intervention for UHI mitigation.

4.3. Integrating LCZ-based UHI mitigation strategies into Outline Zoning Plan in Hong Kong

Based on the above spatial analysis of LCZ characteristics and the estimated UHI intensity at OZP scale, UHI mitigation strategies were developed for OZP areas at four levels: Level I (MUHII > 3 K), Level II (2.5 K < MUHII < 3 K), Level III (1.5 K < MUHII < 2.5 K), and Level IV (MUHII < 1.5 K) .

Planning Level I: OZP areas in Level I mainly include the most densely built metropolitan areas in Hong Kong, covering the CBD areas and residential areas in the mid-western part of the northern Hong Kong Island, as well as commercial and residential areas in Kowloon peninsula. These areas are mainly covered by high-rise LCZs (LCZ1 & LCZ4). The MUHII of in these OZP areas is expected to be above 3 K. Thus, UHI mitigation actions are essential to these areas. Improving the existing urban environment through urban renewal is strongly recommended. The urban renewal schemes need to control building coverage ratio and building height carefully, to achieve sky view factor elevation without compromising urban density. Further intensified development is not recommended only if with sufficient reasons and proper mitigation actions.

Planning Level II: The OZP areas in Level II mainly include the eastern part of the norther Hong Kong Island, as well as New Town regions of Tseung Kwan O, Kwun Tong, Tsuen Wan, Tsing Yi, Tuen Mun, Yuen Long, Tai Po and Sha Tin. These areas are mostly in residential and commercial land use, which are also associated with dense traffic and high population density. High-rise LCZs are the dominant LCZ types in most of the OZP areas. These OZP areas have more diverse urban built environments than those in Level I. There is a decreasing trend of urban density from the central areas to the periphery. Thus, the estimated UHI intensity in the OZP areas has a wider range than that in Level I. The MUHII is expected to be spanning from 2.5 K to 3 K.

UHI mitigation actions through urban renewal are highly recommended for the hot spot areas in the OZP areas. Further development in the periphery areas could be allowed if balanced well in building volume density and sky view factor. Regulating urban development density, determining appropriate LCZ types and proportion in OZP areas, controlling building height & building coverage ratio are essential.

Planning Level III: OZP areas in Level III are mainly distributed in the western and eastern part of Hong Kong Island, middle of Kowloon Peninsula, the northwestern part of the New Territories and Islands Districts. The dominant LCZ types in these OZP areas vary from high-rise LCZs (mainly in Hong Kong Island) to low-rise LCZs (mainly in northwestern part of the New Territories). The estimated maximum UHI intensity ranges from 1.5 K to 2.5 K.

OZP areas show a high potential for future urban development because of the existing low-density land use development. The planning schemes need to achieve a balance between urban density and local climate conditions. The UHI estimation model could be used to evaluate the UHI conditions of different planning schemes for urban development.

Planning Level IV: OZP areas in Level IV are generally in low construction density, mainly distributed in the northern part of the New Territories, the southern part of Hong Kong Island, and Islands District. The dominant LCZ types are low-rise or mid-rise LCZs. The estimated maximum UHI intensity is below 1.5 K.

These areas also show a high potential for future urban development. It needs to determine appropriate LCZ types and proportion in the development schemes, and control building height and building coverage ratio to achieve proper construction density. The configuration of open space needs to be carefully designed to preserve spatial links with the surrounding natural spaces, and facilitate the cool and fresh air to penetrate into urban areas.

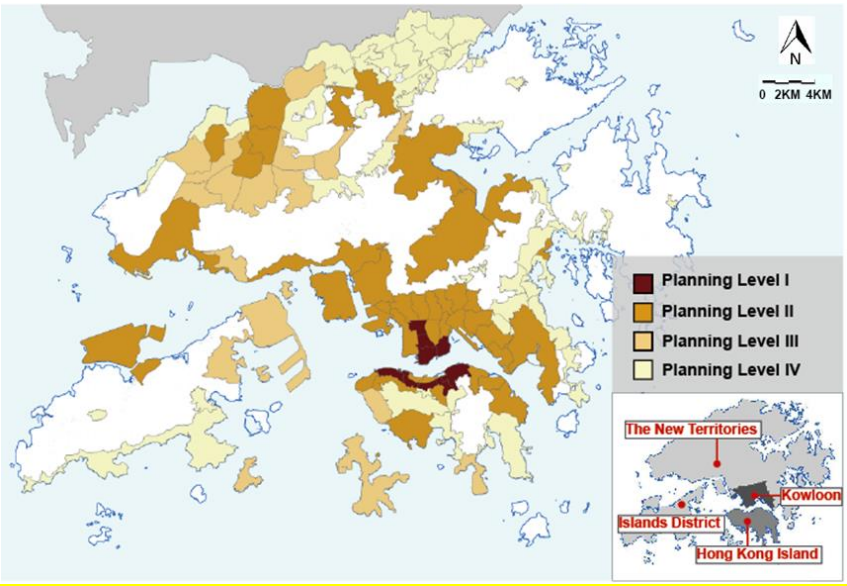

Figure 14. Integration of LCZ-based UHI mitigation strategies into Outline Zoning Plans in Hong Kong

4.4. Developing LCZ-based UHI mitigation strategies at local scale

According to the UHI estimation model of Hong Kong, optimized configuration of buildings, streets and green spaces is essential to mitigate UHI conditions at local/site scale. A wider setback of buildings from the zone boundaries needs to be imposed to increase urban openness and permeability, which would benefits in promoted radiative and convective cooling (**Figure 15**). Green space with high pervious surface cover is helpful for UHI mitigation, but dense buildings along street canyons usually restrict the cool air of green space at local scale. Thus, more dispersed green space could benefit a larger number of neighbourhoods than the green space in a concentrated form. Specially, green space configured on the side of streets is more recommended compared to those enclosed by high-rise buildings within land use zones (**Figure 15**).

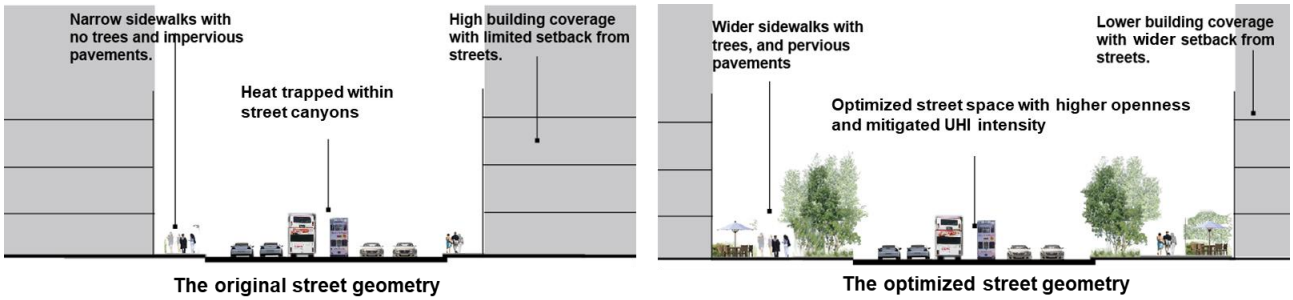

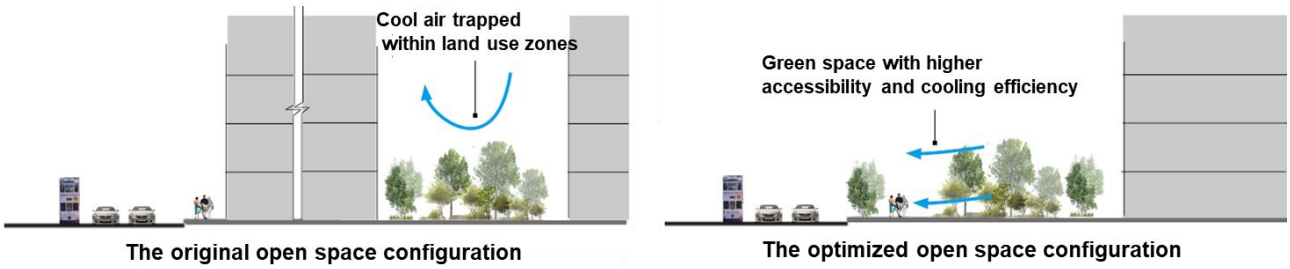

Figure 15. Planning strategies for UHI mitigation at local scale

5. Conclusion

This study has conducted mobile traverse measurements to monitor local climate variations in Hong Kong based on LCZ framework. The measurement results were processed and analyzed with urban morphology data using GIS to establish LCZ datasets. Bivariate and multivariate analysis were performed to quantify the connections between urban morphology and UHI conditions, based on which a UHI estimation model and the corresponding UHI estimation map were established.

For climatic planning practice, this study shows how the LCZ classification system could be applied to land surface classification, site selection, experimental design as well as data documentation and analysis for UHI studies. An integrative method of statistical analysis and spatial mapping has been employed to establish the urban morphology-based UHI estimation model of Hong Kong, which not only supports quantitative knowledge of key urban morphology parameters influencing local UHI development, but also provides intuitive spatial information about critical urban areas with urgent need for UHI mitigation. The UHI estimation map and LCZ classification map were further analysed at OZP level, to evaluate the urban morphology characteristics and the associated UHI intensity risks of OZP areas, and develop LCZ-based planning strategies for UHI mitigation.

The key findings of this study are summarized as follows: (1). LCZ framework is applicable for classifying land surface properties and standardizing UHI observations in the subtropical high-density city of Hong Kong. (2). Nocturnal UHI conditions at LCZ scale are significantly influenced by local urban forms, and the urban morphology-based UHI estimation model can explain around 50% of UHI variations. (3). the UHI estimation map and LCZ-based UHI mitigation planning map

are the core results of this study, which support standardized spatial information for climatic planning in Hong Kong, and for cross comparison with LCZ-based UHI studies in different climate regions.

A limitation of this study is that it only focused on UHI conditions in the early night-time period in summer, when outdoor human activities are intense with high exposure risks to significant UHI effects. Further heat risk analysis during the daytime and other seasons is necessary, especially in the early afternoon with the air temperature at its peak level. In addition, obvious UHI variations in the dominant high-rise LCZ classes of LCZ1 and LCZ4 have been observed through mobile traverse measurements, which indicates the needs for further subclassification and refinement of LCZ framework in the high-density and heterogenous urban environments in Hong Kong.

Funding: This study is supported by Guangdong Philosophy and Social Science Foundation (Grant No. GD22CGL38), Guangzhou Science and Technology Programme (Grant No. 202201020541), Guangzhou Philosophy and Social Science Planning 2022 Annual Project (Grant No. 2022GZQN19), Guangdong Basic and Applied Basic Research Foundation (Grant No. 2022A1515010171), and the Science and Technology Program of Guangzhou University (Grant No. PT252022006).

Acknowledgements: The authors deeply thank Professor Edward Ng, Mr. Max Lee, and Mr. Fung Wai Lui of the Chinese University of Hong Kong for the guidance and support of this study.

References

Buttstädt, M., & Schneider, C. (2014). Thermal load in a medium-sized European city using the example of Aachen, Germany. *Erdkunde*, 71-83.

Cao, Q., Huang, H., Hong, Y., Huang, X., Wang, S., Wang, L., & Wang, L. (2022). Modeling intra-urban differences in thermal environments and heat stress based on local climate zones in central Wuhan. *Building and Environment, 225*, 109625.

Chàfer, M., Tan, C. L., Cureau, R. J., Hien, W. N., Pisello, A. L., & Cabeza, L. F. (2022). Mobile measurements of microclimatic variables through the central area of Singapore: An analysis from the pedestrian perspective. *Sustainable Cities and Society, 83*, 103986.

Chen, L., Ng, E., An, X., Ren, C., Lee, M., Wang, U., & He, Z. (2010). Sky view factor analysis of street canyons and its implications for daytime intra- urban air temperature differentials in high- rise, high- density urban areas of Hong Kong: a GIS- based simulation approach. *International Journal of Climatology, 32*(1), 121-136.

Chu, H., Venevsky, S., Wu, C., & Wang, M. (2019). NDVI-based vegetation dynamics and its response to climate changes at Amur-Heilongjiang River Basin from 1982 to 2015. *Science of the total environment, 650*, 2051-2062.

Cilek, M. U., & Cilek, A. (2021). Analyses of land surface temperature (LST) variability among local climate zones (LCZs) comparing Landsat-8 and ENVI-met model data. *Sustainable Cities and Society, 69*, 102877.

Dosio, A., Mentaschi, L., Fischer, E. M., & Wyser, K. (2018). Extreme heat waves under 1.5 C and 2 C global warming. *Environmental Research Letters, 13*(5), 054006.

Fung, W. Y. (2010). *Characterizing urban heat island and its effects in Hong Kong.* The Hong Kong Polytechnic University.

Giridharan, R. (2005). *Urban design factors influencing outdoor temperature in high-risehigh-density residential developments in the coastal zone of HongKong.* (Doctoral Doctoral), University of Hong Kong.

Giridharan, R., Lau, S., Ganesan, S., & Givoni, B. (2007). Urban design factors influencing heat island intensity in high-rise high-density environments of Hong Kong. *Building and Environment, 42*(10), 3669-3684.

Goggins, W. B., Chan, E. Y., Ng, E., Ren, C., & Chen, L. (2012). Effect modification of the association between short-term meteorological factors and mortality by urban heat islands in Hong Kong. *PLoS One, 7*(6), e38551.

Gu, Y., & You, X.-y. (2022). A spatial quantile regression model for driving mechanism of urban heat island by considering the spatial dependence and heterogeneity: An example of Beijing, China. *Sustainable Cities and Society, 79*, 103692.

Guo, A., Yang, J., Xiao, X., Xia, J., Jin, C., & Li, X. (2020). Influences of urban spatial form on urban heat island effects at the community level in China. *Sustainable Cities and Society, 53*, 101972.

HKGovernment. (2021). Hong Kong : The Facts.

Ho, H. C., Lau, K. K.-L., Ren, C., & Ng, E. (2017). Characterizing prolonged heat effects on mortality in a sub-tropical high-density city, Hong Kong. *International journal of biometeorology, 61*(11), 1935-1944.

Houet, T., & Pigeon, G. (2011). Mapping urban climate zones and quantifying climate behaviors–an application on Toulouse urban area (France). *Environmental Pollution, 159*(8-9), 2180-2192.

Hua, J., Zhang, X., Ren, C., Shi, Y., & Lee, T.-C. (2021). Spatiotemporal assessment of extreme heat risk for high-density cities: A case study of Hong Kong from 2006 to 2016. *Sustainable Cities and Society, 64*, 102507.

Jiang, S., Zhan, W., Dong, P., Wang, C., Li, J., Miao, S., . . . Wang, C. (2022). Surface air temperature differences of intra-and inter-local climate zones across diverse timescales and climates. *Building and Environment, 222*, 109396.

Kotharkar, R., & Bagade, A. (2018). Evaluating urban heat island in the critical local climate zones of an Indian city. *Landscape and urban planning, 169*, 92-104.

Lau, K. K.-L., Chung, S. C., & Ren, C. (2019). Outdoor thermal comfort in different urban settings of sub-tropical high-density cities: An approach of adopting local climate zone (LCZ) classification. *Building and Environment, 154*, 227-238.

Leconte, F., Bouyer, J., Claverie, R., & Pétrissans, M. (2015). Using Local Climate Zone scheme for UHI assessment: Evaluation of the method using mobile measurements. *Building and Environment, 83*, 39-49.

Leconte, F., Bouyer, J., Claverie, R., & Pétrissans, M. (2016). Analysis of nocturnal air temperature in districts using mobile measurements and a cooling indicator. *Theoretical and Applied Climatology*, 1-12.

Leung, Y. K. (2004). Climate Change in Hong Kong. *Hong Kong Meteorological Society Bulletin*.

Leung, Y. K., & Ng, T. S. (1997). *Regional temperature variation in winter of Hong Kong*: Hong Kong Observatory.

Li, Q., Vilela, P., Tariq, S., Nam, K., & Yoo, C. (2022). Multiple land-use fugacity model to assess the transport and fate of polycyclic aromatic hydrocarbons in urban and suburban areas. *Urban Climate, 45*, 101263.

Lin, P., Lau, S. S. Y., Qin, H., & Gou, Z. (2017). Effects of urban planning indicators on urban heat island: a case study of pocket parks in high-rise high-density environment. *Landscape and urban planning, 168*, 48-60.

Liu, L., Lin, Y., Liu, J., Wang, L., Wang, D., Shui, T., . . . Wu, Q. (2017). Analysis of local-scale urban heat island characteristics using an integrated method of mobile measurement and GIS-based spatial interpolation. *Building and Environment, 117*, 191-207.

Masson-Delmotte, V., Zhai, P., Pörtner, H.-O., Roberts, D., Skea, J., Shukla, P. R., . . . Pidcock, R. (2018). Global warming of 1.5 C. *An IPCC Special Report on the impacts of global warming of, 1*(5).

Memon, R. A., Leung, D. Y., & Liu, C.-H. (2009). An investigation of urban heat island intensity (UHII) as an indicator of urban heating. *Atmospheric Research, 94*(3), 491-500.

Mok, H. Y., Wu, M. C., & Cheng, C. Y. (2011). Spatial variation of the characteristics of urban heat island effect in Hong Kong. *Journal of Civil Engineering and Architecture, 5*(9), 779-786.

Morakinyo, T. E., Ren, C., Shi, Y., Lau, K. K.-L., Tong, H.-W., Choy, C.-W., & Ng, E. (2019). Estimates of the impact of extreme heat events on cooling energy demand in Hong Kong. *Renewable Energy, 142*, 73-84.

Mughal, M., Li, X.-X., & Norford, L. K. (2020). Urban heat island mitigation in Singapore: Evaluation using WRF/multilayer urban canopy model and local climate zones. *Urban Climate, 34*, 100714.

Mushore, T. D., Dube, T., Manjowe, M., Gumindoga, W., Chemura, A., Rousta, I., . . . Mutanga, O. (2019). Remotely sensed retrieval of Local Climate Zones and their linkages to land surface temperature in Harare metropolitan city, Zimbabwe. *Urban Climate, 27*, 259-271.

Ng, E., Yau, R., Wong, K. S., & Ren, C. (2012). Final Report of Hong Kong Urban Climatic Map and Standards for Wind Environment- Feasibility Study.

Nwakaire, C. M., Onn, C. C., Yap, S. P., Yuen, C. W., & Onodagu, P. D. (2020). Urban Heat Island Studies with emphasis on urban pavements: A review. *Sustainable Cities and Society, 63*, 102476.

Oukawa, G. Y., Krecl, P., & Targino, A. C. (2022). Fine-scale modeling of the urban heat island: a comparison of multiple linear regression and random forest approaches. *Science of the total environment, 815*, 152836.

Perera, N., & Emmanuel, R. (2018). A "Local Climate Zone" based approach to urban planning in Colombo, Sri Lanka. *Urban Climate, 23*, 188-203.

Perkins-Kirkpatrick, S., & Lewis, S. (2020). Increasing trends in regional heatwaves. *Nature communications, 11*(1), 1-8.

Ren, C., Ng, E. Y. y., & Katzschner, L. (2011). Urban climatic map studies: a review. *International Journal of Climatology, 31*(15), 2213-2233.

Ren, C., Wang, K., Shi, Y., Kwok, Y. T., Morakinyo, T. E., Lee, T. c., & Li, Y. (2021). Investigating the urban heat and cool island effects during extreme heat events in high-density cities: A case study of Hong Kong from 2000 to 2018. *International Journal of Climatology, 41*(15), 6736-6754.

Ren, C., Yang, R., Cheng, C., Xing, P., Fang, X., Zhang, S., . . . Kwok, Y. T. (2018). Creating breathing cities by adopting urban ventilation assessment and wind corridor plan–the

implementation in Chinese cities. *Journal of Wind Engineering and Industrial Aerodynamics, 182*, 170-188.

Sakakibara, Y., & Owa, K. (2005). Urban–rural temperature differences in coastal cities: Influence of rural sites. *International Journal of Climatology, 25*(6), 811-820.

Shi, Y., Katzschner, L., & Ng, E. (2018). Modelling the fine-scale spatiotemporal pattern of urban heat island effect using land use regression approach in a megacity. *Science of the total environment, 618*, 891-904.

Shi, Y., Lau, K. K.-L., Ren, C., & Ng, E. (2018). Evaluating the local climate zone classification in high-density heterogeneous urban environment using mobile measurement. *Urban Climate, 25*, 167-186.

Shipley, B. (2016). *Cause and correlation in biology: a user's guide to path analysis, structural equations and causal inference with R*: Cambridge University Press.

Siu, L. W., & Hart, M. A. (2013). Quantifying urban heat island intensity in Hong Kong SAR, China. *Environmental monitoring and assessment, 185*(5), 4383-4398.

Stewart, I. D. (2011). *Redefining the urban heat island.* University of British Columbia. Retrieved from https://circle.ubc.ca/handle/2429/38069

Stewart, I. D., & Oke, T. R. (2012). Local climate zones for urban temperature studies. *Bulletin of the American Meteorological Society, 93*(12), 1879-1900.

Tan, Z., Lau, K. K.-L., & Ng, E. (2016). Urban tree design approaches for mitigating daytime urban heat island effects in a high-density urban environment. *Energy and Buildings, 114*, 265-274.

Tan, Z., Lau, K. K.-L., & Ng, E. (2017). Planning strategies for roadside tree planting and outdoor comfort enhancement in subtropical high-density urban areas. *Building and Environment, 120*, 93-109.

Wang, R., Ren, C., Xu, Y., Lau, K. K.-L., & Shi, Y. (2018). Mapping the local climate zones of urban areas by GIS-based and WUDAPT methods: A case study of Hong Kong. *Urban Climate, 24*, 567-576.

Wang, Z., Zhao, H., & Peng, Z. (2021). Spatiotemporal analysis of pedestrian exposure to submicron and coarse particulate matter on crosswalk at urban intersection. *Building and Environment, 204*, 108149.

Weier, J., & Herring, D. (2000). Measuring Vegetation (NDVI & EVI). from http://earthobservatory.nasa.gov/Features/MeasuringVegetation/

Wu, M., Leung, Y., Lui, W., & Lee, T. (2009). A study on the difference between urban and rural climate in Hong Kong. *Meteor, 35*(2), 71-79.

Yan, C., Guo, Q., Li, H., Li, L., & Qiu, G. Y. (2020). Quantifying the cooling effect of urban vegetation by mobile traverse method: A local-scale urban heat island study in a subtropical megacity. *Building and Environment, 169*, 106541.

Yang, J., Jin, S., Xiao, X., Jin, C., Xia, J. C., Li, X., & Wang, S. (2019). Local climate zone ventilation and urban land surface temperatures: Towards a performance-based and wind-sensitive planning proposal in megacities. *Sustainable Cities and Society, 47*, 101487.

Yang, J., Zhan, Y., Xiao, X., Xia, J. C., Sun, W., & Li, X. (2020). Investigating the diversity of land surface temperature characteristics in different scale cities based on local climate zones. *Urban Climate, 34*, 100700.

Yin, C., Yuan, M., Lu, Y., Huang, Y., & Liu, Y. (2018). Effects of urban form on the urban heat island effect based on spatial regression model. *Science of the total environment, 634*, 696-704.

Yu, Z., Chen, S., & Wong, N. H. (2020). Temporal variation in the impact of urban morphology on outdoor air temperature in the tropics: A campus case study. *Building and Environment, 181*, 107132.

Yuan, B., Zhou, L., Hu, F., & Zhang, Q. (2022). Diurnal dynamics of heat exposure in Xi'an: A perspective from local climate zone. *Building and Environment, 222*, 109400.

Zheng, Y. (2016). *Planning Strategies for Urban Heat Island Mitigation: An Application of Local Climate Zone into the High-density City of Hong Kong.* The Chinese University of Hong Kong (Hong Kong).

Zheng, Y., Li, W., Fang, C., Feng, B., Zhong, Q., & Zhang, D. (2023). Investigating the Impact of Weather Conditions on Urban Heat Island Development in the Subtropical City of Hong Kong. *Atmosphere*, *14*(2), 257.

Zheng, Y., Ren, C., Xu, Y., Wang, R., Ho, J., Lau, K., & Ng, E. (2017). GIS-based mapping of Local Climate Zone in the high-density city of Hong Kong. *Urban Climate*. doi: 10.1016/j.uclim.2017.05.008

Zou, Z., Yan, C., Yu, L., Jiang, X., Ding, J., Qin, L., . . . Qiu, G. (2021). Impacts of land use/land cover types on interactions between urban heat island effects and heat waves. *Building and Environment, 204*, 108138.

Mapping the spatial distribution of nocturnal urban heat island based on Local Climate Zone framework

Yingsheng Zheng[a,b], Chao Ren[c], Yuan Shi[d], Steve H.L. Yim[e,f,g], Derrick Y.F. Lai[h], Yong Xu[i*], Can Fang[a], Wenjie Li[a]

a. College of Architecture and Urban Planning, Guangzhou University, Guangzhou, China

b. School of Architecture, The Chinese University of Hong Kong, Hong Kong SAR, China

c. Division of Landscape Architecture, Department of Architecture, Faculty of Architecture, The University of Hong Kong, Hong Kong, SAR, China

d. Department of Geography and Planning, University of Liverpool, Liverpool, UK

e. Asian School of the Environment, Nanyang Technological University, Singapore

f. Lee Kong Chian School of Medicine, Nanyang Technological University, Singapore

g. Earth Observatory of Singapore, Nanyang Technological University, Singapore

h. Department of Geography and Resource Management, The Chinese University of Hong Kong, Hong Kong SAR, China

i. School of Geography and Remote Sensing, Guangzhou University, Guangzhou, China

Corresponding Author:
Yong XU
School of Geography and Remote Sensing, Guangzhou University
E-mail: xu1129@gzhu.edu.cn

Mapping the spatial distribution of nocturnal urban heat island based on Local Climate Zone framework

Abstract

A spatial understanding of street-scale urban heat island (UHI) is essential but challenging in Hong Kong, due to its highly heterogeneous urban environment and a limited weather station monitoring network. Night-time mobile measurements were conducted during the summertime of 2014 to monitor UHI variation at local level. Three measurement routes and a total of 80 sample sites were selected according to the Local Climate Zone (LCZ) framework. The measured climatic data and urban morphology data were synergized and analyzed at LCZ scale through Geographical Information System (GIS). Stepwise Multiple Linear Regression (MLR) and Partial Least Square Regression (PLSR) were applied to quantify the connections between urban form and local UHI conditions of LCZ. Mean sky view factor, total street length, and pervious surface fraction of LCZ sites have been found to be the most explanatory variables of local UHI intensity, and over 50% of UHI variations can be explained by both statistical models of stepwise MLR and PLSR. An UHI evaluation map of urban areas in Hong Kong has been developed based on the statistical models, through which UHI hotspots have been identified. LCZ-based UHI mitigation strategies were further developed for climatic planning of Outline Zoning Plan areas. The results indicate that urban forms have significant influences on UHI development at local scale, and an optimal design of urban morphology is necessary for UHI mitigation and climate adaptation.

Key Words: Urban Heat Island; Local Climate Zone; Urban Morphology; Mobile Traverse Measurement; Spatial Mapping; Hong Kong

1.Introduction

1.1. Challenges in climatic planning for urban heat island mitigation

Under the influence of local urbanization and global climate change, many cities over the world have experienced significant temperature increase in past decades (Masson-Delmotte, Zhai, Pörtner et al., 2018). The occurrence frequency, magnitude, and duration of high-temperature episodes are expected to continue rising in the second half of the 21st century (Dosio, Mentaschi, Fischer et al., 2018; Perkins-Kirkpatrick & Lewis, 2020). Urban heat island (UHI) effect which caused by the process of urbanization with changes in land surface structure and human behaviours, tends to be reinforced by high temperature periods. It results in additional hot days at local scale, associated with elevated energy consumption for cooling and increased heat-related health risks (Goggins, Chan, Ng et al., 2012; Ho, Lau, Ren et al., 2017; Morakinyo, Ren, Shi et al., 2019). Therefore, it is essential to identify hotspot areas of UHI and take climatic planning interventions for UHI mitigation.

1.2. Needs for refined spatial understanding of local UHI in the high-density city of Hong Kong

Hong Kong is a high-density city with a highly heterogeneous urban environment and mountainous-coastal geography. Due to the spatial variability of urban forms and geographical conditions, local thermal environments and the associated heat exposure risks vary significantly in Hong Kong (Hua, Zhang, Ren et al., 2021). In high-density urban areas with crowded buildings and dense population, UHI effects exacerbate the strength of high temperatures, and the high temperature weather generally accompanied by high air pressure and weak air flow further exacerbates the magnitude of UHI effects (Zou, Yan, Yu et al., 2021). Residents living in high-density urban areas are exposed to the strengthened high temperature weather and urban heat islands. In such cases, a refined spatial understanding of urban morphology and local UHI conditions is needed to support the planning decision-making for UHI mitigation.

Weather station network operated by Hong Kong Observatory provides long-term meteorological data in high temporal resolution, based on which spatial interpolation techniques

could be applied in the heat risk assessment at city level (Morakinyo et al., 2019). However, as automatic weather stations are sparsely distributed in relatively open spaces, it is still hard to reveal the intra-urban variations of UHI at fine scale (Shi, Katzschner, & Ng, 2018). Remote sensing technique is another commonly used method in the spatial assessment of UHI through retrieving land surface temperature based on satellite images (Nwakaire, Onn, Yap et al., 2020). It is known that diurnal profiles of surface UHI differ from that of canopy UHI. Large SUHI generally occurs during the daytime while large canopy UHI generally occurs at night, and therefore spatial assessment of canopy UHI through remote sensing techniques at fine scale may introduce estimation error (Shi, Katzschner, et al., 2018).

Compared to the above methods, mobile traverse measurement method is more applicable to the refined spatial assessment of UHI for its advantages in low cost, time efficiency, and high spatial resolution (Liu, Lin, Liu et al., 2017; Yan, Guo, Li et al., 2020). The climatic data collected through mobile measurements at street level is close to the local climatic conditions that pedestrians are exposed to. It could be employed to quantify the influence of urban forms on the climatic variation at local level (Chàfer, Tan, Cureau et al., 2022; Z. Wang, Zhao, & Peng, 2021).

1.3. Application of Local Climate Zone framework into the spatial assessment of UHI

To systematically differentiate the varying land surface types, Stewart and Oke (2012) have developed the Local Climate Zone (LCZ) framework as a land surface classification system to standardize the observation and report of UHI studies. The LCZ framework consists of 17 basic classes, including ten building classes and seven land cover classes. Previous studies of LCZ classification have shown that the existing LCZ classes can well describe the land surface properties and thermal environment variations at local scale (Jiang, Zhan, Dong et al., 2022; Francois Leconte, Bouyer, Claverie et al., 2015). Moreover, LCZ framework has proposed a set of guidelines in the aspects of representative site selection, site metadata documentation, weather control and time control for UHI observations and report. Following the standardized framework of LCZ, local climatic studies in different climatic regions over the world with varied built environment could be compared.

In the high-density city of Hong Kong, the highly heterogeneous land cover conditions have been described and quantified in LCZ classification maps through GIS method and remote sensing method (R. Wang, Ren, Xu et al., 2018; Zheng, Ren, Xu et al., 2017). The LCZ classification maps have been evaluated and validated by Shi, Lau, Ren et al. (2018) based on mobile traverse measurements, and the study found that the LCZ framework can well differentiate local thermal variation. The LCZ framework has been further applied in standardizing the observation and analysis of thermal comfort and thermal sensation in different LCZ types (Lau, Chung, & Ren, 2019; Tan, Lau, & Ng, 2017).

Many previous UHI studies in Hong Kong have conducted in situ measurements to monitor local UHI conditions, but mainly focused on certain LCZ types, such as high-rise residential developments and compact commercial areas (Giridharan, Lau, Ganesan et al., 2007; Lin, Lau, Qin et al., 2017; Tan, Lau, & Ng, 2016). The quantitative relationships between local UHI intensity and urban forms have not been fully explored based on UHI observations in a comprehensive set of sample sites. Knowledge about the spatial distribution pattern of UHI intensity at LCZ level is still limited, especially in the critical time period under typical hot summer weather conditions. Thus, standardized UHI observations and refined understanding about how urban morphology influences the spatial distribution of UHI in Hong Kong are needed for climatic planning and adaptation.

This study aims to (1) apply the LCZ framework to standardize the procedures of UHI observations in Hong Kong, and conduct traverse measurements to monitor local climate conditions in selected high-density urban areas under the prevailing summer weather condition of Hong Kong, (2) investigate the relationships between urban morphology parameters and UHI intensity at LCZ scale, and develop a morphological-based UHI estimation model through statistical analysis, (3) formulate a UHI estimation map as an intuitive information support of critical urban areas with urgent needs for UHI mitigation, and (4) integrate the LCZ-based UHI mitigation strategies into the statutory plan of Outline Zoning Plan in Hong Kong.

2.Method

2.1. Study area

Hong Kong is a high-density city located on the southeast coast of China, one of the core cities in the Guangdong-Hong Kong-Macao Greater Bay Area. The total land area of Hong Kong is about 1,114 square kilometers, of which more than 75% is a mountain country park reserve, and less than 25% of the land is allowed for urban development. The total population is about 7.4 million, with the highest subregion population density exceeding 55,000 people per square kilometre (HKGovernment, 2021).

Hong Kong has a subtropical maritime monsoon climate. Summertime in Hong Kong is associated with high air temperature, high relative humidity and weak winds, which may cause thermal discomfort and other heat-related health problems. Large population, limited land resources, and high urbanization level shape the high-density urban environment in Hong Kong, and considerable UHI intensity has been observed in high-density urban areas of Hong Kong.

2.2. Experimental design of mobile traverse measurement for UHI observation

(1). Sample sites selection and measurement routes design

The GIS-based Local Climate Zone classification map of Hong Kong developed by Zheng et al. (2017) was applied to identify the critical regions and potentially appropriate sites for urban heat island monitoring. Main LCZ types of urban areas of Hong Kong are LCZ1- LCZ6 (**Figure 1**), and dominant LCZ types in city centers are LCZ1 (Compact High-rise) and LCZ4 (Open High-rise). High density urban areas of northern Hong Kong Island (HKI), Kowloon Peninsula (KL) as well as the new town of Tuen Mun (TM) in the New Territories have been selected as study areas (**Figure 2**). A total of 80 typical LCZ sites (in 300m grid size) have been selected, including 32 sites in HKI, 33 sites in KL, and 15 sites in TM. Sample sites cover six LCZ types of LCZ1 – LCZ6. HKI and TM areas mainly comprise high-rise LCZ types of LCZ1 and LCZ4, while KL area covers six LCZ types from LCZ1 to LCZ6. Traverse measurement routes have been designed to pass through the central

part of sample sites, and the total length of HKI, KL, and TM routes are 16km, 25km and 12km respectively (**Figure 3**). A couple of pilot measurements were performed to ensure the measurement time was controlled within two hours to limit the background air temperature change during the measurement (Stewart, 2011).

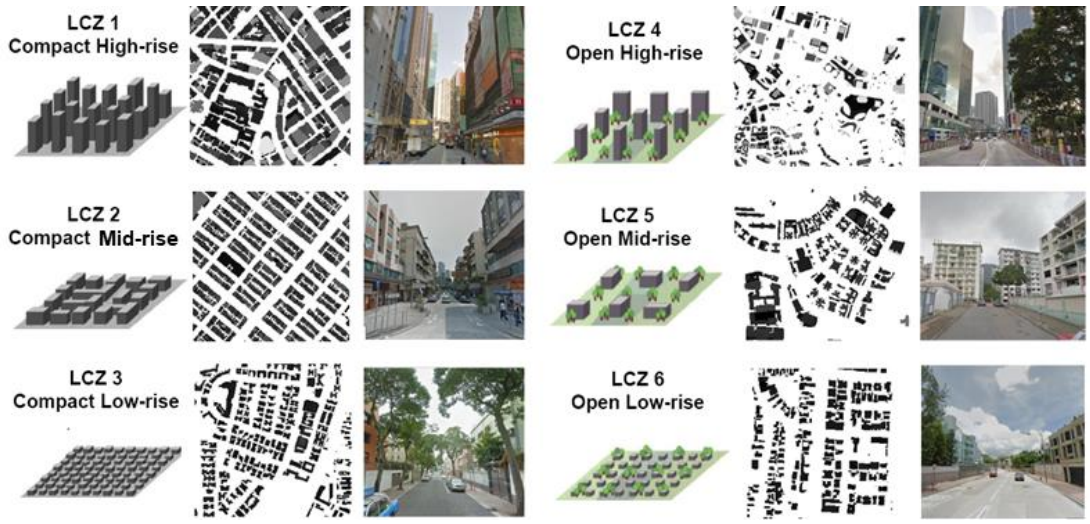

Figure 1. Examples of LCZ classes in Hong Kong (Zheng et al., 2017)

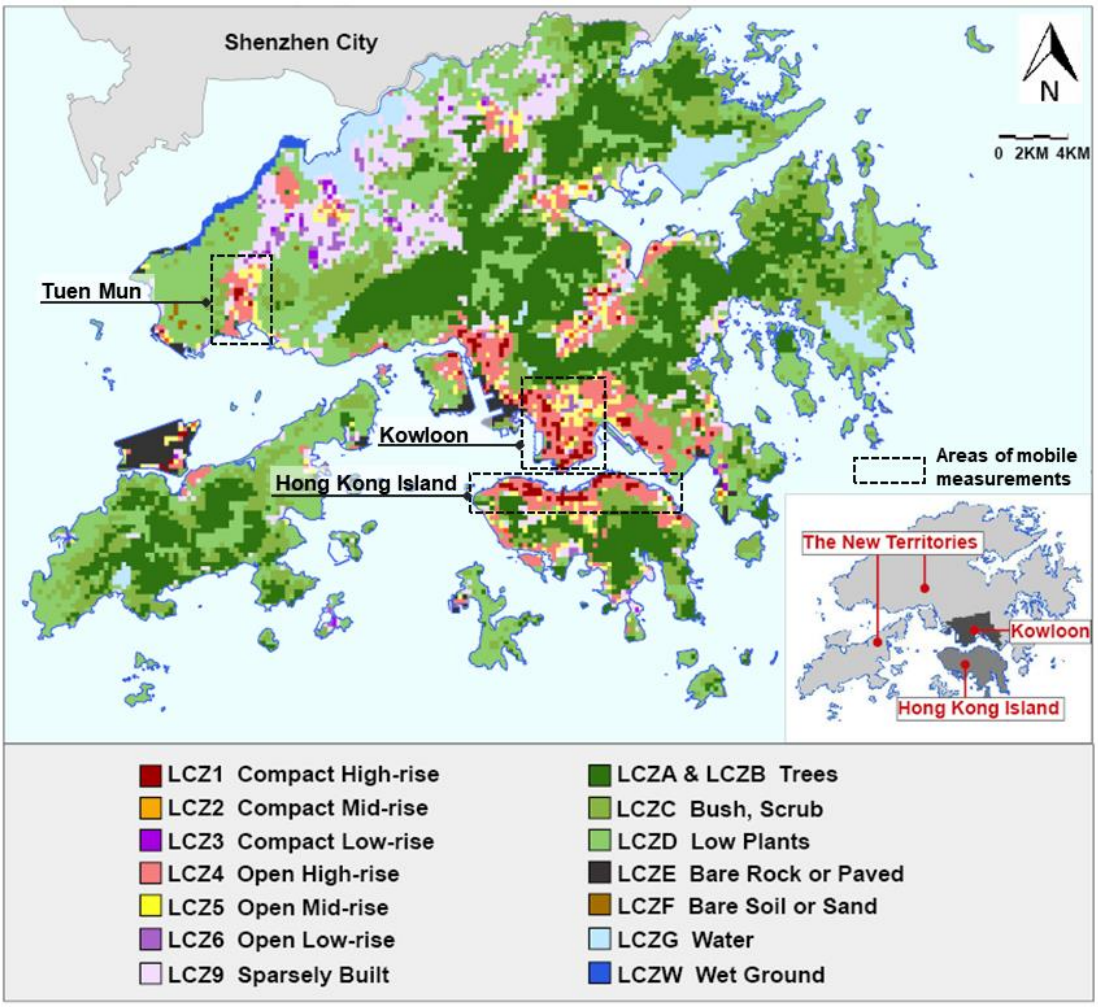

Figure 2. Study areas of traverse measurements based on the LCZ classification map in Hong Kong

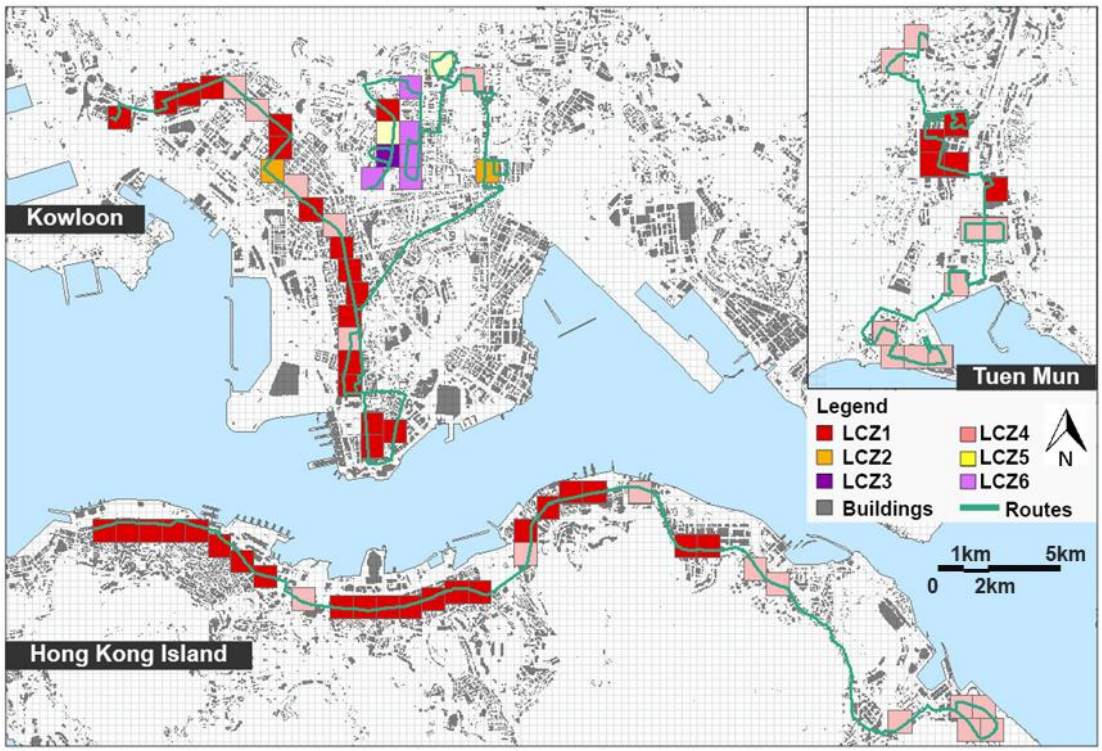

Figure 3. Sample sites selection and traverse measurement routes design

(2). Weather control and measurement time selection

Weather control and time selection is critical for UHI observation and analysis, as the spatial distribution patterns of UHI varies in different background weather conditions and the diurnal circle. Clear sky condition is ideal for UHI development, but it has low occurrence frequency below 2.5% in the summer of Hong Kong. Summertime peak UHI intensities mainly occurred in partly cloudy conditions with daily mean cloud amount of 2-7 Oktas (Zheng, Li, Fang et al., 2023). Thus, typical hot summer days with partly cloudy and weak wind conditions were selected for UHI observations.

Although the stationary observation records in Hong Kong show that UHI intensity is generally maximized in deep night or early morning, and the peak air temperature generally occurs at noon or early afternoon (Zheng, 2016), early night period of 20:00-22:00 would be more critical for UHI measurement since that: (1). Early night time when people get off work or school, urban areas would have more intense outdoor human activities than that at noon or at late night, as noontime or early afternoon when air temperature reaches peak in the whole day in summer, people generally prefer to stay indoor to avoid high temperature and strong solar radiation. (2). Daytime UHI is not that obvious as nocturnal UHI. High-density urban areas is highly possible to have cooler air temperature than

rural areas at noon and early afternoon, i.e. urban cool island effects, mainly due to the shading effects and heat absorption/storage by dense buildings (Ren, Wang, Shi et al., 2021). Significant UHI intensity at early night would lead to air temperature elevation in urban areas and cause thermal discomfort or heat-related health problems to pedestrians. Based on the above consideration, early night period of 20:00-22:00 was determined as the critical time period for mobile traverse measurement of UHI effects.

2.3. Data

(1). Traverse measurement data

A total of five mobile measurements were completed under the typical hot weather condition of Hong Kong, to monitor local atmospheric environments of selected LCZ sample sites (**Table 1**). There was no rainfall recorded in the past 24 hours before each measurement at the nearby weather stations of study areas.

Table 1. Background information of traverse measurements

Study Region	Measurement Date	Number of Typical LCZ Sample Sites						
		Sum	LCZ1	LCZ2	LCZ3	LCZ4	LCZ5	LCZ6
HKI	Jul 16, 2014 Aug 26, 2014	32	24	--	--	8	--	--
KL	Jul 30, 2014	33	17	2	1	6	2	5
TM	Aug 25, 2014 Sep 2, 2014	15	5	--	--	10	--	--

Air temperature and relative humidity were measured and recorded by TESTO 480 temperature and humidity probe and data logger (**Figure 4**). The air temperature and relative humidity probe of TESTO 480 was mounted on top of the van, 2.5m above ground. The estimated system accuracy of the air temperature is +/-0.5 K within the range from -20 K to +70 K, while the accuracy of the relative humidity is +/- 1% from 0 to 90%, and +/- 1.4 % from 90% to 100%. Data were recorded by the data logger of TESTO 480 at one-second interval while the Garmin 62s GPS system also recorded the location and driving velocity at one-second interval simultaneously. A driving

recorder was installed on the van to record the road conditions. During measurements, the van traveled at an average speed of around 20 km/h with its maximum speed controlled within 50 km/h.

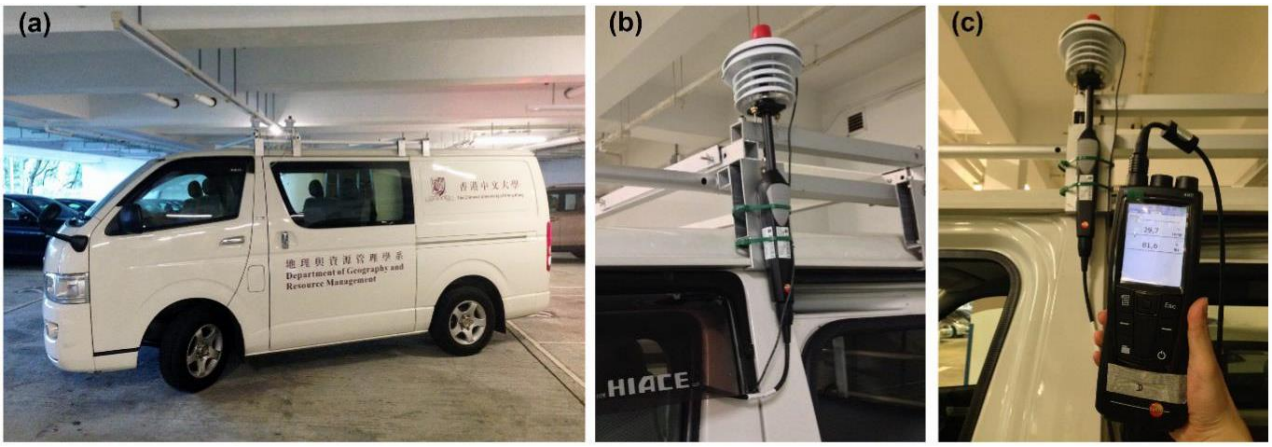

Figure 4. Measurement equipment
(a. Vehicle; b. Mounting of Testo 480 sensor; c. Testo 480 sensor and data logger)

The measured data was divided into two datasets for statistical modelling. Data in the HKI and KL areas was applied as the training dataset to quantify the correlation between UHI intensity and urban morphology parameters and develop the UHI estimation model. Data in TM was used as the validation dataset to evaluate the predictive accuracy of the UHI estimation model.

(2). Urban morphology data

Urban morphology data including buildings, streets, topography and land use in GIS format, as well as four remote sensing images of Landsat 8 (October 5, 2013, December 31, 2013, August 8, 2015, and October 18, 2015) were employed to quantify urban morphology parameters of LCZ sample sites following the GIS-based LCZ classification method (Zheng et al., 2017) (**Figure 5**). The urban morphology parameters of LCZ include building height (BH), building surface fraction (BSF, i.e. building coverage ratio), building volume density (BVD), sky view factor (SVF), aspect ratio (H/W), pervious surface fraction (PSF), impervious surface fraction (ISF), street coverage ratio (SCR), street width (SW), and elevation (DEM).

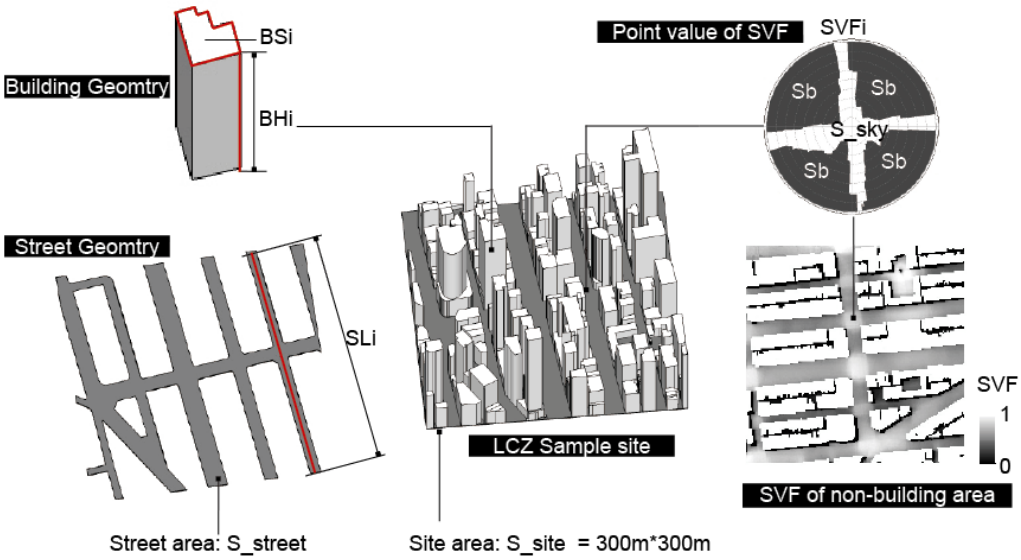

Figure 5. Urban morphology parameters calculation (Zheng et al., 2017)

Table 2. Definition and calculation methods of urban morphology parameters

Parameters	Definition	Basic Data	Calculation methods	Description
BH	Area weighted mean building height of sample sites	Building data	$\mathrm{BH} = \frac{\sum_{i=1}^{n} BSi * BHi}{\sum_{i=1}^{n} BSi}$	n is the number of buildings of the LCZ sample site. BSi is the ground area of a building. BHi is the height of a building. $\sum_{i=1}^{n} BSi$ is the total building cover area of the site. $\sum_{i=1}^{n} BSi * BHi$ is the total building volume of the site.
BSF	Building surface fraction of sample sites	Building data	$\mathrm{BSF} = \frac{\sum_{i=1}^{n} BSi}{S\_site}$	n is the number of buildings of the LCZ sample site. S_site is the total area of the site.
SVF	Areal mean SVF of non-building areas in sample sites (Chen, Ng, An et al., 2010)	Building and topography data	$\mathrm{SVF} = \frac{\sum_{i=1}^{n} SVFi}{n}$ $\mathrm{SVFi} = \frac{S\_Sky}{(S\_Sky + \sum Sb)}$	SVFi is the SVF value of a certain point in non-building area (point area 1m*1m) in the LCZ sample site. n is the number of SVF points (1m*1m) in non-building area of the site. S_Sky and $\sum Sb$ represent the area of sky and the area occupied by buildings in a certain point respectively. $S_{Sky} + \sum Sb$ represents the entire hemispheric environment in a certain point.
H/W	Areal mean aspect ratio of sample sites	Building and street data	$\mathrm{H/W} = \frac{\mathrm{BH}}{\mathrm{SW}}$	The ratio of mean building height to mean

				street width in the LCZ sample site.
BVD	Building volume density of sample sites (Ng, Yau, Wong et al., 2012)	Building data	$\mathrm{BVD} = \frac{\sum_{i=1}^{n} BSi * BHi}{S\_site}$	n is the number of buildings of the LCZ sample site. BSi is the ground area of a building. BHi is the height of a building. $\sum_{i=1}^{n} BSi$ is the total building cover area of the site. $\sum_{i=1}^{n} BSi * BHi$ is the total building volume of the site.
PSF	Pervious surface fraction of sample sites	Remote sensing data	$\mathrm{PSF} = \frac{\sum S\_per}{S\_site}$ $\sum S\_per$ is the total area of pervious surface, with NDVI above 0.2 (Weier & Herring, 2000)	$\sum S\_per$ is the total area of pervious surface, with NDVI above 0.2
ISF	Impervious surface fraction of sample sites	Building and remote sensing data	$\mathrm{ISF} = 1 - \mathrm{BSF} - \mathrm{PSF}$	Impervious surface fraction is defined as the fraction of surface not covered by pervious surface or buildings.
SCR	Street coverage ratio of sample sites	Street data	$\mathrm{SCR} = \frac{\sum S\_street}{S\_site}$	$\sum S\_street$ is the total area of streets in the site. S_site is the area of sample sites.
SL	Total street length of sample sites	Street data	$\mathrm{SW} = \sum_{i=1}^{n} SLi$	n is the number of streets in the LCZ sample site. $\sum_{i=1}^{n} SLi$ is the total length of streets in the site.
SW	Mean street width of sample sites	Street data	$\mathrm{SW} = \frac{\sum S\_street}{\sum_{i=1}^{n} SLi}$	n is the number of streets in the LCZ sample site. $\sum_{i=1}^{n} SLi$ is the total length of streets in the site. $\sum S\_street$ is the total area of streets in the site.
Elevation	Mean elevation of sample sites	Topography data	--	--

(3). Stationary observation data

Meteorological data are collected from the Hong Kong Observatory for calculating UHI magnitude of LCZ sample sites and conducting temporal adjustments for measured air temperature. Determination of rural reference for UHI study is difficult for Hong Kong because local climate vary across different rural areas owing to the mountainous and coastal geographical conditions. Stations located near the coast such as Cheung Chau station and Waglan Island stations have been excluded

from consideration, as the recorded daily temperature profiles could be significantly influenced by the seawater temperature (Sakakibara & Owa, 2005). Ta Kwu Ling (TKL) and Lau Fu Shan (LFS) stations have been commonly recognized as rural stations of Hong Kong (Fung, 2010; Memon, Leung, & Liu, 2009; Siu & Hart, 2013). TKL station is in the northeastern rural area with a small population and lush vegetation (Figure 6). LFS station is controversial due to its surrounding low-rise neighborhoods and proximity to high-rise residential developments in Tin Shui Wai, and some studies have classified LFS as a rural station (Leung, 2004; Leung & Ng, 1997), while recent studies have recognized it as an urban or suburban station as LFS station shows similar diurnal temperature profiles with the urban stations located in new towns of Hong Kong (Memon et al., 2009; Wu, Leung, Lui et al., 2009). Based on the above consideration, TKL station is determined as the rural reference in this study. UHI intensity of LCZ sample sites (UHII) was calculated as the mean air temperature difference between LCZ sample sites and TKL station during traverse measurements according to the definition of UHI (Kotharkar & Bagade, 2018; Stewart & Oke, 2012):

$$\text{UHII} = \Delta T_{U-R} = T_{LCZ\ Sites} - T_{TKL} \quad (1)$$

Figure 6. Panoramic view of rural reference station: TKL station

2.4. Post-processing of traverse measurement data

(1). Exclusion of contaminated data

Air temperature data measured when the mobile traverse vehicle with low driving speed is possible to be affected by heat release from nearby vehicles and insufficient ventilation of sensor. Previous study by Buttstädt and Schneider (2014) has excluded data collected at a driving speed lower than 18 km/h in order to ensure sufficient sensor ventilation. François Leconte, Bouyer, Claverie et al. (2016) have pointed out that low-driving-speed (below 15 km/h) data may have thermal

perturbations from other vehicles stopped nearby. Therefore, this study has not considered the data with driving speed lower than 15 km/h.

(2). Temporal adjustment and altitude correction of measured air temperature

As local climate conditions change with time during traverse measurements, temporal adjustment of measured data is necessary for synchronous analysis. Due to the geographical diversity and spatial heterogeneity of urban morphology in Hong Kong, this study has selected reference stations operated by Hong Kong Observatory for three traverse measurement regions separately. Hong Kong Park (HKP) and Shaw Kai Wan (SKW) stations in Hong Kong Island have been determined as reference stations for HKI region. Hong Kong Observatory headquarter station (HKOH), Kings Park (KP), Kowloon Town (KLT), and Sham Shui Po (SSP) stations in Kowloon have been determined as the reference stations for KL region, and TU1 station has been determined as a reference station for TM region (Mok, Wu, & Cheng, 2011).

Mean cooling rates during measurement time (8 pm - 10 pm) have been calculated based on hourly air temperature data of reference stations in each day. 9 pm is the reference time for the linear temporal adjustment. Measured data has been adjusted proportionally to the time difference between 9 pm and the measurement time. **Table 3** shows the mean cooling rates of reference stations between 20:00 and 22:00 in five measurement days. The mean cooling rates of reference stations were all below 0.25 K/h, and the overall temperature changes during two-hour measurements ranged from 0.15 K to 0.5 K.

Due to the elevation difference between LCZ sample sites and the reference rural station, the measured air temperature was corrected to the same elevation of TKL station (15m above mean sea level) to calculate the UHI intensity. Air temperature of each measured point has been corrected to the same elevation of TKL station (15m), to calculate the UHI intensity. The temperature lapse rate for UHI calculation was 0.01 K/m, as suggested by previous study in Hong Kong (Giridharan, 2005).

Table 3. Cooling rates of reference stations during the traverse measurements (8 pm - 10 pm)

Date	Mean Cooling Rate of Reference Stations (K/h)			
	HKI	KL	TM	Mean

	HKP	SKW	HKOH	KP	KLT	SSP	TU1	
Jul 16	0.15	0	*n/a*	*n/a*	*n/a*	*n/a*	*n/a*	0.075
Jul 30	*n/a*	*n/a*	0.15	0.1	0.2	0.25	n/a	0.175
Aug 25	*n/a*	*n/a*	*n/a*	*n/a*	*n/a*	*n/a*	0.25	0.25
Aug 26	0.15	0.3	*n/a*	*n/a*	*n/a*	*n/a*	*n/a*	0.225
Sep 2	*n/a*	*n/a*	*n/a*	*n/a*	*n/a*	*n/a*	0.2	0.2

(3). Collation of measured data into GIS

GPS information, which records the corresponding geographical location of each measurement data, was firstly imported into the GIS system in vector points. Secondly, the measured data (after temporal adjustment and exclusion of low-speed data) was related to each GPS point according to the measurement time. The measured data points were converted into high-resolution raster layer (in 1m resolution) in GIS. Then, the raster layer was processed through zonal statistics in GIS to calculate the mean air temperature of each LCZ site. Thirdly, mean air temperature of each LCZ site was subtracted by the mean air temperature of TKL station during 8 pm - 10 pm to get the UHI intensity of sample sites.

2.5. Bivariate and multivariate analysis

Bivariate analysis methods of Pearson Correlation and Partial Correlation were used to access the discrete association between every urban morphology parameter and UHI intensity. Pearson Correlation measures the linear correlation between two variables, which is an important approach to address the collinearity issue between the independent variables. However, multicollinearity is a common feature of urban morphology dataset, which can lead to inflation of the variance of predictive variables and cause biased inference statistics in multivariate analysis(Yu, Chen, & Wong, 2020). Therefore, Partial Correlation was compared with Pearson Correlation to examine the relationship between every two variables, with the effects of other variables removed (Chu, Venevsky, Wu et al., 2019; Shipley, 2016). It is essential for enhancing the reliability of statistical model when multicollinearity exists among the independent variables.

Multivariate analysis methods of stepwise Multiple Linear Regression (stepwise MLR) and Partial Least Squares (PLS) were conducted to identify the predictive variables of UHI intensity and establish the UHI estimation model at local scale. Bootstrap resampling method was employed to evaluate confidence intervals of UHI intensity (Houet & Pigeon, 2011). To identify the best fitting model, different combinations of urban morphology parameters were compared based on the Akaike Information Criterion (AIC)(Guo, Yang, Xiao et al., 2020; Yin, Yuan, Lu et al., 2018). According to the model selection rule of AIC, the combination of independent variables with minimum AIC value is preferred to establish the urban morphology based UHI estimation model. Based on the model, a UHI estimation map was formulated in GIS.

The workflow of this study is summarized as follows (**Figure 7**).

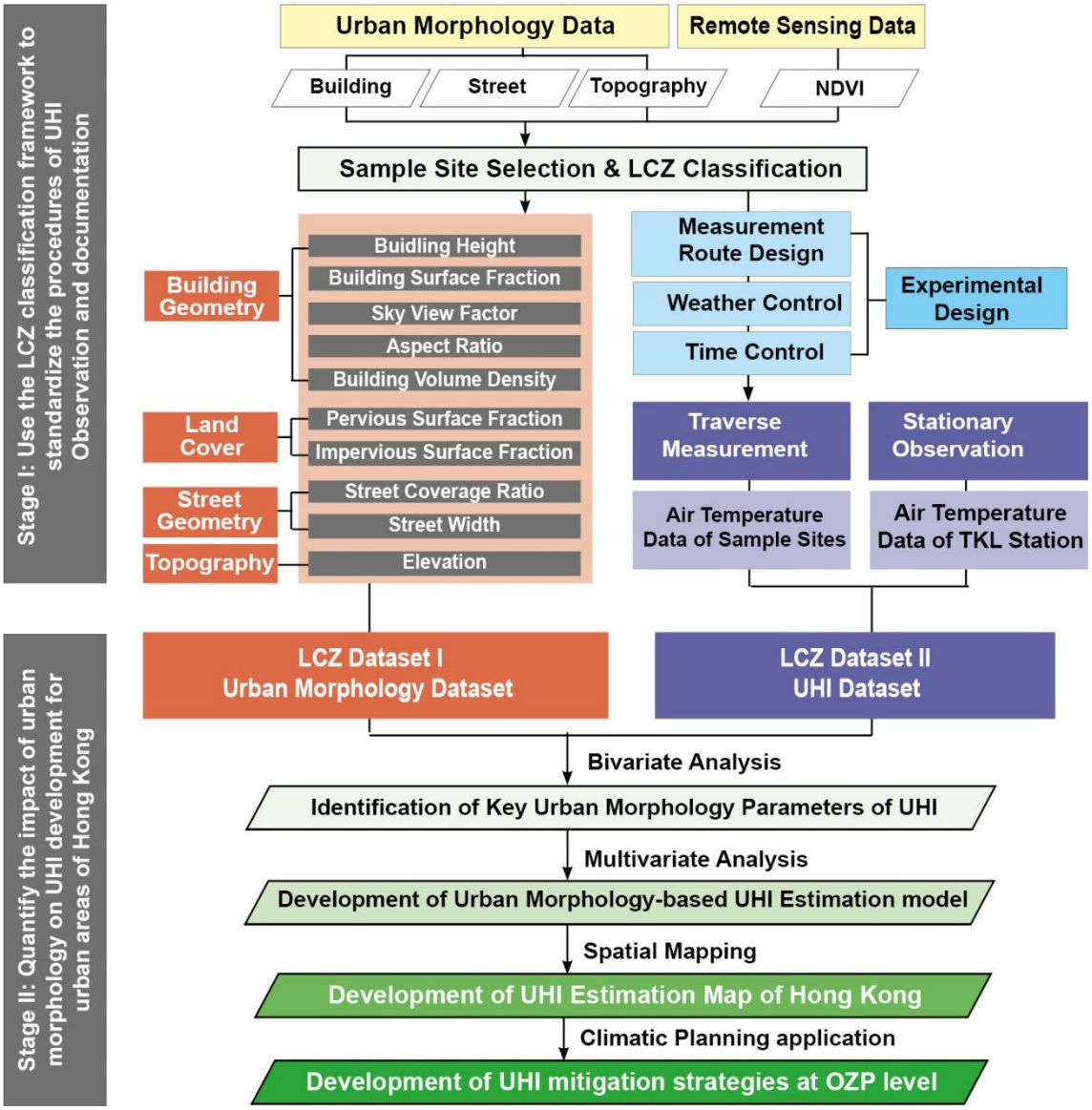

Figure 7. Workflow of this study

3. Results

3.1. UHI intensity and urban morphology statistics of LCZ sample sites

Figure 8 presents the mean UHI intensity of LCZ sample sites based on traverse measurement results. On average, a 3 K variation of UHI intensity has been observed, with maximum and minimum UHI intensity of around 4.2 K and 1.0 K, respectively. Wan Chai, Causeway Bay, North Point in HKI, as well as Jorden and Tin Hau Temple in KL were hot spot areas which have observed UHI intensity higher than 3.5 K. Sai Ying Pun, Sheung Wan, Admiralty and Fortress Hill in HKI, as well as Prince Edward and Yau Ma Tei in KL have observed UHI intensity of 3.0 - 3.5 K. All the above hot spot sites are LCZ1 (compact high-rise), except Tin Hau Temple is LCZ4 (open high-rise). The

sample sites in TM, mainly classified as LCZ4, experienced comparatively lower UHI intensity under 2.5 K.

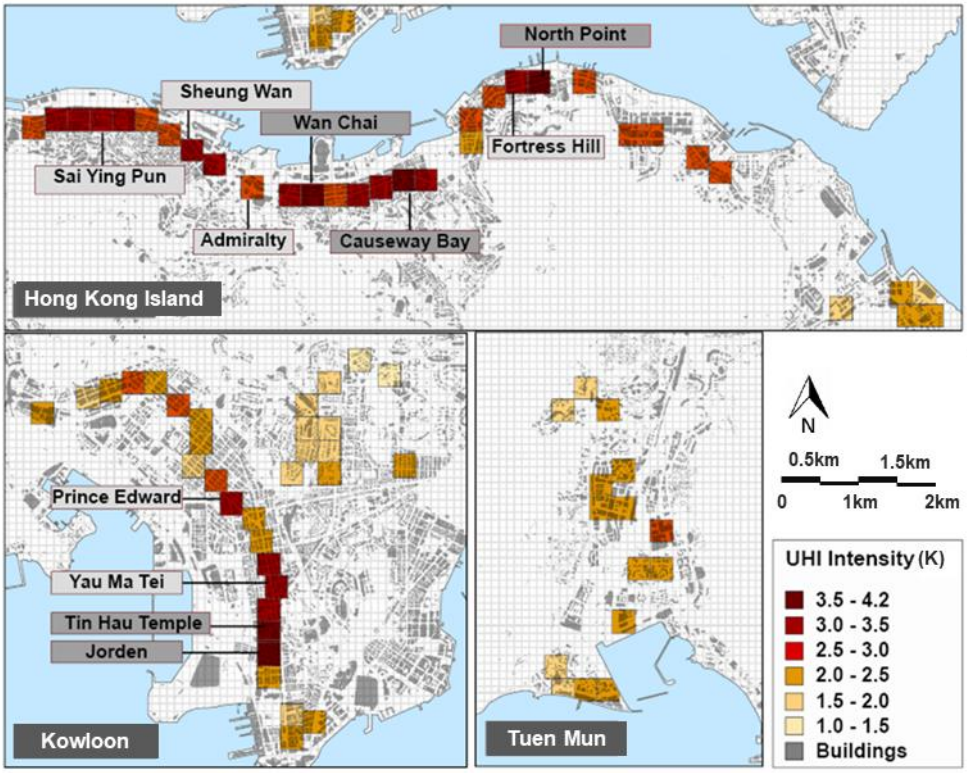

Figure 8. Mean UHI intensity of LCZ sample sites based on traverse measurements (Sample Size: 80)

UHI intensities and urban morphology parameters of LCZ sample sites in the six LCZ classes were shown in **Figure 9** and **Figure 10**. LCZ1 experienced the highest mean UHI level above 2.5 K among the six classes, and it showed wide range of 1.58 K – 4.49 K. LCZ2 and LCZ4 also observed considerable UHI intensity, with the mean values above 2.0 K. The mean value of LCZ4 was slightly higher than that of LCZ2, but it had wider range spanning from 1.08 K to 3.62 K. The high UHI intensities observed in some LCZ sample sites are possibly due to the influence of surrounding high-density urban environments. The open mid-rise class of LCZ5 and low-rise classes (LCZ3 and LCZ6) have recorded averaged UHI intensity below 2.0 K. LCZ5 had the lowest mean UHI level of 1.15 K. LCZ6 documented a slightly elevated UHI intensity compared to LCZ3 and LCZ5, which may be influenced by the heat release from the freeway near the sites.

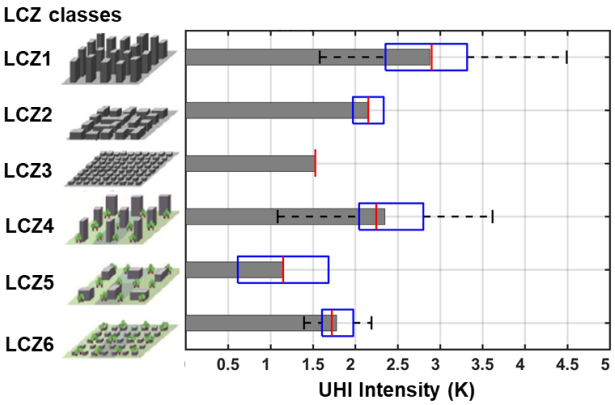

LCZ Type	UHI Intensity (K)					
	Mean	Median	Max	Min	Std Dev	Sample Size
LCZ1	2.88	2.90	4.49	1.58	0.62	46
LCZ2	2.15	2.15	2.33	1.97	0.26	2
LCZ3	1.53	1.53	1.53	1.53	-	1
LCZ4	2.36	2.25	3.62	1.08	0.53	24
LCZ5	1.15	1.15	1.68	0.61	0.75	2
LCZ6	1.78	1.72	2.19	1.39	0.29	5

Figure 9. UHI intensity of LCZ classes based on traverse measurement results (Sample Size: 80)

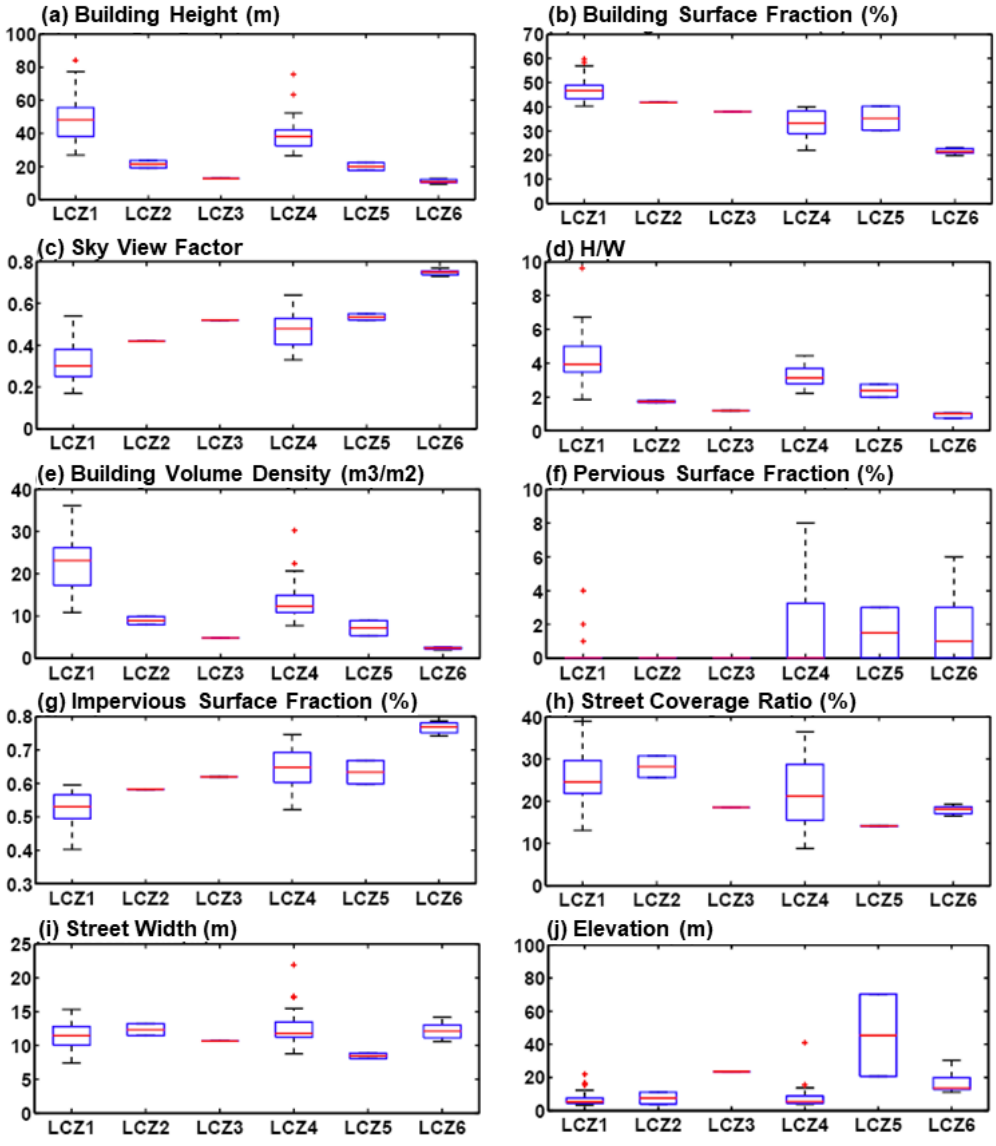

Figure 10. Boxplot of urban morphology parameters in LCZ sample sites (Sample Size: 80)

3.2. LCZ-based UHI estimation models by stepwise MLR and PLSR

(1). Bivariate analysis

The measurement data was divided into two datasets for statistical modelling. Data in the HKI and KL areas were used as the training dataset, as HKI and KL are early built high-density urban areas in Hong Kong. The training dataset was applied for quantifying the correlation between urban morphology parameters and UHI intensity, and develop the urban morphology-based UHI estimation model. TM measurement route is comparatively shorter with LCZ types consisting of LCZ4, so the data in TM was applied as the validation dataset for evaluating the predictive performance of the UHI estimation model.

First, bivariate correlation analysis methods (Pearson Correlation and Partial Correlation methods) were employed to analyze the discrete relationship between UHI intensity and each urban morphology parameter (**Table 4** and **Table 5**). Urban morphology parameters were classified into three categories: (1) building morphology parameters, including BH, BSF, SVF, H/W, and BVD; (2) land cover parameters: PSF and ISF; (3) traffic-related parameters: SCR, SL, and SW. The Pearson Correlation coefficients between UHI intensity and urban morphology parameters with the absolute value above 0.5 are as follows: (1) SVF (R = -0.67); (2) H/W (R = 0.51); (3) BVD (R = 0.52); (4) PSF (R = -0.62); (5) SCR (R = 0.59); and (9) SL (R = 0.66) (**Table 4**). Moreover, results show that collinearity exists between urban morphology parameters. For example, 3-d building geometry parameters of SVF, H/W, BVD are correlated to BH with R values of -0.56, 0.82 and 0.93, respectively, while SVF, H/W, BVD, and PSF are correlated to BSF with R values of -0.75, 0.55, 0.75, and -0.81, respectively.

In partial correlation analysis (**Table 5**), most of partial correlation coefficients between UHI intensity and multiple morphology parameters decrease to varying degrees compared to the results of Pearson Correlation analysis, with the influence of other urban morphology parameters removed. According to the analysis of Pearson correlation and partial correlation, SVF, PSF, and SL were identified as the most important indicators of UHI intensity in the building geometry, land cover, and street geometry categories respectively. SVF, PSF and SL were therefore applied as input variables for MLR and PLSR analysis.

Table 4. Pearson correlations between UHI intensity and multiple urban parameters based on training dataset (Training sample size: 65)

	Building Geometry					Land Cover		Street Geometry/ Traffic		
	BH (m)	**BSF (%)**	**SVF**	**H/W**	**BVD (m^3/m^2)**	**PSF (%)**	**ISF (%)**	**SCR (%)**	**SL (m)**	**SW (m)**
UHII (K)	0.49	0.43	-0.67	0.51	0.52	-0.62	0.47	0.59	0.66	-0.05
BH (m)	1.00	0.48	-0.56	0.82	0.93	-0.41	0.03	0.30	0.28	0.24
BSF (%)	0.48	1.00	-0.75	0.55	0.75	-0.81	-0.01	0.37	0.48	-0.17
SVF	-0.56	-0.75	1.00	-0.64	-0.71	0.79	-0.29	-0.59	-0.68	0.16
H/W	0.82	0.55	-0.64	1.00	0.84	-0.43	-0.04	0.12	0.37	-0.31
BVD (m^3/m^2)	0.93	0.75	-0.71	0.84	1.00	-0.62	0.01	0.37	0.41	0.09
PSF (%)	-0.41	-0.81	0.79	-0.43	-0.62	1.00	-0.57	-0.62	-0.64	0.04
ISF (%)	0.03	-0.01	-0.29	-0.04	0.01	-0.57	1.00	0.54	0.41	0.16
SCR (%)	0.30	0.37	-0.59	0.12	0.37	-0.62	0.54	1.00	0.80	0.31
SL (m)	0.28	0.48	-0.68	0.37	0.41	-0.64	0.41	0.80	1.00	-0.16
SW (m)	0.24	-0.17	0.16	-0.31	0.09	0.04	0.16	0.31	-0.16	1.00

Table 5. Partial correlations between UHI intensity and multiple urban parameters based on training dataset (Training sample size: 65)

	Building Geometry					Land Cover		Street Geometry/ Traffic		
	BH (m)	**BSF (%)**	**SVF**	**H/W**	**BVD (m^3/m^2)**	**PSF (%)**	**ISF (%)**	**SCR (%)**	**SL (m)**	**SW (m)**
UHII (K)	0.24	-0.16	-0.33	-0.16	-0.06	-0.14	0.04	-0.19	0.34	-0.20
BH (m)		-0.13	0.08	0.59	0.60	0.13	0.07	0.17	-0.24	0.55
BSF (%)	-0.13		-0.37	-0.29	0.46	-0.82	-0.75	-0.17	0.08	-0.31
SVF	0.08	-0.37		-0.24	0.01	-0.20	-0.22	-0.43	0.22	0.00
H/W	0.59	-0.29	-0.24		0.24	-0.16	-0.08	-0.31	0.25	-0.80
BVD (m^3/m^2)	0.60	0.46	0.01	0.24		-0.01	-0.04	0.00	0.10	0.18
PSF (%)	0.13	-0.82	-0.20	-0.16	-0.01		-0.89	-0.16	0.09	-0.22

ISF (%)	0.07	-0.75	-0.22	-0.08	-0.04	-0.89		-0.02	0.02	-0.13
SCR (%)	0.17	-0.17	-0.43	-0.31	0.00	-0.16	-0.02		0.82	0.16
SL (m)	-0.24	0.08	0.22	0.25	0.10	0.09	0.02	0.82		-0.14
SW (m)	0.55	-0.31	0.00	-0.80	0.18	-0.22	-0.13	0.16	-0.14	

Partialed with respect to all the other variables.

(2). Multivariate analysis

Forward stepwise MLR and PLSR were applied to establish urban morphology-based UHI estimation models. To prevent over-fitting caused by multicollinearity of explanatory variables, predictors were selected following the procedures suggested by Oukawa, Krecl, and Targino (2022) that variables with the highest correlation with UHI intensity in the three categories (building geometry, land cover, and street geometry/traffic) were identified and selected as the input variables in stepwise MLR and PLSR analysis. Based on the results of the bivariate analysis in the above section, SVF, PSF, and SL were selected as representative parameters of building geometry, land cover, and street geometry/traffic categories respectively, as input variables of multivariate analysis. In stepwise MLR analysis, forward selection started with no independent variable, and tested the influence of each newly added variables on the model. The testing process was based on stopping rule of Akaike Information Criterion (AIC). It kept variables that contributed most to the fitting performance of the model, and repeated testing until no newly-added variable further improved the model.

Table 6 shows the results of forward stepwise MLR analysis. In the forward step analysis, SVF was the first entered variable which was evaluated as the most decisive predictor of UHI intensity, as it can explain around 44% of the UHI variation independently, with the AIC value of 114.6. SL was the second entered variable, through which the predictive performance increased to 0.54 and the AIC value decreased to 104.4. When PSF was entered in the stepwise MLR model, the predictive performance remained the same, while the AIC value had slight increase to 106.7. Thus, a combination of SVF and SL were determined as the predictors of the finalized UHI estimation model

by stepwise MLR (R^2 = 0.54, RMSE = 0.52, AIC = 104.4). **Table 7** presents the best fitting model developed by stepwise MLR, which indicates that every 0.1 decreases in SVF, or 1km increase in the total street length (SL) of LCZ sites is associated with a rise of UHI intensity by 0.23 K, and 0.48 K, respectively.

Table 6. Model-fitting results of UHI intensity and urban geometric parameters based on training dataset (Training sample size: 65)

Forward Step-wise MLR					
Step	Parameter	Action	R^2	10-fold Cross Validation R^2	AIC
1	SVF	Entered	0.44	0.40	114.6
2	SL	Entered	0.54	0.51	104.4
3	PSF	Entered	0.54	0.49	106.7
4	*Best Model*	*Specific*	*0.54*	*0.51*	*104.4*

Table 7 Planning-based statistical model of UHI intensity using Stepwise MLR (Training sample size: 65)

Summary of Fit						
R^2	Adjusted R^2	RMSE	Mean of Response	P value	Observations	10-fold Cross Validation R^2
0.54	0.53	0.52	2.64	<0.0001 *	65	0.51

Parameter Estimates					
Independent Variable	Estimate	Std Error	Prob>|t|	VIF	Estimate (Z-value)
Intercept	2.53	0.46	<.0001*	n/a	n/a
SVF	-2.23	0.60	0.0006*	1.68	-0.43
SL	4.8×10^{-4}	1.3×10^{-4}	0.0004*	1.68	0.41
Stepwise MLR Model	$UHII = 2.53 - 2.23\times SVF + 4.8\times10^{-4}\times SL$				

The PLSR with variables' importance of projection (VIP) approach (Li, Vilela, Tariq et al., 2022) was implemented to develop the UHI estimation model based on the NIPALS algorithm. SVF, PSF, and SL were applied as input variables for PLSR analysis. As **Table 8** shows, the minimum number of latent factors is one, and all the three input variables of SVF, PSF, and SL have the VIP value above 0.8. The latent factor developed by PLSR analysis can explain 80.39% variation of independent variables (SVF, SL and PSF) and 52.56% of dependent variable (UHI intensity). Bootstrap method was employed to evaluate confidence intervals of parameter estimates of UHI

estimation model through 5000 bootstrapping replications (Gu & You, 2022). The results show that the original PLSR model has higher predictive performance (R^2 = 0.53) than bootstrap-based models (R^2 = 0.28).

Method	Number of Factors	Percent Variation Explained for Cumulative X		Percent Variation Explained for Cumulative Y		Number of VIP > 0.8
NIPALS	1	80.39 %		52.56 %		3
Parameter Estimates						
		Original	Bootstrap Method (5000 bootstrap samples)			
			Mean	Median	95% Confidence Interval Upper	95% Confidence Interval Lower
Intercept		2.71	2.71	2.71	3.02	2.48
SVF		-1.50	-1.52	-1.50	-1.19	-1.93
SL		0.0003	0.0003	0.0003	0.0004	0.0003
PSF		-1.72	-1.75	-1.73	-1.30	-2.31
R2/Adjusted R2		0.53/0.52	0.28/0.27	0.28/0.26	-	-
PLSR Model		UHII = 2.71 - 1.50×SVF + 3.0×10-4×SL - 1.72×PSF				

Table 9 compared UHI estimation models developed by MLR and PLSR. It shows that the two methods have similar performance in predicting UHI intensity, and stepwise MLR has a slightly higher adjusted R^2 (0.53) than PLSR (adjusted R^2=0.52). The model by PLSR gives a more comprehensive consideration of the influence of building geometry (SVF), vegetated land cover (PSF) and street geometry/traffic conditions(SL) on UHI development, while stepwise MLR only takes SVF and SL into account through automatic variable selection procedures. Hence, the finalized model is determined as the PLSR model. It the PLSR model, for every 0.1 decrease in SVF, 10% decrease in PSF, or 1km increase in the total street length of LCZ sites, UHI intensity is associated with a rise of 0.15 K, 0.17 K, and 0.30 K, respectively.

Table 8. PLSR model summary in predicting UHI intensity at LCZ scale

Method	Number of Factors	Percent Variation Explained for Cumulative X		Percent Variation Explained for Cumulative Y		Number of VIP > 0.8
NIPALS	1	80.39 %		52.56 %		3
Parameter Estimates						
		Original	Bootstrap Method (5000 bootstrap samples)			
			Mean	Median	95% Confidence Interval Upper	95% Confidence Interval Lower
Intercept		2.71	2.71	2.71	3.02	2.48
SVF		-1.50	-1.52	-1.50	-1.19	-1.93

SL	0.0003	0.0003	0.0003	0.0004	0.0003
PSF	-1.72	-1.75	-1.73	-1.30	-2.31
R^2/Adjusted R^2	0.53/0.52	0.28/0.27	0.28/0.26	-	-
PLSR Model	UHII = 2.71 - 1.50×SVF + 3.0×10-4×SL - 1.72×PSF				

Table 9. Comparison of UHI estimation models by Stepwise MLR and PLSR

Summary of Fit						
	R^2	Adjusted R^2	RMSE	Mean of Response	P value	Observations
Stepwise MLR	0.54	0.53	0.52	2.64	<0.0001*	65
PLSR	0.53	0.52	0.52	2.64	<0.0001*	65
UHI Estimation Models by Stepwise MLR and PLSR						
	Intercept	SVF	SL	PSF	UHI Estimation Model	
Stepwise MLR	2.52	-2.23	4.8×10^{-4}	n/a	UHII= 2.53 – 2.23×SVF + 4.8×10^{-4}×SL	
PLSR	2.71	-1.50	3.0×10^{-4}	-1.72	UHII = 2.71 - 1.50×SVF + 3.0×10^{-4}×SL - 1.72×PSF	
Finalized Model (PLSR)	UHII = 2.71 - 1.50×SVF + 3.0×10-4×SL - 1.72×PSF					

(3). Model validation

Traverse measurement data in TM was used to validate the UHI estimation model by PLSR. **Figure 11** illustrates the comparison of the observed data and the predicted data. Although there is variation between the measured and the predicted values, the overall pattern is predicted by the PLSR method. The statistical model explains 56% of UHI intensity diversity in TM, and the root mean square error is 0.19 K. The measured UHI intensity ranges from 1.6 K to slightly above 2.7 K, while the predicted value ranges from 1.4 K to 2.6 K.

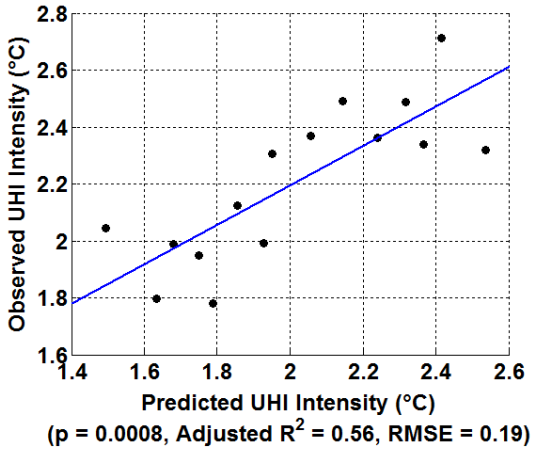

Figure 11. Validation of PLSR model based on traverse measurement data in Tuen Mun region (Validation sample size: 15)

3.3. UHI estimation map of urban areas in Hong Kong

According to the urban morphology-based UHI estimation model, an UHI estimation map for Outline Zoning Plan (OZP) (Ren, Ng, & Katzschner, 2011; Ren, Yang, Cheng et al., 2018) areas of Hong Kong has been developed (**Figure 12**). The raster grid of the map is 300m, which is consistent with the scale of LCZ unit. The UHI intensity of each raster grid was calculated using the urban morphology analysis maps of SVF, SL and PSF. As the UHI estimation map shows, hot spot areas with UHI intensity above 3 K are mainly distributed in KL and HKI areas. LCZ1 is the dominant LCZ type of hot spot areas according to the LCZ classification map (**Figure 2**). Large areas in Kowloon and northern HKI experience high-level UHI intensity ranging from 2.5 K to 3 K. Some areas in Tsuen Wan and Kwun Tong also have UHI intensity above 2.5 K. Open high-rise residential areas (LCZ4), which are mainly distributed in northern HKI, Kwun Tong, Sha Tin, Yuen Long, and TM, generally experience UHI intensity from 1.5 K to 2.5 K. The low-rise LCZ classes of LCZ5 and LCZ6, highly concentrated in the Sai Kung district and the northern part of Hong Kong, have UHI intensity of 0.5 K – 1.5 K.

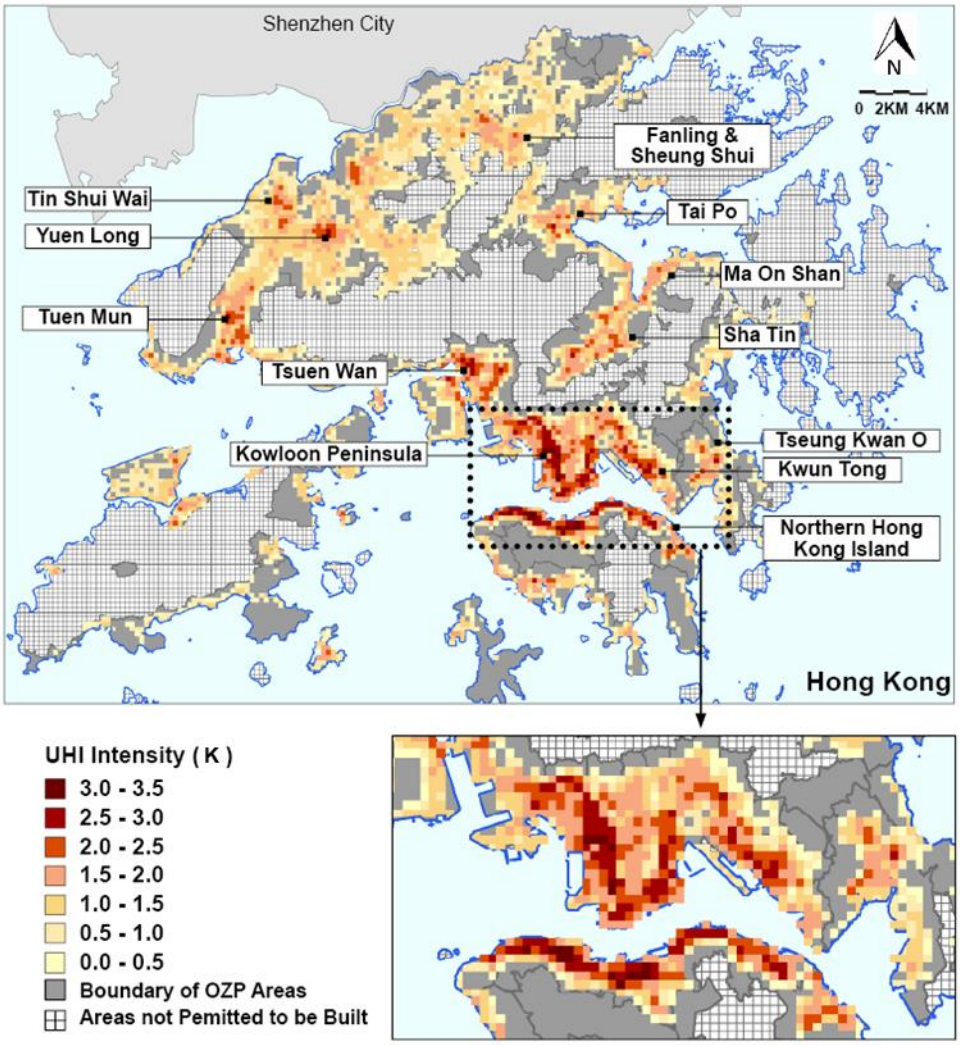

Figure 12. UHI Intensity Estimation Map for urban areas (covered by LCZ1-LCZ6) of Hong Kong

3.4. Identification of critical Outline Zoning Plan areas for UHI mitigation

Outline Zoning Plan (OZP) is the key statutory plan of Hong Kong at district level, which integrates various planning considerations in the provision of development, covering urban development purposes, environmental planning, natural landscape/habitat conservation, and cultural heritage/townscape conservation. Thus, the maximum UHI intensity (MUHII) of OZP was evaluated based on the UHI estimation map to identify critical planning zones for UHI mitigation (**Figure 13, Table 10**). 8% of OZP areas suffer MUHII above 3°C, which are distributed in KL Peninsula and the northern part of Hong Kong Island. LCZ sites with UHI intensity of 2.5°C - 3°C have been found in OZP areas along the northern coastline of Hong Kong Island, the western and eastern part of Kowloon, as well as New Towns such as Yuen Long, Tun Mun, Tsuen Wan, Sha Tin, Kwun Tong, and Tseung Kwan O. The OZP areas with MUHII above 2.5°C are generally covered by high-rise

LCZs. 34% OZP areas have MUHII from 1.5°C to 2.5°C, mainly located in marginal areas. OZP areas with MUHII under 1°C are dominated by mid-rise LCZs or low-rise LCZs.

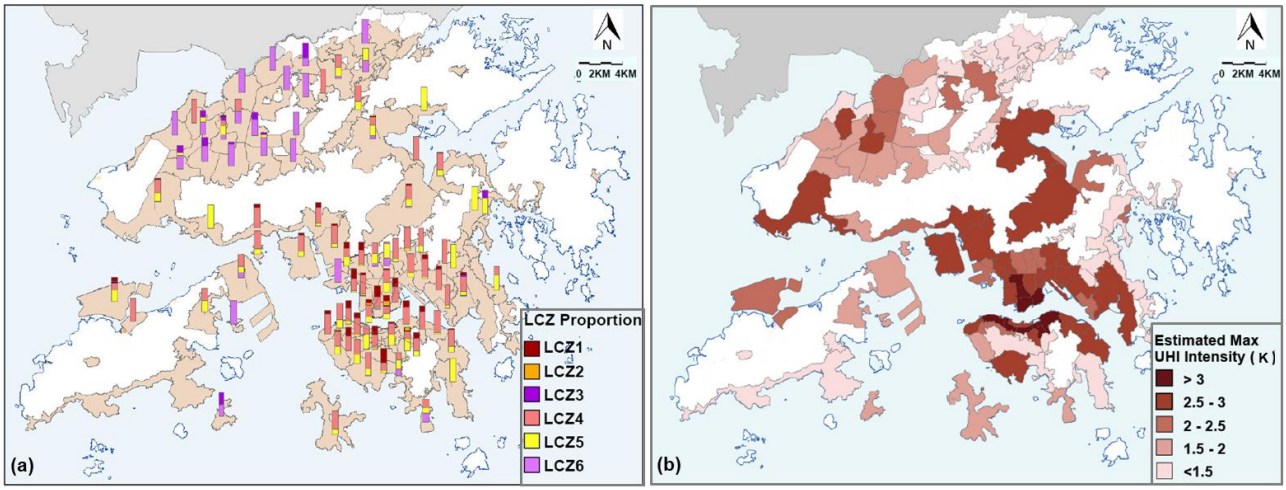

Figure 13. LCZ proportion and estimated maximum UHI intensity of OZP areas in Hong Kong ((a). LCZ proportion map (b). Estimated Maximum UHI intensity map)

Table 10. Frequency distribution of maximum UHI intensity in OZP areas

Maximum UHI Intensity (K)	>3	2.5 - 3	2 - 2.5	1.5 - 2	<1.5
Percentage of OZP areas	8%	24%	17%	17%	34%

4. Discussion

4.1. Applying LCZ framework in UHI observations and interdisciplinary communication

Spatial understanding of local climatic conditions is essential to the mitigation and adaptation of heat risks (Yuan, Zhou, Hu et al., 2022). This study applied LCZ framework in the experimental design, site selection, as well as data documentation and analysis of mobile traverse measurements. Sample sites and measurement routes were determined based on the LCZ classification map. LCZ sample sites consisted of built-up LCZ types of LCZ1-LCZ6. Measurement routes were designed to cover typical high-density urban areas of Hong Kong. Obvious intra-urban variations of local climatic conditions were monitored by the mobile measurements, and the results were analysed at LCZ scale.

Besides the application in standardizing the procedures of UHI observations , LCZ framework was employed to synergize climatic and urban morphology data to establish standardized LCZ datasets. LCZ datasets not only allow parametric analysis to investigate the links between urban morphology parameters and UHI intensity, but also provide spatial information for developing the

UHI estimation map based on the statistical models. The LCZ classification map and the UHI estimation map demonstrate the spatial distribution of urban morphology and UHI intensity using an easy-to-understand way, which may assist cross-field communication and cooperation between researchers, planners and policy makers (Perera & Emmanuel, 2018; Yang, Jin, Xiao et al., 2019).

4.2. Quantifying connections between urban morphology parameters and UHI development at local scale

Obvious intra-urban variation of UHI has been observed in the high-density and heterogenous urban environment of Hong Kong through mobile measurement. The results indicate that urban morphology has significant influence on UHI development. LCZ parameters in building density, street density, and impervious land cover has positive connections with UHI intensity, while elevation shows the opposite effect on UHI intensity. Quantitative connections between LCZ parameters of SVF, SL, PSF, and UHI intensity have been established through multivariate analysis of stepwise MLR and PLSR. Intra-urban variations of UHI intensity were characterized through the UHI estimation map, based on which urban areas with critical UHI conditions were identified.

Mobile measurement, numerical modelling and remote-sensing image analysis methods have been widely applied in quantifying the links between urban morphology and thermal environment at LCZ scale across different cities (Cilek & Cilek, 2021; Mughal, Li, & Norford, 2020; Yang, Zhan, Xiao et al., 2020). Kotharkar and Bagade (2018) have conducted mobile traverse surveys in winter of Nagpur, India. The study has found significant thermal variations across traditional LCZ types and LCZ subclasses, which helps identifying hot spots for prioritized UHI mitigation measures. Cao, Huang, Hong et al. (2022) employed numerical simulation methods to model the climatic conditions and thermal comfort at LCZ scale in Wuhan. Compact LCZ types have been found to be hotter and drier than open LCZ types both in daytime and nighttime, which may be due to the lack of open space and vegetation in urban core areas. Mushore, Dube, Manjowe et al. (2019) examined land surface temperature of LCZs based on remote sensing data of Landsat 8 in Harare, and found that LCZ types with high building surface cover had higher land surface temperature, while LCZ types with high

natural cover such as vegetation and water were cooler. Previous studies using different climatic observation and simulation methods have widely identified that compact LCZ types with the low natural surface cover of vegetation and water need planning intervention for UHI mitigation.

4.3. Integrating LCZ-based UHI mitigation strategies into Outline Zoning Plan in Hong Kong

Based on the above spatial analysis of LCZ characteristics and the estimated UHI intensity at OZP scale, UHI mitigation strategies were developed for OZP areas at four levels: Level I (MUHII > 3 K), Level II (2.5 K < MUHII < 3 K), Level III (1.5 K < MUHII < 2.5 K), and Level IV (MUHII < 1.5 K) .

Planning Level I: OZP areas in Level I mainly include the most densely built metropolitan areas in Hong Kong, covering the CBD areas and residential areas in the mid-western part of the northern Hong Kong Island, as well as commercial and residential areas in Kowloon peninsula. These areas are mainly covered by high-rise LCZs (LCZ1 & LCZ4). The MUHII of in these OZP areas is expected to be above 3 K. Thus, UHI mitigation actions are essential to these areas. Improving the existing urban environment through urban renewal is strongly recommended. The urban renewal schemes need to control building coverage ratio and building height carefully, to achieve sky view factor elevation without compromising urban density. Further intensified development is not recommended only if with sufficient reasons and proper mitigation actions.

Planning Level II: The OZP areas in Level II mainly include the eastern part of the norther Hong Kong Island, as well as New Town regions of Tseung Kwan O, Kwun Tong, Tsuen Wan, Tsing Yi, Tuen Mun, Yuen Long, Tai Po and Sha Tin. These areas are mostly in residential and commercial land use, which are also associated with dense traffic and high population density. High-rise LCZs are the dominant LCZ types in most of the OZP areas. These OZP areas have more diverse urban built environments than those in Level I. There is a decreasing trend of urban density from the central areas to the periphery. Thus, the estimated UHI intensity in the OZP areas has a wider range than that in Level I. The MUHII is expected to be spanning from 2.5 K to 3 K.

UHI mitigation actions through urban renewal are highly recommended for the hot spot areas in the OZP areas. Further development in the periphery areas could be allowed if balanced well in building volume density and sky view factor. Regulating urban development density, determining appropriate LCZ types and proportion in OZP areas, controlling building height & building coverage ratio are essential.

Planning Level III: OZP areas in Level III are mainly distributed in the western and eastern part of Hong Kong Island, middle of Kowloon Peninsula, the northwestern part of the New Territories and Islands Districts. The dominant LCZ types in these OZP areas vary from high-rise LCZs (mainly in Hong Kong Island) to low-rise LCZs (mainly in northwestern part of the New Territories). The estimated maximum UHI intensity ranges from 1.5 K to 2.5 K.

OZP areas show a high potential for future urban development because of the existing low-density land use development. The planning schemes need to achieve a balance between urban density and local climate conditions. The UHI estimation model could be used to evaluate the UHI conditions of different planning schemes for urban development.

Planning Level IV: OZP areas in Level IV are generally in low construction density, mainly distributed in the northern part of the New Territories, the southern part of Hong Kong Island, and Islands District. The dominant LCZ types are low-rise or mid-rise LCZs. The estimated maximum UHI intensity is below 1.5 K.

These areas also show a high potential for future urban development. It needs to determine appropriate LCZ types and proportion in the development schemes, and control building height and building coverage ratio to achieve proper construction density. The configuration of open space needs to be carefully designed to preserve spatial links with the surrounding natural spaces, and facilitate the cool and fresh air to penetrate into urban areas.

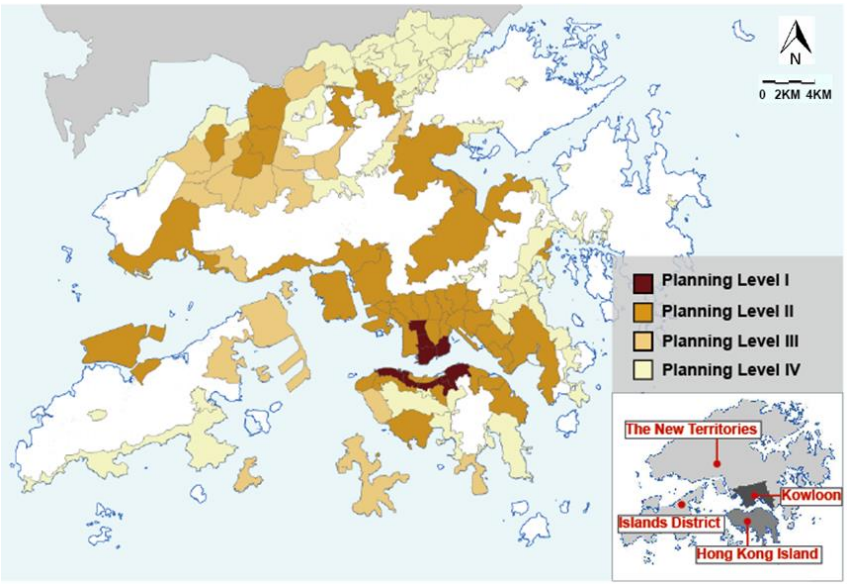

Figure 14. Integration of LCZ-based UHI mitigation strategies into Outline Zoning Plans in Hong Kong

4.4. Developing LCZ-based UHI mitigation strategies at local scale

According to the UHI estimation model of Hong Kong, optimized configuration of buildings, streets and green spaces is essential to mitigate UHI conditions at local/site scale. A wider setback of buildings from the zone boundaries needs to be imposed to increase urban openness and permeability, which would benefits in promoted radiative and convective cooling (**Figure 15**). Green space with high pervious surface cover is helpful for UHI mitigation, but dense buildings along street canyons usually restrict the cool air of green space at local scale. Thus, more dispersed green space could benefit a larger number of neighbourhoods than the green space in a concentrated form. Specially, green space configured on the side of streets is more recommended compared to those enclosed by high-rise buildings within land use zones (**Figure 15**).

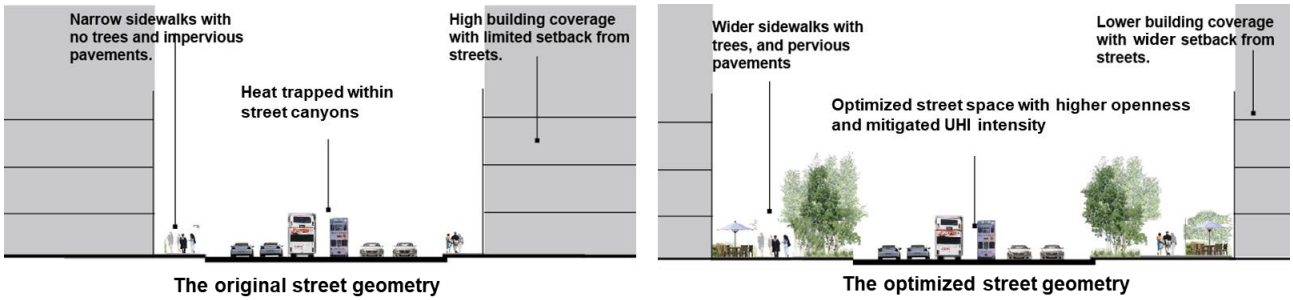

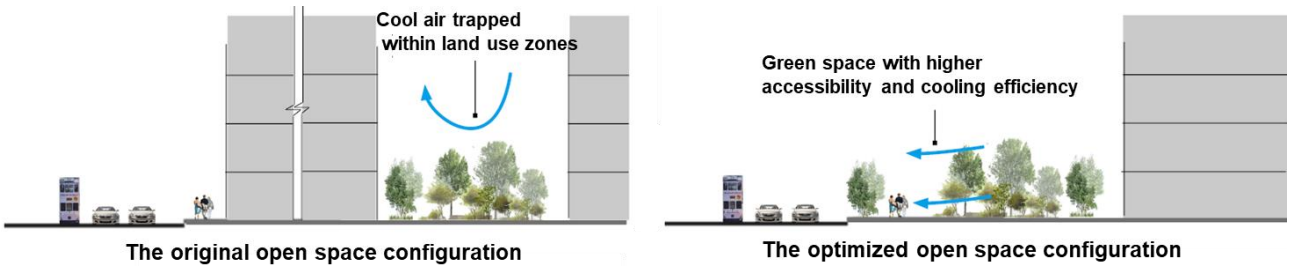

Figure 15. Planning strategies for UHI mitigation at local scale

5. Conclusion

This study has conducted mobile traverse measurements to monitor local climate variations in Hong Kong based on LCZ framework. The measurement results were processed and analyzed with urban morphology data using GIS to establish LCZ datasets. Bivariate and multivariate analysis were performed to quantify the connections between urban morphology and UHI conditions, based on which a UHI estimation model and the corresponding UHI estimation map were established.

For climatic planning practice, this study shows how the LCZ classification system could be applied to land surface classification, site selection, experimental design as well as data documentation and analysis for UHI studies. An integrative method of statistical analysis and spatial mapping has been employed to establish the urban morphology-based UHI estimation model of Hong Kong, which not only supports quantitative knowledge of key urban morphology parameters influencing local UHI development, but also provides intuitive spatial information about critical urban areas with urgent need for UHI mitigation. The UHI estimation map and LCZ classification map were further analysed at OZP level, to evaluate the urban morphology characteristics and the associated UHI intensity risks of OZP areas, and develop LCZ-based planning strategies for UHI mitigation.

The key findings of this study are summarized as follows: (1). LCZ framework is applicable for classifying land surface properties and standardizing UHI observations in the subtropical high-density city of Hong Kong. (2). Nocturnal UHI conditions at LCZ scale are significantly influenced by local urban forms, and the urban morphology-based UHI estimation model can explain around 50% of UHI variations. (3). the UHI estimation map and LCZ-based UHI mitigation planning map

are the core results of this study, which support standardized spatial information for climatic planning in Hong Kong, and for cross comparison with LCZ-based UHI studies in different climate regions.

A limitation of this study is that it only focused on UHI conditions in the early night-time period in summer, when outdoor human activities are intense with high exposure risks to significant UHI effects. Further heat risk analysis during the daytime and other seasons is necessary, especially in the early afternoon with the air temperature at its peak level. In addition, obvious UHI variations in the dominant high-rise LCZ classes of LCZ1 and LCZ4 have been observed through mobile traverse measurements, which indicates the needs for further subclassification and refinement of LCZ framework in the high-density and heterogenous urban environments in Hong Kong.

Funding: This study is supported by Guangdong Philosophy and Social Science Foundation (Grant No. GD22CGL38), Guangzhou Science and Technology Programme (Grant No. 202201020541), Guangzhou Philosophy and Social Science Planning 2022 Annual Project (Grant No. 2022GZQN19), Guangdong Basic and Applied Basic Research Foundation (Grant No. 2022A1515010171), and the Science and Technology Program of Guangzhou University (Grant No. PT252022006).

Acknowledgements: The authors deeply thank Professor Edward Ng, Mr. Max Lee, and Mr. Fung Wai Lui of the Chinese University of Hong Kong for the guidance and support of this study.

References

Buttstädt, M., & Schneider, C. (2014). Thermal load in a medium-sized European city using the example of Aachen, Germany. *Erdkunde*, 71-83.

Cao, Q., Huang, H., Hong, Y., Huang, X., Wang, S., Wang, L., & Wang, L. (2022). Modeling intra-urban differences in thermal environments and heat stress based on local climate zones in central Wuhan. *Building and Environment, 225*, 109625.

Chàfer, M., Tan, C. L., Cureau, R. J., Hien, W. N., Pisello, A. L., & Cabeza, L. F. (2022). Mobile measurements of microclimatic variables through the central area of Singapore: An analysis from the pedestrian perspective. *Sustainable Cities and Society, 83*, 103986.

Chen, L., Ng, E., An, X., Ren, C., Lee, M., Wang, U., & He, Z. (2010). Sky view factor analysis of street canyons and its implications for daytime intra- urban air temperature differentials in high- rise, high- density urban areas of Hong Kong: a GIS- based simulation approach. *International Journal of Climatology, 32*(1), 121-136.

Chu, H., Venevsky, S., Wu, C., & Wang, M. (2019). NDVI-based vegetation dynamics and its response to climate changes at Amur-Heilongjiang River Basin from 1982 to 2015. *Science of the total environment, 650*, 2051-2062.

Cilek, M. U., & Cilek, A. (2021). Analyses of land surface temperature (LST) variability among local climate zones (LCZs) comparing Landsat-8 and ENVI-met model data. *Sustainable Cities and Society, 69*, 102877.

Dosio, A., Mentaschi, L., Fischer, E. M., & Wyser, K. (2018). Extreme heat waves under 1.5 C and 2 C global warming. *Environmental Research Letters, 13*(5), 054006.

Fung, W. Y. (2010). *Characterizing urban heat island and its effects in Hong Kong.* The Hong Kong Polytechnic University.

Giridharan, R. (2005). *Urban design factors influencing outdoor temperature in high-risehigh-density residential developments in the coastal zone of HongKong.* (Doctoral Doctoral), University of Hong Kong.

Giridharan, R., Lau, S., Ganesan, S., & Givoni, B. (2007). Urban design factors influencing heat island intensity in high-rise high-density environments of Hong Kong. *Building and Environment, 42*(10), 3669-3684.

Goggins, W. B., Chan, E. Y., Ng, E., Ren, C., & Chen, L. (2012). Effect modification of the association between short-term meteorological factors and mortality by urban heat islands in Hong Kong. *PLoS One, 7*(6), e38551.

Gu, Y., & You, X.-y. (2022). A spatial quantile regression model for driving mechanism of urban heat island by considering the spatial dependence and heterogeneity: An example of Beijing, China. *Sustainable Cities and Society, 79*, 103692.

Guo, A., Yang, J., Xiao, X., Xia, J., Jin, C., & Li, X. (2020). Influences of urban spatial form on urban heat island effects at the community level in China. *Sustainable Cities and Society, 53*, 101972.

HKGovernment. (2021). Hong Kong : The Facts.

Ho, H. C., Lau, K. K.-L., Ren, C., & Ng, E. (2017). Characterizing prolonged heat effects on mortality in a sub-tropical high-density city, Hong Kong. *International journal of biometeorology, 61*(11), 1935-1944.

Houet, T., & Pigeon, G. (2011). Mapping urban climate zones and quantifying climate behaviors–an application on Toulouse urban area (France). *Environmental Pollution, 159*(8-9), 2180-2192.

Hua, J., Zhang, X., Ren, C., Shi, Y., & Lee, T.-C. (2021). Spatiotemporal assessment of extreme heat risk for high-density cities: A case study of Hong Kong from 2006 to 2016. *Sustainable Cities and Society, 64*, 102507.

Jiang, S., Zhan, W., Dong, P., Wang, C., Li, J., Miao, S., . . . Wang, C. (2022). Surface air temperature differences of intra-and inter-local climate zones across diverse timescales and climates. *Building and Environment, 222*, 109396.

Kotharkar, R., & Bagade, A. (2018). Evaluating urban heat island in the critical local climate zones of an Indian city. *Landscape and urban planning, 169*, 92-104.

Lau, K. K.-L., Chung, S. C., & Ren, C. (2019). Outdoor thermal comfort in different urban settings of sub-tropical high-density cities: An approach of adopting local climate zone (LCZ) classification. *Building and Environment, 154*, 227-238.

Leconte, F., Bouyer, J., Claverie, R., & Pétrissans, M. (2015). Using Local Climate Zone scheme for UHI assessment: Evaluation of the method using mobile measurements. *Building and Environment, 83*, 39-49.

Leconte, F., Bouyer, J., Claverie, R., & Pétrissans, M. (2016). Analysis of nocturnal air temperature in districts using mobile measurements and a cooling indicator. *Theoretical and Applied Climatology*, 1-12.

Leung, Y. K. (2004). Climate Change in Hong Kong. *Hong Kong Meteorological Society Bulletin*.

Leung, Y. K., & Ng, T. S. (1997). *Regional temperature variation in winter of Hong Kong*: Hong Kong Observatory.

Li, Q., Vilela, P., Tariq, S., Nam, K., & Yoo, C. (2022). Multiple land-use fugacity model to assess the transport and fate of polycyclic aromatic hydrocarbons in urban and suburban areas. *Urban Climate, 45*, 101263.

Lin, P., Lau, S. S. Y., Qin, H., & Gou, Z. (2017). Effects of urban planning indicators on urban heat island: a case study of pocket parks in high-rise high-density environment. *Landscape and urban planning, 168*, 48-60.

Liu, L., Lin, Y., Liu, J., Wang, L., Wang, D., Shui, T., . . . Wu, Q. (2017). Analysis of local-scale urban heat island characteristics using an integrated method of mobile measurement and GIS-based spatial interpolation. *Building and Environment, 117*, 191-207.

Masson-Delmotte, V., Zhai, P., Pörtner, H.-O., Roberts, D., Skea, J., Shukla, P. R., . . . Pidcock, R. (2018). Global warming of 1.5 C. *An IPCC Special Report on the impacts of global warming of, 1*(5).

Memon, R. A., Leung, D. Y., & Liu, C.-H. (2009). An investigation of urban heat island intensity (UHII) as an indicator of urban heating. *Atmospheric Research, 94*(3), 491-500.

Mok, H. Y., Wu, M. C., & Cheng, C. Y. (2011). Spatial variation of the characteristics of urban heat island effect in Hong Kong. *Journal of Civil Engineering and Architecture, 5*(9), 779-786.

Morakinyo, T. E., Ren, C., Shi, Y., Lau, K. K.-L., Tong, H.-W., Choy, C.-W., & Ng, E. (2019). Estimates of the impact of extreme heat events on cooling energy demand in Hong Kong. *Renewable Energy, 142*, 73-84.

Mughal, M., Li, X.-X., & Norford, L. K. (2020). Urban heat island mitigation in Singapore: Evaluation using WRF/multilayer urban canopy model and local climate zones. *Urban Climate, 34*, 100714.

Mushore, T. D., Dube, T., Manjowe, M., Gumindoga, W., Chemura, A., Rousta, I., . . . Mutanga, O. (2019). Remotely sensed retrieval of Local Climate Zones and their linkages to land surface temperature in Harare metropolitan city, Zimbabwe. *Urban Climate, 27*, 259-271.

Ng, E., Yau, R., Wong, K. S., & Ren, C. (2012). Final Report of Hong Kong Urban Climatic Map and Standards for Wind Environment- Feasibility Study.

Nwakaire, C. M., Onn, C. C., Yap, S. P., Yuen, C. W., & Onodagu, P. D. (2020). Urban Heat Island Studies with emphasis on urban pavements: A review. *Sustainable Cities and Society, 63*, 102476.

Oukawa, G. Y., Krecl, P., & Targino, A. C. (2022). Fine-scale modeling of the urban heat island: a comparison of multiple linear regression and random forest approaches. *Science of the total environment, 815*, 152836.

Perera, N., & Emmanuel, R. (2018). A "Local Climate Zone" based approach to urban planning in Colombo, Sri Lanka. *Urban Climate, 23*, 188-203.

Perkins-Kirkpatrick, S., & Lewis, S. (2020). Increasing trends in regional heatwaves. *Nature communications, 11*(1), 1-8.

Ren, C., Ng, E. Y. y., & Katzschner, L. (2011). Urban climatic map studies: a review. *International Journal of Climatology, 31*(15), 2213-2233.

Ren, C., Wang, K., Shi, Y., Kwok, Y. T., Morakinyo, T. E., Lee, T. c., & Li, Y. (2021). Investigating the urban heat and cool island effects during extreme heat events in high-density cities: A case study of Hong Kong from 2000 to 2018. *International Journal of Climatology, 41*(15), 6736-6754.

Ren, C., Yang, R., Cheng, C., Xing, P., Fang, X., Zhang, S., . . . Kwok, Y. T. (2018). Creating breathing cities by adopting urban ventilation assessment and wind corridor plan–the

implementation in Chinese cities. *Journal of Wind Engineering and Industrial Aerodynamics, 182*, 170-188.

Sakakibara, Y., & Owa, K. (2005). Urban–rural temperature differences in coastal cities: Influence of rural sites. *International Journal of Climatology, 25*(6), 811-820.

Shi, Y., Katzschner, L., & Ng, E. (2018). Modelling the fine-scale spatiotemporal pattern of urban heat island effect using land use regression approach in a megacity. *Science of the total environment, 618*, 891-904.

Shi, Y., Lau, K. K.-L., Ren, C., & Ng, E. (2018). Evaluating the local climate zone classification in high-density heterogeneous urban environment using mobile measurement. *Urban Climate, 25*, 167-186.

Shipley, B. (2016). *Cause and correlation in biology: a user's guide to path analysis, structural equations and causal inference with R*: Cambridge University Press.

Siu, L. W., & Hart, M. A. (2013). Quantifying urban heat island intensity in Hong Kong SAR, China. *Environmental monitoring and assessment, 185*(5), 4383-4398.

Stewart, I. D. (2011). *Redefining the urban heat island.* University of British Columbia. Retrieved from https://circle.ubc.ca/handle/2429/38069

Stewart, I. D., & Oke, T. R. (2012). Local climate zones for urban temperature studies. *Bulletin of the American Meteorological Society, 93*(12), 1879-1900.

Tan, Z., Lau, K. K.-L., & Ng, E. (2016). Urban tree design approaches for mitigating daytime urban heat island effects in a high-density urban environment. *Energy and Buildings, 114*, 265-274.

Tan, Z., Lau, K. K.-L., & Ng, E. (2017). Planning strategies for roadside tree planting and outdoor comfort enhancement in subtropical high-density urban areas. *Building and Environment, 120*, 93-109.

Wang, R., Ren, C., Xu, Y., Lau, K. K.-L., & Shi, Y. (2018). Mapping the local climate zones of urban areas by GIS-based and WUDAPT methods: A case study of Hong Kong. *Urban Climate, 24*, 567-576.

Wang, Z., Zhao, H., & Peng, Z. (2021). Spatiotemporal analysis of pedestrian exposure to submicron and coarse particulate matter on crosswalk at urban intersection. *Building and Environment, 204*, 108149.

Weier, J., & Herring, D. (2000). Measuring Vegetation (NDVI & EVI). from http://earthobservatory.nasa.gov/Features/MeasuringVegetation/

Wu, M., Leung, Y., Lui, W., & Lee, T. (2009). A study on the difference between urban and rural climate in Hong Kong. *Meteor, 35*(2), 71-79.

Yan, C., Guo, Q., Li, H., Li, L., & Qiu, G. Y. (2020). Quantifying the cooling effect of urban vegetation by mobile traverse method: A local-scale urban heat island study in a subtropical megacity. *Building and Environment, 169*, 106541.

Yang, J., Jin, S., Xiao, X., Jin, C., Xia, J. C., Li, X., & Wang, S. (2019). Local climate zone ventilation and urban land surface temperatures: Towards a performance-based and wind-sensitive planning proposal in megacities. *Sustainable Cities and Society, 47*, 101487.

Yang, J., Zhan, Y., Xiao, X., Xia, J. C., Sun, W., & Li, X. (2020). Investigating the diversity of land surface temperature characteristics in different scale cities based on local climate zones. *Urban Climate, 34*, 100700.

Yin, C., Yuan, M., Lu, Y., Huang, Y., & Liu, Y. (2018). Effects of urban form on the urban heat island effect based on spatial regression model. *Science of the total environment, 634*, 696-704.

Yu, Z., Chen, S., & Wong, N. H. (2020). Temporal variation in the impact of urban morphology on outdoor air temperature in the tropics: A campus case study. *Building and Environment, 181*, 107132.

Yuan, B., Zhou, L., Hu, F., & Zhang, Q. (2022). Diurnal dynamics of heat exposure in Xi'an: A perspective from local climate zone. *Building and Environment, 222*, 109400.

Zheng, Y. (2016). *Planning Strategies for Urban Heat Island Mitigation: An Application of Local Climate Zone into the High-density City of Hong Kong.* The Chinese University of Hong Kong (Hong Kong).

Zheng, Y., Li, W., Fang, C., Feng, B., Zhong, Q., & Zhang, D. (2023). Investigating the Impact of Weather Conditions on Urban Heat Island Development in the Subtropical City of Hong Kong. *Atmosphere*, *14*(2), 257.

Zheng, Y., Ren, C., Xu, Y., Wang, R., Ho, J., Lau, K., & Ng, E. (2017). GIS-based mapping of Local Climate Zone in the high-density city of Hong Kong. *Urban Climate*. doi: 10.1016/j.uclim.2017.05.008

Zou, Z., Yan, C., Yu, L., Jiang, X., Ding, J., Qin, L., . . . Qiu, G. (2021). Impacts of land use/land cover types on interactions between urban heat island effects and heat waves. *Building and Environment, 204*, 108138.